KU LEUVEN

FACULTEIT WETENSCHAPPEN

Recovery of rare earths from lamp phosphor waste: a solvometallurgical approach

Brent GRYMONPREZ

Promotor: Dr. Nerea Rodriguez Rodriguez
Co-promotor: Prof. Dr. Koen Binnemans

Proefschrift ingediend tot het
behalen van de graad van
Master of Science in Chemistry

Academiejaar 2018-2019

Preface

The original objective of this master thesis was to combine two solvometallurgical techniques together in a flowsheet to successfully recover valuable rare earth elements from lamp phosphor waste. The rare earth elements and their value, what solvometallurgy is and how it differs from traditional hydrometallurgy, how the lamps work from which the phosphor waste is obtained and already investigated techniques to recover these rare earth elements from the phosphor waste with varying rates of success are discussed first, along with the two techniques on which this master thesis was to be built further on. One of these two techniques uses an ionic liquid, so a section is dedicated to this as well.

The first of these two techniques can selectively dissolve the red YOX phosphor (Y_2O_3:Eu^{3+}) using the ionic liquid protonated betaine bis(trifluoromethylsulfonyl)imide ([Hbet][Tf_2N]). After that, the dissolved yttrium and europium can be removed again from the ionic liquid very well using oxalic acid, and the oxalates can be heated to turn it back into usable YOX phosphor. The second technique uses methanesulfonic acid and a high temperature to dissolve the green LAP phosphor ($LaPO_4$:Ce^{3+},Tb^{3+}) and then uses solvent extraction to separate the valuable terbium from the less valuable lanthanum and cerium.

In the end, things ran a bit differently due to some issues, but a new flowsheet is proposed which is faster and uses less expensive chemicals.

Many thanks go to Prof. Dr. Koen Binnemans for giving me the chance of working on this interesting topic, for thinking of the concept to combine the two techniques together into a possible elegant flowsheet, and for guiding the research towards more feasible options when the original plan turned out to be less appealing.

Next, also many thanks to Dr. Nerea Rodriguez Rodriguez for being such an awesome mentor/promotor, for all the feedback, for helping tackle the issues encountered along the way, for taking a picture used in this master thesis, for performing the OLI simulations and for performing the microwave digestions in the HF room as I was a bit too uncomfortable to enter it after seeing some nasty pictures of HF burns.

Many thanks to David Dupont for discovering that the YOX phosphor can be dissolved and recovered using the aforementioned ionic liquid, and to Lukas Gijsemans, Federica Forte and Bieke Onghena for discovering the solubility of the LAP phosphor in methanesulfonic acid and successfully separating the terbium from lanthanum and cerium using solvent extraction. Without their research, the original flowsheet might not have been thought off and the new flowsheet might not even be discovered.

Also, many thanks for everyone in (and outside) the research group for showing me how all the fantastic machines work, where to find certain chemicals and advice for some experiments, notably Brecht Dewulf for the TXRF experiments and Giacomo Damilano for the vacuum distillation experiment.

Summary

The objective of this master thesis is to set up a flowsheet to recover the precious rare earth elements from lamp phosphors used in (compact) fluorescent lamps. These lamp phosphors are substances which emit visible light after being excited. Mostly yttrium, europium and terbium are of interest, the former two being used in the YOX phosphor (Y_2O_3:Eu^{3+}) which emits red light, the latter in the LAP phosphor ($LaPO_4$:Ce^{3+},Tb^{3+}) which emits green light. These elements are quite expensive due to the limited sources from which they are available, and as all rare earths occur together, the supply and demand of most elements do not match, making some very expensive and other rather cheap. Yttrium, europium and terbium are mostly used for lamp phosphors, but these are currently not recycled due to the other substances that accompany it in the lamps like other less valuable phosphors and contamination by other parts of the lamps. Even though (compact) fluorescent lamps are slowly being phased out in favor for LEDs, recovering these elements can still be beneficial for the rare earth element market, and there already possible applications to use these elements for instead.

It was originally attempted to combine two reported techniques previously developed in the research group, both of these belonging to the quite new branch of solvometallurgy. Solvometallurgy is similar to hydrometallurgy, but water takes a much smaller role. The first technique uses the ionic liquid (a salt with a melting point below 100 °C) protonated betaine bis(trifluoromethylsulfonyl)imide (shortened to [Hbet][Tf_2N]) to selectively dissolve the red YOX phosphor, and from the ionic liquid the yttrium and europium can be precipitated using a stoichiometric amount of oxalic acid. The obtained oxalates can then be calcined to produce new YOX phosphor, with fluorescent properties equal to the starting material. The second technique uses methanesulfonic acid (MSA) to dissolve the green LAP phosphor at a rather high temperature, then dilutes the obtained rare earth rich methanesulfonic acid to separate the valuable rare earth terbium from the less valuable rare earth lanthanum and cerium. First the red YOX phosphor would be dissolved selectively, then the green LAP phosphor, but the first technique had not been tested on real waste yet, and the second was only tested on waste from which some phosphors had already been removed. After setting up the flowsheet, the objective was to scale the flowsheet up so it might be used in industry.

Due to some issues and disadvantages, the flowsheet had some steps replaced and other steps added compared to the original objective to make it all work. The research consisted of quite a portion of trial and error to fix the issues. The main issues were the HALO phosphor leaching along the other phosphors, contaminating the pregnant leach solutions heavily with calcium phosphate, and the characterization of the phosphor waste received from the supplier not matching the actual content and the waste containing large pieces of glass, plastic and metal, giving unreliable results. For the latter problem, the waste was sieved to remove most of the junk and characterized using microwave digestion. The former problem was solved by selectively removing the HALO phosphor using methanesulfonic acid at room temperature.

The very slow leaching of the YOX phosphor using the ionic liquid was successfully replaced by leaching with 2.5 vol% MSA in water at 80 °C. This aqueous MSA solution is what appears at the end of the solvent extraction to separate terbium from lanthanum and cerium. The yttrium and europium can be extracted completely from the pregnant leach solution using 70 vol% di-(2-ethylhexyl)phosphor acid (D2EHPA) in xylene, but the stripping of yttrium and

europium from this is not optimal yet and needs some further research This part is also contaminated with some calcium, originating from traces of unremoved HALO.

The main issues left were closing the loops to make the flowsheet as sustainable as possible. The MSA containing the dissolved HALO phosphor can be purified using vacuum distillation. Removing the HALO phosphor from the MSA using solvent extraction was not possible as the tested extractants are transferred from the organic phase they were dissolved in to the MSA instead of extracting the calcium and phosphate from the MSA. The barren 2.5 vol% MSA in water after extracting the yttrium and europium should be separable via a pressure swing distillation as a simulation shows that MSA and water form an azeotropic mixture with a specific composition depending on the ambient pressure.

The new proposed flowsheet works quite well in the end and only needs some small improvements and a few tests. The flowsheet is given below.

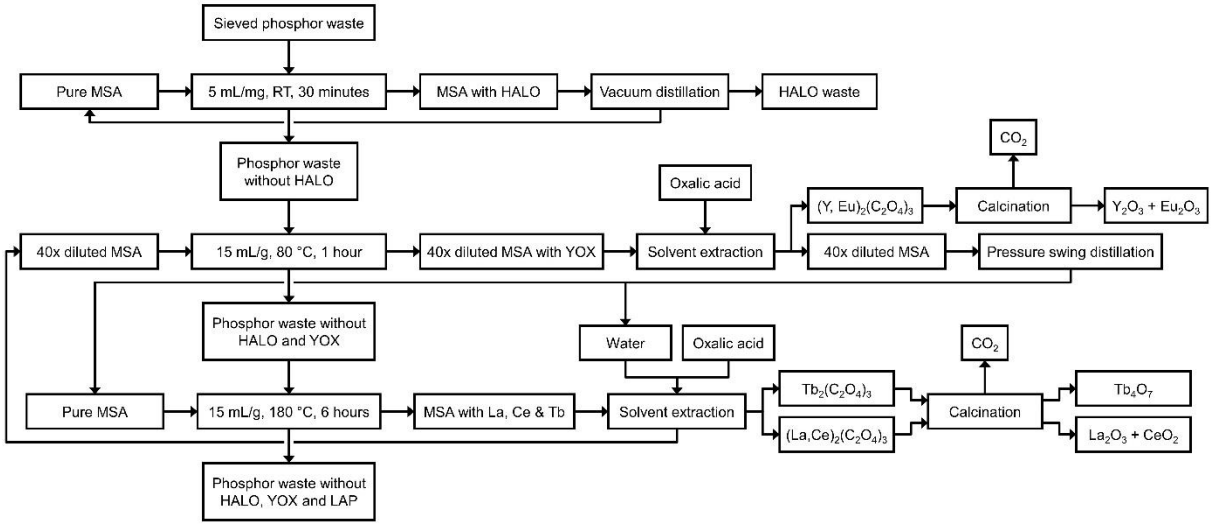

Samenvatting

Het doel van deze masterproef is het opzetten van een stroomdiagram om kostbare zeldzame aarden terug te winnen van lampfosfors gebruikt in TL-buizen en spaarlampen. Deze lampfosfors zijn stoffen die zichtbaar licht uitzenden na excitatie. Vooral yttrium, europium en terbium zijn het meest interessant, de eerste twee worden gebruikt in de YOX-fosfor (Y_2O_3:Eu^{3+}) die rood licht uitzendt, de laatste wordt gebruikt in de LAP-fosfor ($LaPO_4$:Ce^{3+},Tb^{3+}) die groen licht uitzendt. Deze elementen zijn redelijk duur door de beperkte bronnen waaruit ze beschikbaar zijn, en aangezien alle zeldzame aarden samen voorkomen, komen vraag en aanbod van de meeste elementen niet overeen, zodat sommige erg duur worden en andere meer goedkoop. Yttrium, europium en terbium worden vooral gebruikt in lampfosfors, maar deze worden momenteel niet gerecycleerd omdat er andere stoffen bijzitten zoals minder kostbare fosfors en vervuiling door andere delen van de lamp. Hoewel spaarlampen en TL-buizen langzaamaan vervangen worden door LEDs, kan het terugwinnen van deze elementen toch een positief effect hebben op de markt van de zeldzame aarden, en er zijn al mogelijke applicaties om deze elementen in te gebruiken.

Het was origineel de bedoeling om twee eerder gerapporteerde technieken te combineren die eerder in de onderzoeksgroep werden ontwikkeld, beide behorend tot de redelijk nieuwe tak van de solvometallurgie. Solvometallurgie is gelijkaardig aan hydrometallurgie, maar water neemt een veel kleinere rol in. De eerste techniek gebruikt de ionische vloeistof (een zout met een smeltpunt onder 100 °C) geprotoneerd betaine bis(trifluoromethylsulfonyl)imide (afgekort tot [Hbet][Tf_2N]) om de rode YOX-fosfor selectief op te lossen, en het yttrium en europium kunnen dan neergeslagen worden uit de ionische vloeistof met een stoichiometrische hoeveelheid oxaalzuur. The verkregen oxalaten kunnen dan gecalcineerd worden tot nieuwe YOX-fosfor, met fluorescentie-eigenschappen identiek aan het startmateriaal. De tweede techniek gebruikt methaansulfonzuur (in het Engels afgekort tot MSA) om de groene LAP-fosfor op te lossen aan een redelijk hoge temperatuur, om dan de verkregen methaansulfonzuur rijk aan zeldzame aarden te verdunnen om het kostbare terbium te scheiden van de minder kostbare lanthaan en cerium. Eerst zou de rode YOX-fosfor selectief opgelost worden, dan de groene LAP-fosfor, maar de eerste techniek was nog niet getest op echt fosforafval, en de tweede techniek was alleen maar getest op afval waarvan sommige fosfors al werden verwijderd. Na het opzetten van een stroomdiagram was het doel om het stroomdiagram op te schalen zodat het mogelijk in de industrie gebruikt kan worden.

Door enkele problemen en nadelen werden er enkele stappen in het stroomdiagram vervangen en andere toegevoegd vergeleken met het originele doel om het allemaal te laten werken. Het onderzoek bestond voor een redelijk deel uit vallen en opstaan om de problemen op te lossen. De hoofdproblemen waren de HALO-fosfor die mee oploste met de andere fosfors, en zo de geladen uitloogoplossingen zwaar onzuiver maken met calciumfosfaat, en de karakterisatie van het fosforafval verkregen van de leverancier dat niet overeenkwam met de werkelijke samenstelling en het afval dat stukjes glas, plastiek en metaal bevatten, en de resultaten zo onbetrouwbaar maakten. Voor het laatste probleem werd het fosforafval gezeefd om de meeste rommel te verwijderen en dan gekarakteriseerd met microgolf-digestie. Het eerste probleem werd opgelost door de HALO-fosfor selectief te verwijderen met methaansulfonzuur aan kamertemperatuur.

Het erg trage oplossen van de YOX-fosfor met de ionische vloeistof was succesvol vervangen door het op te lossen met 2,5 vol% methaansulfonzuur in water bij 80 °C. Deze waterige methaansulfonzuur-oplossing is een eindproduct van de solventextractie om terbium van lanthaan en cerium te scheiden. Het yttrium en europium kunnen dan volledig geëxtraheerd worden van de beladen uitloogoplossing met 70 vol% di-(2-ethylhexyl)fosforzuur (D2EHPA) in xyleen, maar het verwijderen van yttrium en europium hiervan is nog niet optimaal en heeft verder onderzoek nodig. Dit deel is ook gecontamineerd met wat calcium, afkomstig van resten HALO die niet verwijderd werden.

De overblijvende problemen was het sluiten van de lussen om het stroomdiagram zo duurzaam mogelijk te maken. Het methaansulfonzuur met de opgeloste HALO-fosfor kan gezuiverd worden met vacuümdestillatie. Het verwijderen van de HALO-fosfor van het methaansulfonzuur met solventextractie was niet mogelijk aangezien de geteste extractanten van de organische fase waarin ze opgelost zijn naar de methaansulfonzuur overgingen in plaats van de calcium en fosfaat van de methaansulfonzuur te onttrekken. Het 2,5 vol% methaansulfonzuur in water na het extraheren van yttrium en europium zou gescheiden kunnen worden met een drukwisseldestillatie aangezien een simulatie toont dat methaansulfonzuur en water een azeotroop mengsel vormen met een specifieke compositie afhankelijk van de omgevingsdruk.

Het nieuwe voorgestelde stroomdiagram werkt uiteindelijk redelijk goed en heeft enkel nog wat verbeteringen en tests nodig. Het stroomdiagram staat hieronder.

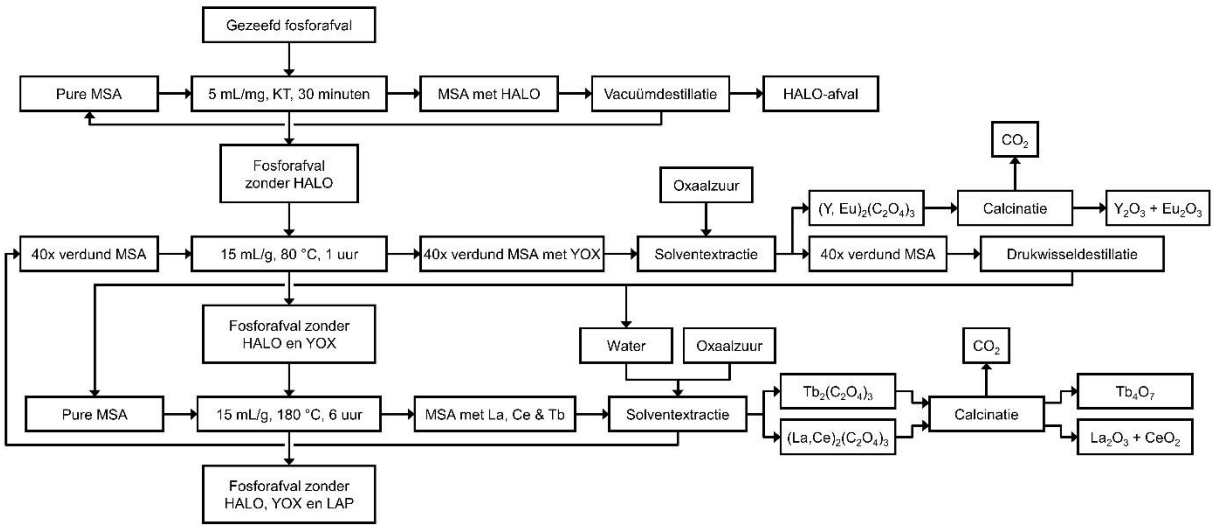

List of used symbols and abbreviations

Molecules and substances

Ln	Lanthanide
REE (RE)	Rare earth element
LREE	Light rare earth element
HREE	Heavy rare earth element
BAM	$BaMg_2Al_{16}O_{27}:Eu^{2+}$ or $BaMgAl_{10}O_{17}:Eu^{2+}$, a blue lamp phosphor
CAT	$Ce_{0.65}Tb_{0.35}MgAl_{11}O_{19}$, a green lamp phosphor
HALO	$Ca_{10}(PO_4)_6(F,Cl)_2:Sb^{3+},Mn^{2+}$ or $(Sr,Ca)_{10}(PO_4)_6(F,Cl)_2:Sb^{3+},Mn^{2+}$, a white lamp phosphor
LAP	$LaPO_4:Ce^{3+},Tb^{3+}$, a green lamp phosphor
YOX	$Y_2O_3:Eu^{3+}$, a red lamp phosphor
[Hbet][Tf_2N]	Protonated betaine bis(trifluoromethylsulfonyl)imide, an ionic liquid
ClO^-	Hypochlorite
D2EHPA	Di-(2-ethylhexyl)phosphoric acid
DMF	Dimethylformamide
DMSO	Dimethyl sulfoxide
EDTA	Ethylenediaminetetraacetic acid
HbetCl	Betaine hydrochloride, a precursor of [Hbet][Tf_2N]
$LiTf_2N$	Lithium bis(trifluoromethylsulfonyl)imide, a precursor of [Hbet][Tf_2N]
MSA	Methanesulfonic acid
NiMH	Nickel-metal hydride
PET	Polyethylene terephthalate
PVC	Polyvinyl chloride
TBP	Tributyl phosphate
TMS	Tetramethylsilane ($(CH_3)_4Si$)

Units and quantities

%	Percent
<	Smaller than
>	Larger than
=	Equal to
°C	Degrees Celsius
$_{aq}$	aqueous
$_{f}$	fluid
$_{s}$	solid
µL	Microliter
µm	Micrometer
η	Viscosity
ρ	Density
Å	Angstrom, equal to 0.1 nm
A/O ratio	Aqueous-to-organic ratio, amount of aqueous phase per unit of aqueous phase in a solvent extraction step, dimensionless
atm	Atmosphere

cm	Centimeter
cm^3	Cubic centimeter
d	Diameter
G	Centrifugal velocity
g	Gram
h	Hour
Hz	Hertz
J	Coupling constant, expressed in Hz
K	Kelvin
k	A constant
kg	Kilogram
L	Liter
L%	Leaching efficiency, expressed in percent
L-to-S ratio (LS)	Liquid-to-solid ratio, amount of liquid per unit if weight in a leaching step, expressed in volume or mass divided by mass
M	Molar, moles per liter
m	Meter
MΩ	Megaohm
mbar	Millibar, equal to 100 pascals
mg	Milligram
min	Minute
mL	Milliliter
mol	Mole
mol%	Mole percent
MPa	Megapascal
ms	millisecond
MHz	Megahertz
nm	Nanometer
O/A ratio	Organic-to-aqueous ratio, amount of organic phase per unit of aqueous phase in a solvent extraction step, dimensionless
Pa	Pascal
pH	Acidity
ppm	Parts per million, equal to mg/L
ppb	Parts per billion
q	Quartet
R^2	Coefficient of determination
rpm	Rotations per minute
s	Singlet
S-to-L ratio	Solid-to-liquid ratio, amount of mass per unit of liquid in a leaching step, expressed in mass divided by volume
T	Temperature
t	Time
USD	United States dollar
v	Speed
vol%	Volume percent
wt%	Weight percent

Other

CFL	Compact fluorescent lamp
EoL	End-of-life
ERECON	European Rare Earths Competency Network
FCC	Fluid cracking catalyst
HSE	Health, safety and environment
HydroWEEE	Innovative Hydrometallurgical Processes to recover Metals from WEEE including lamps and batteries
ICP-OES	Inductive Coupled Plasma- Optical Emission Spectrometry
IL	Ionic liquid
ISE	Ion-selective electrode
LED	Light-emitting diode
NMR	Nuclear Magnetic Resonance
MWD	Microwave digestion
PLS	Pregnant leach solution
RT	Room temperature
TOC	Total organic carbon
TXRF	Total Reflection X-Ray Fluorescence (Analysis)
U.S.	United States
UV	Ultraviolet
WEEE	Waste from Electrical and Electronic Equipment

Content

1 Introduction

The original objective of this master thesis was to combine (and upscale) two previously reported techniques developed in the research group of prof. Binnemans to recover rare earth elements from lamp phosphor waste. Before discussing these two techniques, background info is given on what the rare earth elements are, how the lamps and lamp phosphors containing these rare earth elements work, and which recycling techniques have already been discovered to recover (some of) the rare earths from the lamp phosphor waste.

1.1 Rare Earth Elements and the Balance Problem

The rare earth elements (REEs), or the rare earths (REs), are a group of elements containing scandium, yttrium and the lanthanides. The lanthanides are all the elements between, and including, lanthanum and lutetium, positioned on the first row of the f-block in the periodic table, see Figure 1.[1] REEs are also divided in two groups, the light rare earths (LREEs) and the heavy rare earths (HREEs). The LREEs include the elements from lanthanum to neodymium and the HREEs include the elements from gadolinium to lutetium and yttrium; however, the separation depends from source to source and samarium and europium can belong to either.[2]

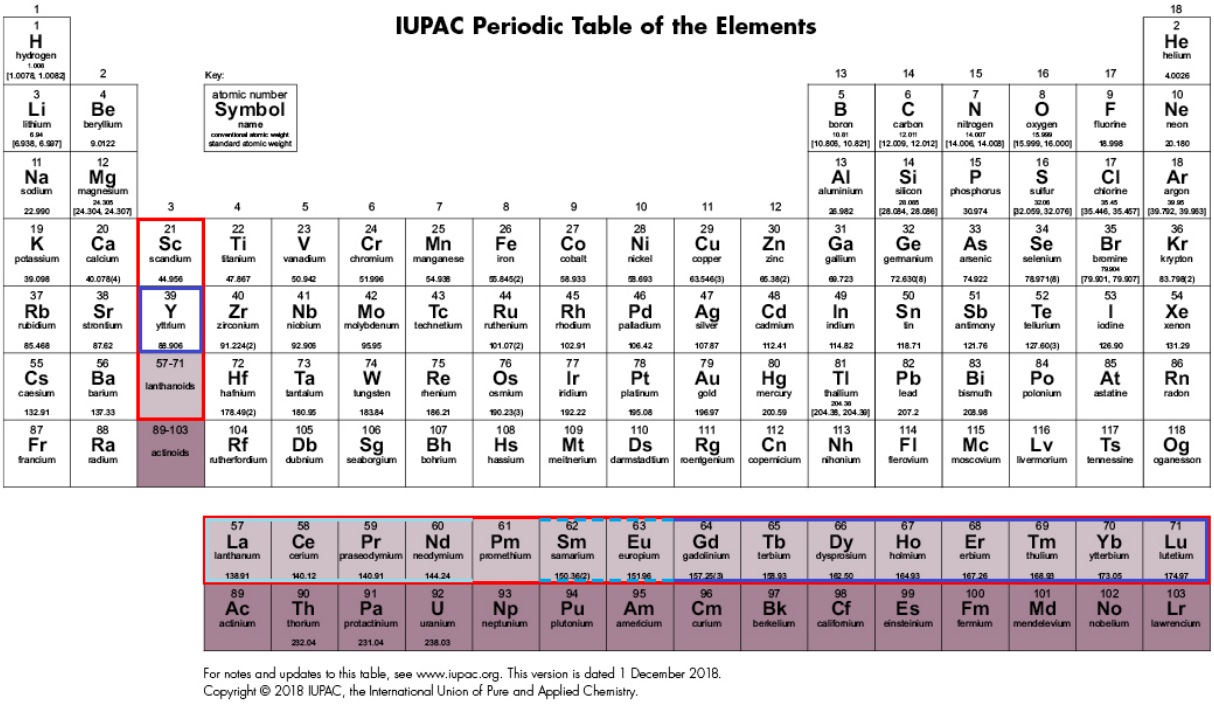

Figure 1: The periodic table with all the REEs marked in red boxes. The LREEs are marked light blue, the HREEs are marked dark blue, and the elements that can be grouped in either are marked with a blue dashed line. (image adapted from https://iupac.org/wp-content/uploads/2018/12/IUPAC_Periodic_Table-01Dec18.jpg).

Although REEs were called “rare” in the past, the abundance of these elements in the Earth’s crust is not that low. Only promethium occurs in the Earth’s crust at very low concentrations (< 10^{-19} %) as all isotopes are radioactive and transmute into other elements. The abundance of the REEs is given in Table 1.[1]

Table 1: Abundance of the REEs in the Earth's crust (differs from source to source),[1] their atomic number and their price as oxide.[a] Holmium, erbium, thulium and ytterbium have no large-volume applications, and lutetium only recently found an application, so not all of these elements have a bulk price.[2]

Element	Symbol	Atomic number	Abundance (ppm)	Price (USD/kg)
Scandium	Sc	21	13.6	1019
Yttrium	Y	39	22	3
Lanthanum	La	57	30	2
Cerium	Ce	58	64	2
Praseodymium	Pr	59	7.1	55
Neodymium	Nd	60	26	42
Promethium	Pm	61	$< 10^{-15}$	-
Samarium	Sm	62	4.5	2
Europium	Eu	63	0.88	38
Gadolinium	Gd	64	3.8	21
Terbium	Tb	65	0.64	452
Dysprosium	Dy	66	3.5	212
Holmium	Ho	67	0.80	-
Erbium	Er	68	2.3	22
Thulium	Tm	69	0.33	-
Ytterbium	Yb	70	2.2	-
Lutetium	Lu	71	0.32	-

There are two clear trends in the abundance of the REEs: (1) heavier elements are less abundant, and (2) elements with an even atomic number are more abundant than its close neighbors with an odd atomic number (Oddo-Harkins rule). This rule is based on the higher stability of the nuclei with an even number of protons and/or neutrons. The ores which contain REEs always contain all of these elements, although some ores contain mostly the LREEs (bastnäsite, monazite) while others are richer in HREEs (xenotime and ion-adsorption ores).[2]

A serious disadvantage of the fact that the REEs occur together is that some applications needing a certain amount of one pure element gives rise to an excess of some other elements compared to its demand on the market, these elements produced in excess need to be stockpiled.[2] This problem of the market demand not matching the abundance of the REEs is called the *balance problem*. The problem can be solved for example by finding new applications for the elements that are more abundant than currently needed or by recycling.[3] Currently, the LREE market is driven by the need for neodymium in Nd-Fe-B magnets, creating a surplus of lanthanum and cerium.[4] A report has been written for the European Commission in which the criticality of various materials was investigated, and all the REEs have a very high supply risk with varying economic importance, a plot of this can be found in Figure 2. Because of this, both the HREEs as the LREEs (when grouped) are deemed critical (a material is critical when the supply risk value is above 1 and the economic importance is above 2.8).[5]

[a] Prices of May 19 2019, converted from China Yuan to USD when necessary using exchange rate of May 19 2019 (1 Yuan = 0.14454 USD). All purities are > 99.5 %, except for samarium (> 99.9 %), terbium (> 99.9 %), yttrium (> 99.99 %) and scandium (> 99.99 %). Found on https://mineralprices.com/rare-earth-metals/

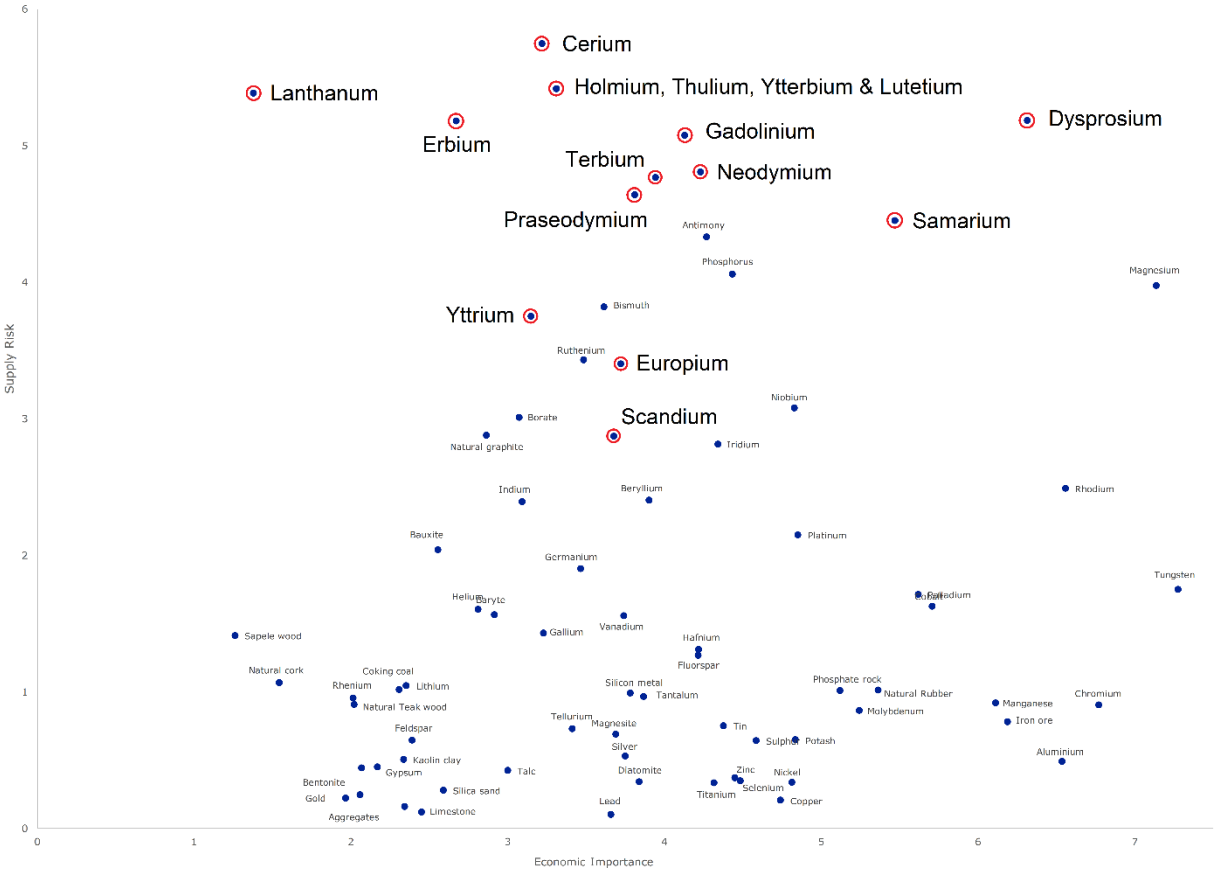

Figure 2: Plot of the supply risk versus the economic importance of 78 individual raw materials with the REEs (scandium included) encircled.[5]

Besides the aforementioned balance problem, REEs are also very critical due to the risk in the supply chain. According to the U.S. Geological Survey, REEs are mostly mined in China, with around 80 % of the total production (~130.000 tons) until 2017. The production of REEs increased dramatically in 2018 when the U.S. started producing REEs again (10 % of the total production) along with smaller quantities from some other countries and China then only produced 70 % of the total production.[6–8] However, it is estimated that 30.000 - 40.000 tons extra is mined illegally in China.[1] Australia produces another 10 – 15 % of the REEs and the rest is mined mostly in Russia, India, Thailand and Brazil, and since 2018 also Burundi and Myanmar.[6–8] However, in an assessment from the European Commission from 2017, it is estimated that China holds 95 % of the REE supply, much more than the U.S. Geological Survey reported from that same year, even when taking into account possibly illegally mined REEs.[5] Since the vast majority is mined in China, this gives the country a monopoly, and trade restrictions can increase the price of the REEs dramatically, e.g. REEs crisis of 2010-2011 when prices increased four to nine fold for some time.[9]

Because of the importance of some REEs and the high supply risk, three ways to reduce the EU's import dependence have been suggested by the European Rare Earth Competency Network (ERECON): (1) substituting critical REEs by less critical metals, (2) investing in sustainable primary mining from old and new REE deposits and (3) investing in urban mines and recycling technologies.[9] Several possible sources of REEs are under investigation, and they include apatite ores ($Ca_{10}(PO_4)_6(OH,F,Cl)_2$) and wastes similar to it,[10–17] bastnäsite ($REEFCO_3$),[18,19] coal and coal by-procucts,[20–27] manganese nodules found on the ocean bed of the Pacific ocean,[28] monazites ($REEPO_4$),[29–35] eudialyte (a very complex zirconium silicate),[36] xenotime (YPO_4) found in the Sinai desert,[37] acid mine drainage,[38] phosphogypsum

(waste from phosphoric acid production), red mud (waste of the aluminium industry), fluorescent lamps, motors, computer monitors,[39] and radioactive waste residues.[40] Studies have also been performed to investigate new geological resources for the REEs in Europe[41] and Australia.[42]

This master thesis focuses on the recovery of REEs from fluorescent lamps. The REEs that are used in lamp phosphors are yttrium, europium, lanthanum, cerium and terbium. Yttrium, europium and terbium are considered as a critical REE because of their use in the lamp phosphors. The red YOX phosphor contains yttrium and europium, and the green LAP phosphor contains terbium. It should be noted that the phosphor market is becoming smaller due to the fluorescent lamps being replaced by LEDs. LEDs only use some of the REEs also used in phosphors, and those are also used in much smaller amounts. Together with the possible recycling of the lamp phosphors, it could result in oversupplies of some of the REEs.[2]

An oversupply of yttrium can be overcome by using it to stabilize the zirconia ceramic (zirconium dioxide, ZrO_2) at higher temperatures. Yttria-stabilized zirconia can be used as crucible material in pyrometallurgical techniques where no slag is present as it can resist temperatures of up to 2200 °C, is not wetted by most metals and is stable in oxidizing atmospheres. Yttrium can also be added to magnesium alloys in high-end applications to increase their high-temperature strength, creep resistance and corrosion resistance. Europium on the other hand has no major applications apart from phosphors, and it is only used as luminescent safety markers in euro banknotes. Since the total volume of europium is very small, an oversupply would not cause big problems. Terbium currently has one other main use in the magnetorestrictive alloy Terfenol-D ($Tb_xDy_{1-x}Fe_2$, x ~ 0.3), a substance which changes its dimensions in the presence of a magnetic field. This alloy is mostly used in magneto-mechanical devices and high-precision liquid-fuel injectors. An oversupply of terbium can be solved by replacing the critical dysprosium used in Nd-Fe-B magnets to increase their maximum working temperature.[2]

Cerium and lanthanum are the most abundant and the second most abundant REE and they are used in the green LAP phosphor. Lanthanum is further used for rechargeable NiMH batteries (used in (hybrid) electric cars), optical glasses (such as wide-angle lenses for cameras) and catalysts like fluid cracking catalysts (FCC) in the petrochemical industry. An oversupply by the declining use of the LAP phosphor and the NiMH batteries can be solved by using it as a stabilizer in PVC or in the mischmetal alloy. Cerium is used mainly in the glass industry as a polishing agent and as an addition to prevent the coloring of glass caused by traces of iron(II) by oxidizing it to the less colorful iron(III) or make the glass opaque to UV light. Cerium is also present as sulfides in some pigments and it is used in car exhaust catalysts. An oversupply (which can be further enhanced by the replacement of combustion-driven cars by electric cars) can be solved by using it in the mischmetal alloy.[2] This alloy is made up of metallic REEs (mostly LREEs are these are more abundant), around half is cerium and it further contains 20 wt% lanthanum, 5 wt% praseodymium and 15 – 20 wt% neodymium. The alloy is very cheap as the LREEs do not need to be separated from each other. It easily burns at rather low temperatures when oxygen is present, and because of this it is usually alloyed with some iron to make lighter flints. The mechanical friction of a lighter liberates small alloy particles and heats them to ignition, creating the sparks that ignite the gas in lighters. Mischmetal is also able to remove oxygen, hydrogen, nitrogen, sulfur, arsenic, bismuth and antimony as solids from molten metal to improve the properties of the metal, and it can be used as a cheap

replacement for samarium in magnets for less sophisticated applications like loudspeakers, headphones, microphones or clamp systems to name a few.[43]

1.2 Hydrometallurgy

In the past, metals were produced only via pyrometallurgy, where high-grade ores were heated to high temperatures. Unfortunately, these rich ores are starting to run out for some elements, and lower-grade ores are the only way to keep producing metals, but these cannot be processed via the traditional techniques. This led to the development of mineral processing and hydrometallurgy, first for copper and gold, and later for many more metals. Aluminium has been produced hydrometallurgically in the Bayer process, the oldest commercialized high-pressure hydrometallurgical process,[44] dating back as far as 1887.[45]

1.2.1 *Basics of hydrometallurgy*

In hydrometallurgy, water plays an important role, and the temperature during operations is much lower than in pyrometallurgical processes.[44] Hydrometallurgy consists of a leaching, a separation and a purification step. During the leaching, the wanted metals (and usually some unwanted metals too) are dissolved using a lixiviant or leaching agent from the material they are part of (which is sometimes already treated to enrich the desired metals in it). During the separation, the desired metals in solution are separated from undesired metals and/or from each other using solvent extraction (using an extractant), ion exchange (using a resin to exchange ions) and/or precipitation (by adding a reagent, changing the pH or evaporating water).[46] Although the focus of this master thesis is more on leaching than on solvent extraction, some background on solvent extraction is given too.

Leaching is performed using acid, base or salt aqueous solutions. Leaching of the ores can be performed *in situ*, in dumps, heaps, at atmospheric pressure, in tanks or under high pressure, depending on the grade of the ores.[46] Acidic solutions are not very selective, and this consumes more acid than needed. Alkaline solutions on the other hand are more selective, but not every metal can be dissolved in these solutions.[44] The efficiency of leaching metals depends on: concentration of the leaching agent, temperature, stirring speed, contact time, solid-to-liquid ratio, and particle size among others.[47] The formed metal solution is called the pregnant leach solution (PLS).

In solvent extraction, an immiscible organic phase containing an extractant is brought in contact with the PLS, and the metals are distributed between the two phases. The extractants can be classified in acidic, neutral or basic extractants, depending on the type of complex that is formed.[46] After solvent extraction, the organic phase is generally scrubbed by contacting it with an aqueous solution in order to remove undesired co-extracted metals. The purified organic phase is then stripped to recover the desired metals by contacting it again with an aqueous phase.[47] This phase can then be sent to the electrowinning step where the metal ions are reduced and deposited on the cathode of an electrolytic cell.[46]

There are parameters to compare different solvent extraction systems and to assess the performance of the systems.[47] As solvent extraction isn't the main topic of this master thesis and these formulas are not used in this master thesis, they are omitted.

The factors affecting the performance of the solvent extraction process are: the type of extractant and diluent (organic phase where the extractant is dissolved in), the extractant concentration, temperature, A/O ratio (the volume ratio of the aqueous and organic phases in contact with each other), mixing time, mixing speed, and pH among others.[47]

Extracting, scrubbing and stripping are generally performed in mixer-settlers. These devices consist of two parts, a mixing part where the aqueous phase and the organic phase are mixed to form an emulsion, and a settler part where the emulsion separates back into its original phases. The two phases flow out at different points at the end of the settler part. Usually, several mixer-settlers are set up in a counter-current fashion where the aqueous feed and the organic phase flow through the mixer-settlers in the opposite direction. This results in a product with a high purity as the fresh, barren organic phase has the largest extraction power and can remove the last traces of metal at the end of the aqueous stream while the partially loaded organic phase can still remove part of the metal at the start of the aqueous stream.[47]

1.2.2 *Production of the REEs via hydrometallurgy*

Initially, the REEs were separated via selective crystallization based on the different solubilities of the REE-sodium double sulfates ($(REE,Na)(SO_4)_2$) in water, but this is very inefficient and has a low productivity as the differences in solubility are very small. After this, ion exchange was used, also a hydrometallurgical step, to separate the REEs based on the difference in binding strength of their EDTA complexes. The REEs were fixed on a column and then eluded using an EDTA solution (or a solution of a similar complexing molecule). Ion exchange has been replaced by solvent extraction due to its low yields, low productivity and environmental difficulties caused by used the toxic solutions.[48]

The REEs are now solely processed via hydrometallurgy. The REEs are first leached from their mined ores using sulfuric acid (H_2SO_4), hydrochloric acid (HCl), nitric acid (HNO_3) or caustic soda (NaOH) depending on the ore. For the REE cation adsorption clays, a different leaching method is used. An ammonium sulfate solution is used to exchange the REE ions adsorbed on the clay for the ammonium ions, producing an aqueous solution of the REE sulfates. The REEs are then processed further before using solvent extraction to separate them.

Every solvent extraction step separates the REEs into two groups, and up to five separation steps are needed to separate some elements fully from the others. Each separation step consists of extracting one or several metals from an aqueous solution to an organic solution (insoluble in the aqueous phase), back-extracting traces of unwanted metal(s) from the organic solution back to an aqueous phase (the latter is recycled back to the extraction) and stripping the purified metal(s) from the organic solution to an aqueous solution for further treatment. Each of these three parts needs several mixer-settlers to transfer the metals from one solution to the other.[48]

1.3 Solvometallurgy

Similar to hydrometallurgy, solvometallurgy also consists in: leaching, metal recovery and purification. Instead of aqueous solution, solvometallurgy uses non-aqueous solvent, e.g., deep-eutectic solvents, molecular organic solvents, ionic liquids, inorganic solvents like concentrated acids, supercritical carbon dioxide. Liquid metal can also be used if the required temperature is below 300 °C. Water can be part of solvents (and is sometimes even necessary), but its content must be less than 50 vol%. In the case of using an ionic liquid, the process can be called ionometallurgy.[44]

There are several advantages of using solvometallurgy. The first advantage is that not a lot of water is consumed so no wastewater is generated. The leaching step and the extraction step can be combined into one single step which simplifies process flow sheets. Solvent leaching is usually more selective, resulting in a lower acid consumption. Ores that consist of easily soluble silicates can be treated as the silica does not form silica gel.[44]

In leaching, polar organic solvents like acetone or alcohols can be used to dissolve the mineral acids used to leach metals from solids, or sometimes organic solvents containing acidic extractants, similar to the organic phase in solvent extraction, can be used as well.[44] For example, HCl and some water dissolved in ethanol can leach scheelite (calcium tungstate),[49] and HCl dissolved in ethylene glycol is capable of leaching iron and antimony selectively from ilmenite while leaving other elements untouched.[50] For the solvent extraction part of solvometallurgy, both phases are organic and should be immiscible.[44]

1.3.1 *Ionic liquids*

Ionic liquids are organic salts (thus consisting of positively and negatively charged ions) which have a melting point below 100 °C, or even below room temperature, making them liquid at low temperatures.[51] These melting points are much lower than those of inorganic salts partially because of the bulky cationic groups which cause a low charge density and steric hindrance that is incompatible with Coulombic attraction forces. The vapor pressure of ionic liquids is very low, meaning that they hardly produce vapors and thus do not form explosive air-vapor mixtures. Most ionic liquids have high ignition points, making them very suitable as solvents.[52] Their thermal stability is very high, and they also have a high ionic conductivity.[51] They are mostly used in electrochemical applications like electrolytes in batteries or as a medium for electrodeposition or electropolishing of metals. They need to be very good at dissolving metal salts and metal oxides for this.[52] Ionic liquids have some disadvantages as well, their physical properties are not always known, their viscosity is higher than common solvents and their toxicity is unknown.[51]

Ionic liquids can be designed according to the properties they need for their applications; choosing the anion and the chain length of the cation can make the ionic liquids either miscible in water or in organic solvents, and the ions can be functionalized so they can act like acids, bases or ligands. Possible cations are positively charged nitrogen compounds like 3-methylimidazoliums or quaternary amines, alkyl cations, phosphoniums or sulfoniums. Possible anions are halides, (alkyl) sulfates, alkyl sulfonates, nitrates, aluminium chloride, triflate ($[CF_3SO_3]^-$), trifluoroacetate ($[CF_3CO_2]^-$) or bis(trifluoromethylsulfonyl)imide

($[(CF_3SO_3)_2N]^-$, shortened to $[Tf_2N]^-$, see further). There are at least one million possibilities for simple ionic liquids, and it is possible to mix them as well, resulting in staggering amounts of possible mixtures.[51]

Ionic liquids can be used as a leaching agent or as a solvent. For example, the ionic liquid 1-methylimidazolium hydrogen sulfate is capable of rather selectively leaching most of the YOX phosphor from treated lamp phosphor waste.[53] On the other hand, the ionic liquid trihexyl(tetradecyl)phosphonium chloride can be used as a solvent for hydrochloric acid to dissolve many metal oxides, and dissolved nickel can be selectively stripped from cobalt, manganese, copper, zinc and iron.[54]

1.3.2 *The ionic liquid protonated betaine bis(trifluoromethylsulfonyl)imide*

There are several other studies regarding ionic liquids for processing metals, but the one used in this master thesis is the ionic liquid $[Hbet][Tf_2N]$ and it consists of the cation protonated betaine and the anion bis(trifluoromethylsulfonyl)imide, as shown in Figure 3.

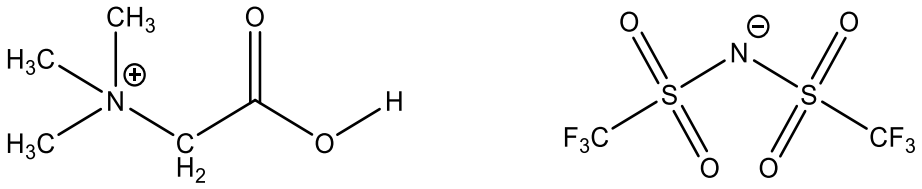

Figure 3: Structure of the cation (left) and the anion (right) of the ionic liquid [Hbet][Tf2N] (protonated betaine bis(trifluoromethylsulfonyl)imide). Notice that the carboxylic acid group of the betaine cation is protonated.

The ionic liquid has a melting point of 57 °C, but can stay liquid at room temperature before it starts crystallizing if some water is present in the ionic liquid. It is soluble in organic solvents like alcohols, DMSO, nitriles, acetic acid and ethyl acetate and other ionic liquids, but it is immiscible with organic solvents like hexane, diethyl ether, chloroform, toluene or benzene. The proton on the carboxylic acid of the betaine cation forms a hydrogen bond with one of the oxygens of the sulfonyl groups of the anion.[52] $[Hbet][Tf_2N]$ is stable up to 200 °C, higher temperatures cause the ionic liquid to degrade.[55]

The mutual solubility of water and ionic liquid increases with temperature, resulting in complete mixing above 55.5 ± 0.2 °C.[52] $[Hbet][Tf_2N]$ contains approximately 13 wt% water[55] when saturated at room temperature, which is more than 3 molecules of water per ion pair (the molecular mass of the ionic liquid at 398.30 g/mol is a lot higher than that of water). $[Hbet][Tf_2N]$ will also dissolve in alkaline aqueous solution at temperatures under 55.5 °C if the water has a pH value above 8, and phase separation occurs again upon acidification.[52]

$[Hbet][Tf_2N]$ is capable of dissolving some metal oxides, including all the oxides of the naturally occurring REE metals except cerium. The solubility of these metal oxides is very high in the ionic liquid as all the ionic liquid can be turned into a metal complex. Iron, cobalt, aluminium and silicon oxides however have a very low solubility in $[Hbet][Tf_2N]$. Usually some water is needed to dissolve the oxides well as the oxides have a hydrophilic surface while the ionic liquid is hydrophobic resulting in a poor wettability, which probably explains why pure ionic liquid has more trouble to dissolve the oxides. The dissolved metals can be stripped from the ionic liquid again by contacting it with acidified aqueous solutions which regenerates the ionic

liquid from the metal complex.[52] Some metals can also be stripped from the ionic liquid by precipitating them with oxalic acids as oxalates. This prevents small losses of [Hbet][Tf_2N] to the aqueous phase which happens when stripping with acidic solutions.[55]

Research has shown that [Hbet][Tf_2N] can be used to selectively leach REE oxides present in low amounts (0.14 wt%) in bauxite residue (also called red mud, the solid waste of extracting aluminium from bauxite ores). 70 – 85 % of the REEs and maximum 45 % of the scandium can be leached from the red mud while iron is leached less than 3 % while its oxide makes up 43 % of the red mud. Almost all of the calcium and sodium is leached as well, and 30 % of aluminum, but silicon and titanium are not leached at all. The metals are stripped from the ionic liquid using an acidic solution and the ionic liquid is regenerated and can be used again for further leaching of the red mud.[56]

[Hbet][Tf_2N] was investigated for the leachability of scandium oxide, and from the results the authors suggest it can be used to selectively leach scandium oxide from tailings or ores which contain large amounts of tantalum and niobium.[57]

Other research showed that [Hbet][Tf_2N] can be used to separate cobalt and the valuable REEs neodymium and dysprosium from unwanted iron in Nd-Fe-B magnets. The (demagnetized) magnets are crushed and roasted to turn the metals into oxides after which they are leached with [Hbet][Tf_2N] and water at 80 °C so the water and ionic liquid form a homogenous phase. The mixture is then cooled to induce a phase separation with the REE, cobalt and some of the iron going to the water phase and most of the iron going to the ionic liquid. Certain salts can be added to reduce the solubility of the ionic liquid in water. The phases are separated and both are stripped by adding oxalic acid. The REEs and cobalt form insoluble oxalates and the water is recycled back to reduce the ionic liquid losses. Aqueous ammonia is then used to separate the cobalt from the REE oxalates, and the latter are calcined to form oxides with a purity above 99.9 %. The iron in the ionic liquid is extracted from the ionic liquid as water soluble oxalate, and the now cleaned ionic liquid can be reused for a new leaching step. The water containing iron can then be treated to remove the iron.[4]

1.4 Fluorescent lamps and their phosphors

Phosphors are inorganic compounds which are able to emit the energy that they have previously absorbed as light. The emission of the phosphor usually happens around 10^{-9} seconds after the excitation of the phosphor,[58] but this can be longer for phosphors which rely on REEs for their luminescence.[1] If the phosphors are excited via photons, the process is called photoluminescence; but there are other kinds of excitation possible.[59]

The lanthanides are usually present in their trivalent state (there are some exceptions), and most of these ions are luminescent. Lanthanide ions have narrow absorption and emission bands due to electronic transitions between its well shielded f-orbitals and the emission of these ions is rather faint, but this can be increased by the antenna effect.[1] In this technique, a chromophore is used close to the lanthanide ion that absorbs energy and transfers it to the lanthanide ion which gets excited into its emissive state.[60] Ce^{3+}, Eu^{2+}, Sm^{2+} and Yb^{2+} have broader peaks in their spectra because of electronic transitions between the f-orbitals and the d-orbitals of the ion.[1]

1.4.1 *Working of fluorescent lamps*

The lamps of interest in this master thesis are the tubular fluorescent lamp and the compact fluorescent lamp (CFL). Both consist of a long glass tube, folded for the CFL, which contains a small amount of mercury vapor (at a partial pressure of about 1 Pa) in an inert gas (a noble gas like neon, argon, krypton or xenon at a pressure of about 400 Pa). The ends of the tube are sealed and contain a coiled tungsten electrode coated with a metal oxide, and the inside of the glass tube is lined with phosphors. The cathode emits electrons which are accelerated by the electric field between the electrodes and ionize the gas inside the tube, forming a plasma. To start the discharge of the gas, a higher voltage is needed than when the light is already on, and a starter or ignitor is used to achieve this. The mercury atoms are excited in the plasma and they emit radiation when falling back to the ground state. The most frequent transitions are those from two excited states (the 6 $^1P_1$ and 6 $^3P_1$ states) to the ground state (6 $^1S_0$), emitting UV radiation with wavelengths of 185.0 and 253.7 nm respectively. Around 66 % of the power input of a fluorescent lamp is turned into radiation this way (62.5 % is UV radiation, the remaining 3.5 % is radiation in the visible spectrum). The phosphors absorb this UV radiation and emit it at lower wavelengths. A large part of the UV radiation is lost, only 24.5 % of the total power input of the lamp is turned into visible light via the phosphors. Together with the 3.5 % of the power turned into visible light by the mercury vapor itself results in an efficiency of 28 %.[61] A schematic of the working is given in Figure 4.

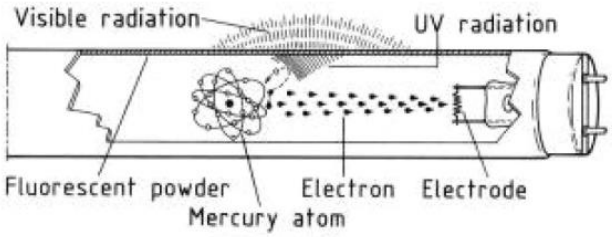

Figure 4: Working of a fluorescent lamp. Note that the mercury atom and the electrons are not to scale.[61]

Between the phosphor layer and the glass there is a layer of alumina (Al_2O_3) and silica (SiO_2) to protect the glass from attack of the mercury (which would cause a loss of mercury and a reduction of the light output of the lamp) and to reflect back UV-light that was not absorbed by the phosphors.[62] This layer is added just for the purpose of improving the efficiency of the lamp and not to prevent the UV-light from leaking out the lamp as the glass tube is composed of soda lime glass with a composition (mainly iron) that absorbs all radiation with a wavelength below 300 nm.[61] This refractive layer is *not* shown in Figure 4.

This lamp powder is made up of REE phosphors: the red phosphor $Y_2O_3:Eu^{3+}$ (YOX); the green phosphors $LaPO_4:Ce^{3+},Tb^{3+}$ (LAP) and $(Ce,Tb)MgAl_{11}O_{19}$ (CAT); and the blue phosphor $BaMgAl_{10}O_{17}:Eu^{2+}$ (BAM). In addition, there is the white halophosphate phosphor $Ca_{10}(PO_4)_6(F,Cl)_2:Sb^{3+},Mn^{2+}$ (HALO), which does not contain any REEs. The lamp phosphors, especially those containing the REEs, are the materials considered in this project, and they are discussed individually below.

1.4.2 *YOX*

The red YOX phosphor consists of yttrium oxide doped with trivalent europium, with the chemical formula $Y_2O_3:Eu^{3+}$. The concentration of europium in the lamp phosphor is usually around 3 mol%. It is the Eu^{3+} ion that is responsible for the strong red emission at a wavelength of 611.5 nm. Adding small amounts of terbium to the phosphor enhances the fluorescence of the phosphor, and causes the host lattice to absorb UV radiation better. The YOX phosphor is also capable of being excited by electrons instead of UV light, so it was used as a red phosphor in cathode ray tubes as well.[58]

Unfortunately, the phosphor does not absorb the UV light emitted by mercury very well, leading to YOX being used in larger amounts than the blue and green phosphors.[2] See Figure 25 in Appendix 1 for the emission spectrum of the red YOX phosphor.

1.4.3 *HALO*

"HALO" is short for halophosphate, which is a doubly activated phosphor. HALO crystallizes in the apatite structure with the chemical structure $Ca_{10}(PO_4)_6(F,Cl)_2:Sb^{3+},Mn^{2+}$,[58] although $(Sr,Ca)_{10}(PO_4)_6(F,Cl)_2:Sb^{3+},Mn^{2+}$ is also reported.[55] Both Sb^{3+} and Mn^{2+} are responsible for the emission of the phosphor; part of the excited antimony ions emits blue radiation while the other part transfers its energy to manganese, which emits orange-yellow radiation. This is because, contrarily to antimony, manganese is not capable of absorbing UV light. By varying the amounts of antimony and manganese, the emitted radiation of both elements combines into white light with varying color temperature.[58] Both elements replace calcium ions in the crystal structure, but no explanation is given for an excess of positive charge in the phosphor caused by replacing Ca^{2+} ions with Sb^{3+} ions. The addition of chloride shifts the emission of manganese to a longer wavelength.[63] The phosphor is deficient in the red color, even if chloride is present, so usually another phosphor is added to make up for this. See Figure 26 in Appendix 1 for a spectrum of the white HALO phosphor.[64] HALO often makes up the largest part of the phosphors present in fluorescent lamps, taking up more mass than the other phosphors combined. It does not contain any REEs and has thus a low economical value.[55]

HALO is produced by firing either high-purity $Ca_2P_2O_7$, $Ca_3(PO_4)_2$ or $CaHPO_4$ (there are different options depending on the source) with $CaCO_3$, CaF_2, NH_4Cl, $MnCO_3$ and Sb_2O_3 at 1150 – 1200 °C. This is done under a reducing atmosphere to prevent the oxidation of Mn^{2+} and Sb^{3+} and in a covered crucible to prevent the evaporation of Sb_2O_3.[58,64] Using NH_4Cl has the drawback that it releases gas when fired. It can be replaced with either $CaCl_2$, or $SrCl_2$. The latter is preferred as $CaCl_2$ tends to liquify, and the presence of strontium does not alter the properties of the final HALO phosphor significantly.[64]

1.4.4 *BAM*

The name BAM stands for "barium magnesium aluminate" and has the chemical formula $BaMg_2Al_{16}O_{27}:Eu^{2+}$ or $BaMgAl_{10}O_{17}:Eu^{2+}$, depending from source to source[55,58,65]. It is produced by firing Al_2O_3, $BaCO_3$, $MgCO_3$ and Eu_2O_3 in a slightly reducing atmosphere in the presence

of a flux at 1100-1200 °C.[58] The reducing atmosphere (e.g. a mixture of H_2-gas and N_2-gas) is used to bring europium from the 3+ state to the 2+ state as Eu^{2+} only exist under limiting conditions.[65] As with other oxygen-dominant phosphors BAM has a good temperature stability.[58] The europium ions are mostly found in two different positions in the $BaMgAl_{10}O_{17}$-crystal: either replacing barium ions or in interstitial positions. The Eu^{2+} ions are responsible for the blue emission of the phosphor with a maximum emission wavelength around 450 nm[58,65]. The structure of the phosphor and some emission spectra can be seen in Figure 27a and Figure 27b respectively in Appendix 1, notice how the spectrum has broad peaks since Eu^{2+} emits via an electronic transition between an f- and a d-orbital.[1]

1.4.5 *LAP*

The green LAP phosphor consists of $LaPO_4:Ce^{3+},Tb^{3+}$ and gets its name from the first three letters of the chemical formula. LAP has an emission maximum at 544 nm, an absorption maximum at 290 nm and a high quantum yield.[58] Commercial LAP phosphor consists of around 60 % lanthanum phosphate, 27 % cerium phosphate and 13 % terbium phosphate.[2] LAP is similar to the HALO phosphor in the way that only cerium is responsible for absorbing the UV light. It emits part of its energy itself and passes part of its energy along to terbium which then emits it. Terbium itself is not able to efficiently absorb UV light of 254 nm emitted by mercury, see Figure 28a in Appendix 1.[59] An emission spectrum of the LAP phosphor is also given in Figure 28b. There are two ways of making this phosphor, the first is firing La_2O_3, Tb_4O_7, $NH_4H_2PO_4$ and CeO_2 or CeF_2 at 1000 – 1250 °C under a reducing atmosphere.[58] The second option is more simple and consists of mixing the pure nitrate or chloride solutions from the hydrometallurgical separation process of the REEs together and then precipitating them using phosphoric acid and ammonium hydroxide, see Equation 1.

$$REE(Cl,NO_3)_{3,aq} + H_3PO_{4,aq} + 3\ NH_{3,aq} \rightarrow REE(PO_4)_s + 3\ NH_4(Cl,NO_3)_{aq} \qquad (1)$$

REE stands for the elements La, Ce and Tb. The precipitate is filtered and heated to improve the structure and morphology.[48]

The LAP phosphor, and REE phosphates in general, are very hard to dissolve due to its monoclinic lattice structure, similar to monazite. The monoclinic lattice structure causes a high chemical stability and thus a lot of energy is needed to break it.[66]

1.4.6 *CAT*

CAT is, like LAP, a green phosphor with the composition $Ce_{0.65}Tb_{0.35}MgAl_{11}O_{19}$. This cerium magnesium aluminate has a maximum emission wavelength of 541 nm and a very high quantum yield (65 %) due to the energy transfer from Ce^{3+} to Tb^{3+}, which then emits the radiation. The phosphor is made either by coprecipitation of the metal hydroxides from aqueous solution using ammonia and firing the precipitate at 700 °C for 2 hours and another hour at 1500 °C, or by firing a mixture of $MgCO_3$, CeO_2 and Tb_4O_7 for five hours at 1500 °C with small amounts of MgF_2 or AlF_3 as crystallizing agents. The firing in both cases should be done under a strongly reducing atmosphere to ensure that both cerium and terbium are present in the trivalent state.[58] A very similar phosphor is $CeMgAl_{10}O_{17}:Tb^{3+}$.[67]

The CAT phosphor has been mostly replaced by the LAP phosphor. There is another green phosphor which contains the REE gadolinium, $GdMgB_5O_{10}:Ce^{3+},Tb^{3+}$, but this one is used even less.[2]

1.5 Existing recycling techniques lamp phosphors

End-of-life (EoL) compact fluorescent lamps (CFLs) and fluorescent tubes are collected and separated in different fractions: (1) glass, to be used in the production of other glass products, (2) metals from the filaments and electrodes, which are generally sent to metal recycling facilities, (3) plastic parts, which are burnt for energy recovery, (4) phosphors powder, and (5) mercury. It is expected that by 2020 the stockpiled lamp powder waste will contain around 25,000 tonnes of REEs. The approximate composition of the lamp phosphor waste is shown in Figure 5.[39]

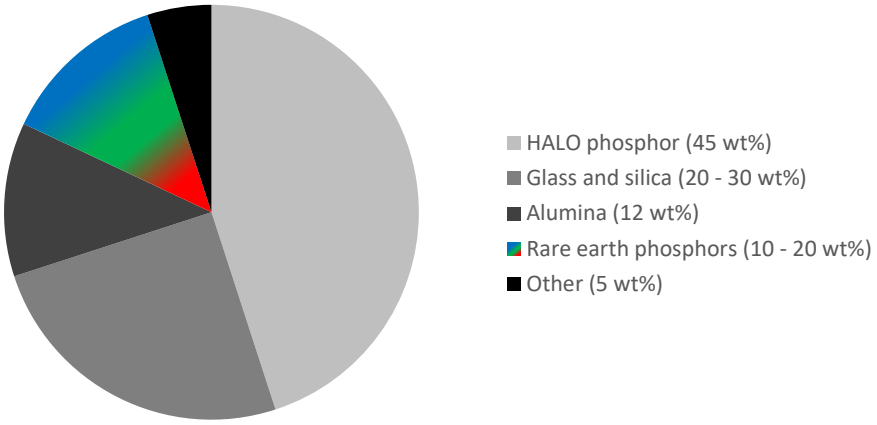

Figure 5: Composition of the lamp phosphor waste after crushing and sieving the lamps. The glass fraction can be as large as 50 wt% if the lamps are crushed to remove the phosphor powder.[62]

First, the fluorescent tubes can have their phosphors blown out after opening the lamp at both sides under reduced pressure to remove the mercury vapor.[62] The lamps that are not straight like the CFLs or special fluorescent tubes are usually crushed under reduced atmosphere to capture the mercury. The aluminium end caps and the larger glass particles are removed from the lamp phosphors and smaller glass particles by using a sieve[62] or a cyclone separator.[68] The aluminium end caps and the glass particles are usually recycled. The lamp phosphors usually contain mercury as well, ranging from half to nearly 90 % of the total amount of mercury vapor initially present.[69]

One technique to remove the mercury present in the lamp phosphors is to heat the phosphors above the boiling point of mercury (357 °C) for several hours so the mercury evaporates. The mercury is then condensed, ready to be used again.[68]

A study has been performed to stabilize and remove the volatile elemental mercury present in lamp phosphor waste by oxidizing the elemental mercury using hypochlorite (ClO^-) in aqueous solutions to form less volatile and more soluble compounds, the proposed reaction is given in Equation 2.[67]

$$ClO^- + Hg^0 + 2\,H^+ \rightarrow Cl^- + Hg^{2+} + H_2O \quad (2)$$

Although protons are needed for the reaction, the reaction does not need to be carried out under (very) acidic conditions as the protons can originate from the autoprotolysis of water. The oxidation reaches an optimum at pH values between 6.5 and 6.9. It was seen that this treatment does not alter the structure of the lamp phosphors.[67]

Leaching the formed mercury compounds is possible with acids, but under the needed circumstances, almost all of the red YOX phosphor and part of the green LAP phosphor are also leached. Also, not all of the mercury is leached, the best result is a leaching efficiency of around 90 % when using 4 M HCl. Either an incomplete oxidation forming low soluble mercury complexes or a strong adsorption to the glass powder or the phosphor powder in the waste is probably what causes the yield to not be 100 %.[67]

There are a few techniques already that recycle lamp phosphors on a large scale. There is the HydroWEEE project that focusses on yttrium (see further),[70] and Solvay[9] and OSRAM (owned by Siemens)[62] are also each running a process. The Belgian waste-processing company named Indaver is working together with Philips Lighting and developed a process to directly re-use the phosphors from EoL lamps manufactured by Philips for new lamps.[9]

Apart from techniques to recycle mercury[62,68] and the HydroWEEE process, all the techniques discussed here to recycle the lamp phosphors are only performed on laboratory scale. The phosphors can be recycled in different ways with varying complexities, the phosphors can be either directly re-used, separated physically without changing the substances themselves, or leached from the waste with varying selectivity. The latter is discussed in its own chapter as it has received more attention.

1.5.1 *Direct re-use of phosphor mixtures*

Although it is perfectly possible to re-use the phosphors after getting rid of the mercury, plastic, metal and glass parts of the lamps, this is usually not done. There are different reasons for this, even though it would be straightforward and would hardly consume any chemicals. First of all, different lamps use different blends of phosphors, so powders collected from one type cannot be used for another. Re-using the phosphors results in an inferior end-product, which is not interesting for lamp manufacturers, and the phosphors deteriorate because of the harsh conditions they are used in (high-energy gas molecules and ions, high energy UV-light and a slow uptake of mercury). Getting only the phosphors out of the lamp is not always that easy either, linear lamps can have the phosphors blown out, but they are contaminated with the alumina binder material. Nonlinear lamps need to be crushed however, and this introduces a lot of fine glass particles to the phosphor which is very hard to remove again, taking up to half of the weight of the sieved fraction.[62]

1.5.2 *Physical separation techniques*

Several methods have been developed to physically separate the phosphors from each other based on their different properties, these methods include froth flotation making use of the

different zeta potentials, pneumatic separation (using either Earth's natural gravity or a centrifuge) relying on the density of the phosphors and dividing the phosphors between two phases depending on their zeta potential.

For instance, the different phosphors have a different zeta-potential depending on the pH, and this can be used to separate them with froth flotation. This is done by adding a "collector", a charged molecule that binds to certain particles depending on their charge. When gas is bubbled through the solution, these collectors cause the formation of a froth (or foam) containing these particles on top of the solution. The foam can then be scraped off and the particles that the collector does not interact with stay behind in the bulk of the solution.[71] Using dodecyl ammonium acetate as collector in an aqueous 10^{-3} M NaCl solution at pH 2.5 can collect 70 % of the white HALO phosphor in the froth while 82 % of the red YOX phosphor and 90 % of the green LAP phosphor stay behind in the solution.[71]

A different technique separates the phosphors pneumatically from the rest of the fine material.[72] Pneumatic separation relies on the settling speeds of spherical particles under gravity in a fluid according to a simplified Stokes' law in Equation 3.[73]

$$v = k_1 d^2 (\rho_s - \rho_f) \quad (3)$$

v is the terminal velocity of the spherical particles, k_1 a constant, d the diameter of the spherical particles, ρ_s the density of the particles and ρ_f the density of the used fluid.[73] The characteristics of the investigated phosphors can be found in Table 2.

Table 2: Densities and mean particle sizes of phosphors from the SPD series of the Toshiba brand.[73]

Phosphor type	Trade name	Formula	Density (g/cm^3)	Median size (µm)
White HALO	SPD-1457HD	$Ca_{10}(PO_4)_6(F,Cl)_2:Sb^{3+},Mn^{3+}$	3.07	13.42
Red YOX	SPD-867JA	$Y_2O_3:Eu^{3+}$	5.12	4.72
Green LAP	SPD-834N	$La(P,B)O_4:Ce^{3+},Tb^{3+}$	5.23	3.72
Blue	SPD-801EJ	$(Sr,Ca,Ba)_{10}(PO_4)_6Cl_2:Eu^{2+}$	4.34	5.18

The HALO phosphor, which does not contain any REEs, can be separated from the other phosphors by using a liquid with a density between 3.07 and 4.34 g/cm^3. Di-iodomethane has a density of 3.3 g/cm^3 (which lies in this density range)[73] and can thus be used to separate the floating HALO phosphor from the sinking rare-earth phosphors. Unfortunately, the relevant phosphors can be enriched in REEs four to five times with a yield of only 2 to 2.5 %. The problems are likely the surface texture and absorptivity and that the density and viscosity of the di-iodomethane rises when phosphors particles are present.[72]

The phosphors containing REE can also be separated using air as medium, and with this technique, the REE content could be increased from 13.3 % to 29.3 % with a yield of only 32.9 %. The phosphors were not reused, but the yttrium and europium were leached instead via the more traditional way of leaching with acids or sodium hydroxide and recovered by precipitating yttrium and europium as an oxalate.[72]

From the simplified Stokes' law in Equation 3 it can be seen that the diameter is more important for the settling speeds than the difference in density, and small, dense particles can settle at the same velocity as larger, less dense particles. This could be the reason why the results are

not very useful in reality.[73] An improvement to the technique using di-iodomethane is using a centrifuge to generate accelerations bigger than Earth's natural gravity to separate HALO from the other phosphors. The full Stokes law is given in Equation 4.

$$v = \frac{d^2 (\rho_s - \rho_f) G}{18 \eta} \quad (4)$$

G is the centrifugal acceleration (depends on the angular velocity and the distance between the particle and the axis of rotation) and η the viscosity of the medium. By using a centrifuge, settling times are reduced.[73] Using a centrifuge to separate the phosphors in di-iodomethane gives better results than letting gravity do its work, but the results are still not that useful. At optimal conditions, the yield is 24 %, the grade of REE phosphors in the sink material is 36 %, and 79 % of the material can be recovered. The sink material still contains a high amount of HALO because the particles aggregate, which causes some negative effects on the separation. To counter this, the surfactant sodium oleate was added (the sodium salt of cis-9-octadecenoic acid), which adsorbs on the surface of the particles and helps the particles to disperse in the di-iodomethane. The best results were obtained when the amount of sodium oleate was around the amount needed to completely fill the particles' surface without forming a second layer of surfactants around it. The sinking fraction now contains 49 % of the REE phosphors with a recovery of 97 %, and more than 90 % of the white HALO phosphor was recovered in the floating fraction. Although this result is a lot better, the different phosphors are still not separated completely from each other. The used di-iodomethane, which contains acetone from washing the filtered fractions, can be regenerated for more than 99.8 % by evaporation of the acetone under reduced pressure.[73]

Another technique to separate certain phosphors from each other also uses the difference in zeta potentials between the phosphors to divide them between a polar/aqueous phase and an apolar/organic phase. This technique was used on either a synthetic mixture of the red YOX phosphor, the blue $(Sr,Ca,Ba)_{10}(PO_4)_6Cl_2:Eu^{2+}$ phosphor and the green LAP phosphor[74] or a mixture of the red YOX phosphor, the blue BAM phosphor and the green $CeMgAl_{10}O_{17}:Tb^{3+}$ phosphor.[75] Each blend has two separation steps to separate the phosphors, and all phosphors were new.

In the case of the YOX /$(Sr,Ca,Ba)_{10}(PO_4)_6Cl_2:Eu^{2+}$/LAP mixture in a 1:1:1 ratio, the green LAP phosphor is extracted first from a polar dimethylformamide (DMF) phase to the apolar heptane phase using stearylamine (dodecylamine) as a surfactant. The other two stay behind in the DMF phase. After separating, filtering and washing the phases, the blue $(Sr,Ca,Ba)_{10}(PO_4)_6Cl_2:Eu^{2+}$ phosphor is extracted from the DMF phase to the heptane phase using 1-octanesulfonic acid as surfactant. The phases are then again separated and the phosphors filtrated. Under the most ideal conditions, the phosphors have purities and recoveries above 90 %: YOX has a grade and a recovery of 95.3 % and 90.9 %, respectively, $(Sr,Ca,Ba)_{10}(PO_4)_6Cl_2:Eu^{2+}$ 90.0 % and 95.2 %, and LAP 92.2 % and 91.8 %, respectively.[74]

In the case of the YOX/BAM/$CeMgAl_{10}O_{17}:Tb^{3+}$ phosphor in a 1:1:1 mixture, the blue BAM phosphor can be extracted to heptane containing 2-thenoyltrifluoroacetone while the red YOX phosphor and the green phosphor stay in the aqueous phase containing potassium sodium tartrate and sodium carbonate (used to regulate the pH). In the second separation, the green phosphor can be extracted to an apolar chloroform phase containing some 1-pentanol phase while YOX stays behind in the aqueous phase. Under the most ideal circumstances, the grades

and recoveries of the three phosphors are all above 80 %. The red YOX phosphor has a grade and recovery of 96.9 % and 95.2 % respectively, the blue BAM phosphor 82.7 % and 98.8 %, and the green $CeMgAl_{10}O_{17}:Tb^{3+}$ phosphor 94.6 % and 82.6 % respectively.[75]

The technique to separate the three phosphors in the YOX /$(Sr,Ca,Ba)_{10}(PO_4)_6Cl_2:Eu^{2+}$/LAP mixture from each other has been applied on real waste phosphor sludge containing only these three phosphors. The sludge was analyzed and contained approximately 40.9 % YOX, 19.1 % $(Sr,Ca,Ba)_{10}(PO_4)_6Cl_2:Eu^{2+}$ and 40.0 % LAP, and some traces of mercury and Al_2O_3 binder material. Because of coagulation of the phosphor particles, the sludge was milled, but it was not possible to extract the blue phosphor, and separating the red and green phosphor had much lower rates than compared to the artificial blend.[76] Pretreating the phosphor sludge first with a nitric acid solution of pH 2 for 5 minutes and then a sodium hydroxide solution of pH 12.5 for 12 minutes to remove the remaining Al_2O_3 binder material gives better results, although a significant amount of strontium from the blue phosphor dissolved during this pretreatment step. In the end, the red YOX phosphor had a grade and recovery of 86.0 % and 80.3 % respectively, the blue $(Sr,Ca,Ba)_{10}(PO_4)_6Cl_2:Eu^{2+}$ phosphor 74.8 % and 95.6 % and the green LAP phosphor 81.2 % and 79.5 % respectively. The grades and recoveries are a bit lower than with the mixture of unused phosphors, but they are still useable, as the recovered phosphors emit the right colors under UV radiation. Unfortunately, this research has not been applied to phosphor mixes containing the white HALO phosphor which is also commonly used in lamps.[76]

1.6 Selective leaching of the different phosphors

The lamp phosphors have different types of structures (oxides, phosphates, aluminates), and can be leached rather selectively using the right conditions. The YOX and HALO phosphors are very easy to dissolve in acid, with HALO leaching at room temperature while YOX needs some mild heating. Leaching HALO increases the acid consumption. The CAT, BAM and LAP phosphors are much harder to dissolve; LAP needs more heating to dissolve, and BAM and CAT are usually treated using alkali fusion with hydroxides at 800 °C followed by acid leaching to dissolve them. Leaching the phosphors in different steps has the advantage of obtaining more pure fractions and reduces unwanted anionic species in the different PLS's.[47]

Several options to leach the different phosphors, some more selective than the other, are discussed in the following sections. Another section discusses the HydroWEEE project, a project on a more industrial scale which partly focuses on recovering yttrium present in the YOX phosphor from lamp phosphor waste. The two REE recovery techniques that this master thesis builds further on are discussed more in depth in their own section. The one to recover the YOX phosphor uses an ionic liquid (IL).

1.6.1 *Leaching of HALO*

The white HALO phosphor can be leached using either HCl and HNO_3 at room temperature. Leaching 10 – 15 minutes with 1 M HNO_3 at room temperature leaches 80 – 90 % of the calcium and 2 – 3 % of the yttrium and europium from the YOX phosphor. The loss of YOX

phosphor is increased almost twofold when the phosphors have been thermally pre-treated to remove mercury as the heat breaks the phosphor aggregates and cracks the particles which increases the total surface area and enhances its leaching.[47] Using a 2 M HCl solution can leach almost 95 % of the calcium from the HALO phosphor in five minutes at room temperature, but the YOX phosphor co-dissolves again, 4.2 % for yttrium and 6.6 % for europium.[77]

The presence of HALO can be a serious problem as it easily dissolves when leaching the YOX phosphor and consumes a lot of acid when doing so. The released phosphoric acid then combines with the dissolved yttrium and europium to form insoluble YPO_4 and $EuPO_4$, lowering the extraction efficiencies of the YOX phosphor.[55]

1.6.2 *Leaching of YOX*

The red YOX phosphor is quite easy to leach using dilute acids. Possible acids are HCl, HNO_3 and acetic acid. The leaching reaction of YOX is given in Equation 5.

$$(Y,Eu)_2O_3 + 6\ H^+ \rightarrow 2\ (Y,Eu)^{3+} + 3\ H_2O \qquad (5)$$

Both HNO_3 and HCl (0.5 M) can leach 90 % of YOX from real phosphor waste at room temperature in 7 days. Under the same conditions 10 % of the LAP is also leached. Higher acid concentrations generally result in better leaching efficiencies, but cerium and terbium are leached preferentially over lanthanum in the LAP phosphor, as lanthanum for example has the lowest leaching efficiency of around 10 % at acid concentrations of 4 M nitric acid after 7 days while cerium and terbium both have a leaching efficiency of around 50 % under the same conditions.[67]

Acetic acid is more selective for YOX compared to the other phosphors, but the leaching efficiency is also lower (75 % for yttrium and 50 % for europium). Nevertheless, traditional acids are not selective enough to leach only the red YOX phosphor. Also traces of mercury in the lamp phosphor waste are leached. Increasing the solid-to-liquid ratio suppresses the leaching of all REEs, so it is not possible to increase the selectivity for some REEs over the others in this way.[67]

Research published in 2008 claims to have found a way to leach the red YOX phosphor from phosphor waste, remove calcium from the HALO phosphor and separate the yttrium and europium from each other. The phosphor waste is leached with a 4 M mixture of sulfuric acid and nitric acid (the exact composition is not given) at 125 °C under a pressure of 5 MPa for 8 hours. 92.8 % of the europium and 96.4 % of the yttrium is leached, and are in the form of sulfate salts. It is suggested, but not performed, to remove the leached calcium from the HALO phosphor via precipitation with oxalic acid.[78] This step might not be performed since the REEs would also precipitate as their oxalates are not very soluble either.[79] These REE sulfate salts are then converted to thiocyanate salts using potassium thiocyanate and they are extracted to methyl ethyl ketone containing trimethyl-benzylammonium chloride in an unknown concentration with a phase ratio of 2 mol solvent per mol water. Yttrium and europium are stripped using an aqueous solution containing 1 M nitric acid and an unknown concentration of *N*-tributyl phosphate. The formed nitrate salts of europium and yttrium are then separated using ethyl alcohol as europium nitrate does not dissolve in ethyl alcohol while yttrium nitrate

does. The separated salts are reduced thermally using hydrogen gas to their metallic state. An economical study shows that this would be profitable. All of the steps have very high yields, but the final yield and recovery is not reported.[78]

1.6.3 *HydroWEEE process*

The HydroWEEE process investigates ways to extract valuable metals via hydrometallurgy from waste electrical and electronic equipment. In this process, the attention is given to the yttrium recovery from lamp phosphor waste, and the rest of the REEs are not targeted. The project also included recycling metals present in cathode ray tubes, spent lithium-ion batteries, printed circuit boards and liquid crystal displays.[80]

Optimal lab-scale leaching conditions were found to be a solid-to-liquid ratio of 20 g/mL, a sulfuric acid concentration of 2 M and a temperature of 90 °C. The leaching efficiency of yttrium is around 85 %, and that of calcium, which is also present in the waste in large amounts, below 10 %. The pregnant leach solution is cooled to precipitate most of the co-dissolved calcium as sulfate, and the yttrium is precipitated with a stoichiometric amount of oxalic acid. The obtained yttrium oxalate has a purity ranging between 90 and 95 wt%, containing approximately 80 % of the total amount of yttrium present in the pregnant leach solution.[81]

Simulations show that 7 tons of yttrium oxalate could be produced by processing 1000 tons of fluorescent lamps a year.[81] Although the yttrium precipitation is not pure enough to be suitable for direct commercialization, which needs at least a purity of 99 %, it can be sold to companies as a feed for final purification.[70]

1.6.4 *Recycling of YOX with the ionic liquid [Hbet][Tf_2N]*

Since the red YOX phosphor is simply a mixture of the oxides of yttrium and europium while other lamp phosphors are either not oxides or are aluminates, makes the ionic liquid [Hbet][Tf_2N] a possible interesting lixiviant which can selectively dissolve the YOX phosphor from lamp phosphor waste. Silicon oxides are normally not leached either, making glass particles present in the lamp phosphor waste not a problem. A study has been performed on the solubility of several lamp phosphors in [Hbet][Tf_2N].[55]

When adding ionic liquid to a mixture consisting of equal weights of the four phosphors YOX, LAP, BAM and HALO, the ionic liquid is not capable of dissolving any blue BAM phosphor or green LAP phosphor from a mixture, and only dissolves a small amount of white HALO phosphor. The red YOX phosphor is leached rather easily under the right circumstances. The reason for this is that the ionic liquid is not able to efficiently solvate the anions (phosphates) from the HALO and LAP phosphors, while the oxide anions of the yttrium and europium oxide are turned into water using the protons of the acid groups of the betaine cations. The dissolution of the YOX phosphor is given in Equation 6 and the formed complex is shown in Figure 6.[55]

$$M_2O_3 + 6\ R^+COOH + 6\ Tf_2N^- \rightarrow 2\ [(RCOO)_3M]^{3+} + 6\ Tf_2N^- + 6\ H_2O \qquad (6)$$

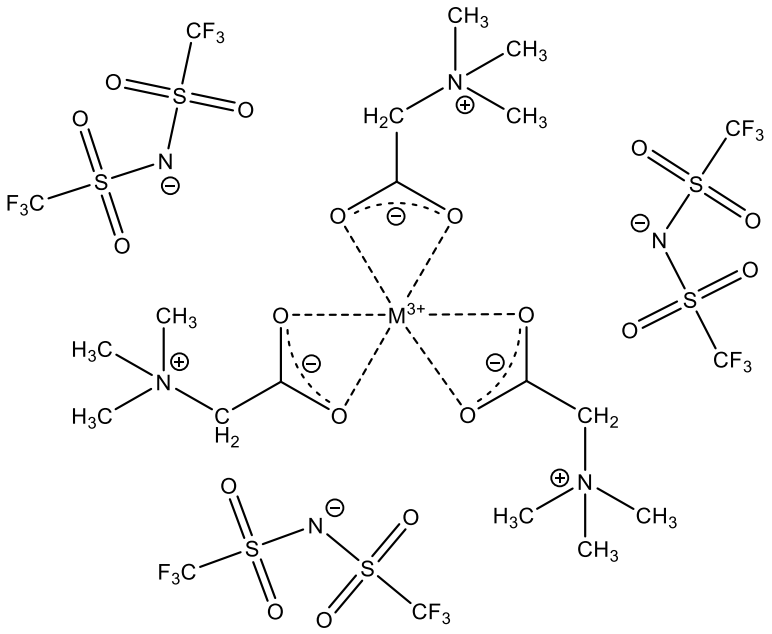

Figure 6: The complex between the trivalent metal cation (yttrium or europium) and three deprotonated betaine molecules along with an equal amount of Tf_2N^- anions to neutralize the charge.

Leaching at 90 °C with ionic liquid containing 5 wt% of water can dissolve up to 40 mg of YOX per g of ionic liquid in 40 hours. A higher solid-to-liquid ratio results in incomplete leaching, even when leaching for longer times. There should be some water present in the ionic liquid as it greatly improves the kinetics of the dissolution reaction. It is thought that this is caused by a lower viscosity and a faster diffusion of protons in the ionic liquid due to the presence of water. Water contents higher than 5 wt% causes more HALO to dissolve and is unwanted. Leaching at lower temperatures also lowers the kinetics severely. This is most likely caused again by the viscosity of the ionic liquid which decreases at higher temperatures, improving the diffusion. At this temperature, less than 0.01 % of the ionic liquid degrades after 24 hours.[55]

To strip the yttrium and europium again from the ionic liquid, a stoichiometric amount of solid oxalic acid is used to precipitate the metal ions as oxalates, regenerating the ionic liquid in the process. The obtained yttrium and europium oxalates can be calcined in an oven at 950 °C for 5 hours to their respective oxides, resulting in a mixed oxide which is basically the YOX phosphor. The luminescence properties of the recycled YOX is equal to that of the starting product as well (see Figure 25 in Appendix 1), making the product useable for making new lamps, which makes this stripping technique the most interesting to use. The research has been performed on mixtures of phosphors, but not in the ratios they appear in phosphor waste.[55] An overview of the whole process is given in Figure 7.

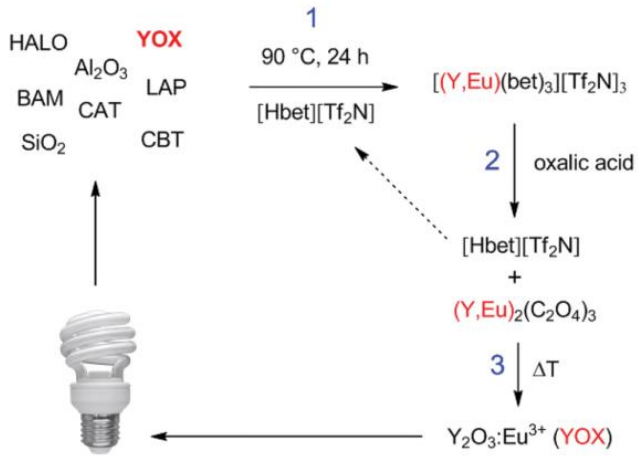

Figure 7: The complete process of (1) leaching the red YOX phosphors from lamp phosphor waste using the ionic liquid [Hbet][Tf_2N], (2) stripping the yttrium and europium with oxalic acid and regenerating the ionic liquid and (3) calcining the precipitate to form new YOX phosphor which can be used to manufacture new lamps.[55]

1.6.5 *Leaching of LAP*

Trying to leach the LAP phosphor with moderately concentrated acids (4 M HNO_3 or HCl) at room temperature does not work as only 0.9 % of the REEs in the phosphor are leached. However, milling the phosphor before the leaching steps greatly enhances the leaching yield of the phosphor with values up to 81 %. This result was obtained by using 1 mm grinding balls and rotating at 600 rpm before leaching the milled phosphor for 4 hours with 4 M HNO_3. During the milling, defects are introduced into the crystal structure by the impact of the grinding process,[77] and the material becomes polycrystalline, increasing the amount of grain boundaries with defects in them and facilitating the leaching.[66] The process was proven to be diffusion-controlled according to its activation energy.[77]

When this technique is used on real phosphor waste, first 95 % of the HALO phosphor is removed by leaching with 2 M HCl for only 5 minutes at room temperature, and almost all of the yttrium and more than 90 % of the europium in the YOX phosphor is then removed using 2 M HCl at a temperature of 70 °C after an hour. The loss of lanthanum, cerium and terbium from the LAP phosphor during these two steps is approximately 1 %. The residue is then milled and leached with 4 M HCl at room temperature for two hours. The LAP phosphor is now leached with an even better yield with 99.0 % for lanthanum, 87.3 % for cerium and 86.3 % for terbium compared to pure LAP phosphor. The reason for this is the presence of glass particles coming from the lamps itself acting as a fine grinding medium, increasing the defects in the LAP phosphor particles and improving the leaching rate. While all the yttrium and lanthanum are removed, some traces of europium (4 %), cerium (12 %) and terbium (13 %) remain in the residue after the third leaching step. These small amounts are likely caused by the low-soluble CAT and BAM phosphors left in the residue which contain these three elements.[77]

To exploit all the crystal defects as optimal as possible, it is possible to leach *during* the milling stage instead of *after* the milling. This constantly reveals fresh, undisturbed surface that was previously unreachable for mechanical activation and therefore harder to leach. Sulfuric acid can leach close to 100 % of the LAP phosphor.[66] This technique can recover up to 98 % of the REEs present in the LAP phosphor using low amounts of H_2SO_4 at room temperature. Although

milling is more energy efficient than leaching at high temperatures or alkali fusion,[77] milling still needs quite some energy to break the chemical bonds.[66]

In alkali fusion the phosphors are pre-treated with an alkaline substance (KOH, $Ba(OH)_2$, NaOH, Na_2CO_3) at high temperatures (800 °C onwards) to turn the phosphates into oxides, see Equation 7, with Ln standing for the lanthanides lanthanum, cerium and terbium.[82–85] During this step, mercury present in the phosphors is evaporated, reducing the hazards of the waste.[82] The oxides are then leached using an acid, the calcium from the HALO phosphor is precipitated as a sulfate and the REEs are precipitated using oxalic acid and are then calcinated to their oxides. If the YOX phosphor isn't removed first, all the REEs are leached together and the end product is a mixed oxide of all the REEs.[83] If NaOH is used for the alkali fusion, alumina present in the waste is turned into $NaAlO_2$, which can be removed from the REE oxides by dissolving it in water. Up to 99.8 % of the REEs can be recovered this way.[84]

$$2\ LnPO_4 + 6\ KOH + \rightarrow Ln_2O_3 + 2\ K_3PO_4 + 3\ H_2O \qquad (7)$$

1.6.6 *Recycling LAP with methanesulfonic acid*

Very recent research has now shown that the LAP phosphor can be leached using concentrated methanesulfonic acid (MSA, CH_3SO_3H).[86] The MSA must be heated to 200 °C to leach LAP completely after approximately forty minutes. Lowering the temperature to 160 °C needs three hours and a half to fully leach the LAP phosphor. The dissolution of the LAP phosphor is given in Equation 8, with Ln standing for the lanthanides lanthanum, cerium and terbium.[86]

$$LnPO_4 + 3\ CH_3SO_3H \rightarrow Ln(CH_3SO_3)_3 + H_3PO_4 \qquad (8)$$

The loaded MSA is diluted ten times in water (REE methanesulfonates are very soluble in aqueous solutions, so this causes no problems) after which terbium is extracted selectively to an organic phase consisting of 70 % di-(2-ethylhexyl)phosphoric acid (D2EHPA) in xylene. Using a three-stage cross-current extraction results in an almost complete extraction of terbium (97.5 %) while no extraction of lanthanum or cerium was observed, resulting in a solution of pure terbium.[86]

The raffinate containing lanthanum, cerium and small amounts of terbium is then diluted four more times, resulting in a dilution factor of 40 compared to the pure loaded MSA. The REEs are extracted to an organic phase consisting of pure D2EHPA extractant in three stages, resulting in an extraction percentage of 100 % for cerium and 98.8 % for lanthanum. At least part of the traces of terbium in the 40x diluted MSA are extracted as well, but no values are given. It could be that all the terbium is extracted as D2EHPA is very selective towards the heavier REEs.[86]

The metals are then stripped from the organic solutions using aqueous oxalic acid, with lanthanum and cerium being stripped more than 99.5 % and terbium only 90 %. The organic phase containing traces of terbium can be recycled to the next extraction cycle to prevent losses. The obtained oxalates can then be calcined to either pure Tb_4O_7 or a mixture of mostly Ce_2O and La_2O_3 with a trace of terbium in an oven (4 hours at 700 °C). The flowsheet of the whole process is given in Figure 8.[86]

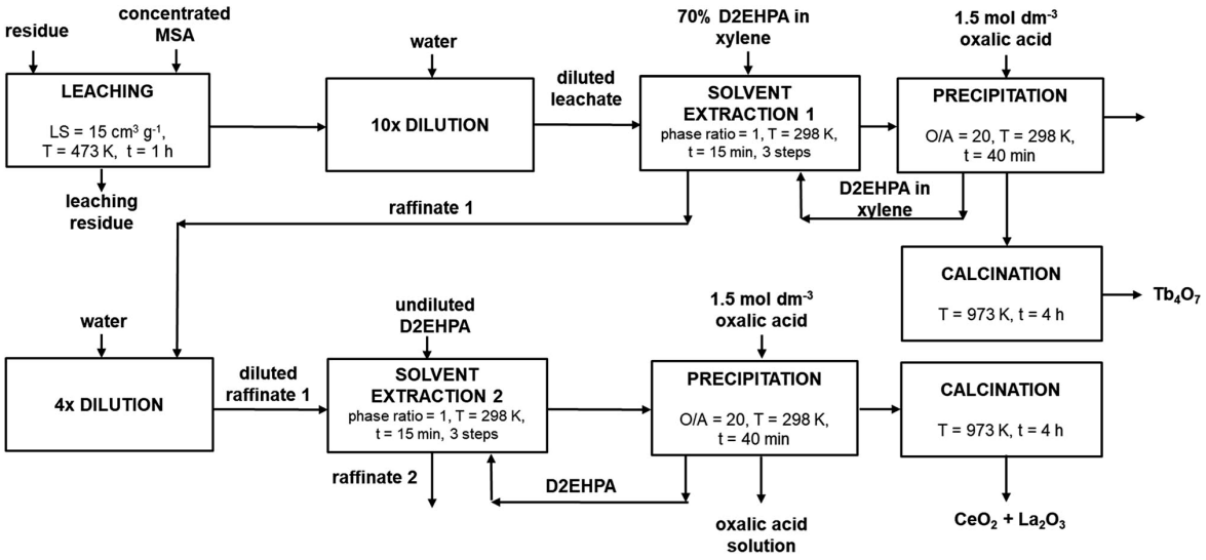

Figure 8: The flow-sheet of the process to dissolve the green LAP phosphor, split the terbium from the lanthanum and cerium and convert these elements to their oxides.[86]

This technique has been applied on real residue that was processed earlier in the HydroWEEE process, meaning that most of the yttrium and europium was already removed. Unfortunately, not all of the yttrium and europium was removed as part of these formed insoluble phosphates with the phosphate ions from the HALO phosphor. These yttrium and europium phosphates are now dissolved along with the LAP phosphor. During the leaching of this residue, most of the yttrium and a large part of the europium are leached, while not all of the terbium and cerium are leached. This is probably because the CAT and CBT phosphors also contain terbium and cerium, but these two phosphors are aluminates and borates and are not soluble in MSA. Lanthanum is only present in the LAP phosphor and not in CAT and CBT, and the lanthanum was leached almost completely, backing up this hypothesis.[86]

The final result of applying these techniques is a mixed oxide containing 76.2 wt% Y_2O_3, 13.1 wt% Tb_4O_7, 8.6 wt% Eu_2O_3, 1.8 wt% Gd_2O_3 and 0.4 wt% La_2O_3 from the terbium part of the process, and a mixed oxide containing 55.8 wt% La_2O_3, 43.8 wt% CeO_2 and 0.4 wt% Tb_4O_7 from the lanthanum/cerium part of the process.[86] If yttrium and europium were removed completely from the lamp phosphor waste it would make the mixed oxide containing terbium a lot more pure.[86]

1.6.7 *Simultaneous leaching of all REEs*

An attempt was made to leach all the REEs (the YOX and LAP phosphors) at once from lamp phosphor waste using supercritical carbon dioxide (333 K, 15 MPa) containing tri-*n*-butyl phosphate (TBP), nitric acid and water. After the leaching, the carbon dioxide was gasified, leaving behind the metal complexes. Tests on simulated wastes were very promising, but when it was repeated on real phosphor waste, only the YOX phosphor could be leached almost completely after two hours (99.7 % for yttrium and 99.8 % for europium), but the leaching efficiencies of lanthanum, cerium and terbium were below 7 %. No info was given about what happened with possible other phosphors during the experiments.[87]

Leaching with 2 M HNO_3 for several days was also tested. The leachate contained iron and mercury next to the REEs, but no leaching efficiencies were reported. The PLS was contacted with kerosene with a low aromatic content containing up to 1 M Cyanex 923 (a mix of trialkylphosphine oxides) with a phase ratio of 1, and all elements were extracted with the following extraction efficiencies: > 95 % for yttrium, europium, terbium, 85 % for cerium and 67 % for lanthanum. Iron and mercury were also extracted, but to a lower extent. The extraction of all elements can be enhanced by decreasing the concentration of nitrate in the pregnant leach solution to 0.5 M as the extraction of nitric acid by Cyanex 923 is inhibited. The loaded organic phase was stripped with aqueous solutions of nitric acid, hydrochloric acid, oxalic acid or acetic acid of varying concentrations. 4 M HCl was able to completely strip all the REEs from the organic phase while leaving all the iron and mercury in the organic phase. The remaining iron and mercury could be stripped with nitric acid, making it possible to re-use the organic phase. 0.5 M oxalic acid could completely strip iron with less than 5 % of the REEs and 12.5 % of the Hg co-stripped; therefore, oxalic acid could be used as scrubbing agent to remove iron before the stripping of the REEs.[88]

1.7 The objective of this master thesis: combining the two techniques

This master thesis builds further on the two techniques previously researched to recover REEs from (mostly pure, unused) lamp phosphors with promising results. These techniques were mentioned in their own sections: selectively leaching the YOX phosphor using the ionic liquid [Hbet][Tf_2N] and turning it back to new YOX phosphor (see section 1.6.4) and leaching the LAP phosphor with methanesulfonic acid and separating terbium from lanthanum and cerium (see section 1.6.6). Both techniques have some limitations though, recycling the YOX phosphor with the ionic liquid [Hbet][Tf_2N] has not been tested on real phosphor waste yet. Recovering terbium, lanthanum and cerium from the LAP phosphor has only been performed on HydroWEEE residue still containing traces of the YOX phosphor which heavily contaminate the pure terbium fraction, so this technique can only be used if the YOX phosphor can be removed first.

The objective of this master thesis is to integrate these two techniques into a flowsheet to recover the REEs from real phosphor waste. First the waste would be leached with [Hbet][Tf_2N] to remove YOX, then the residue would be leached with MSA to remove LAP which should not be contaminated anymore with yttrium and europium. Part of the objective is also to re-use the [Hbet][Tf_2N] as much as possible in the research. If the flowsheet using these two techniques is to be successful, they are to be scaled up to test if the flowsheet can be performed on an industrial scale. The intended flowsheet is given in Figure 9.

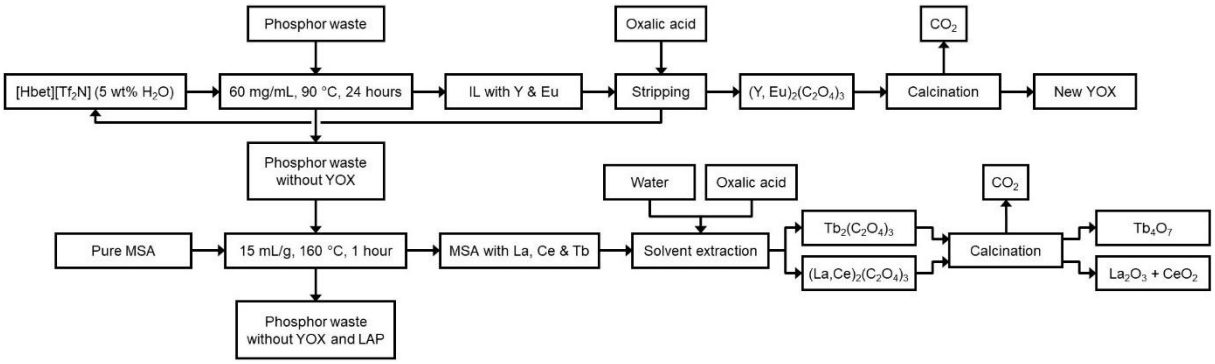

Figure 9: Intended flowsheet by integrating the two techniques.

2 Methods

2.1 Chemicals

The chemicals used in this work are listed in Table 3. All chemicals were used as received, unless otherwise stated. Milli-Q water was prepared by a Millipore Milli-Q® Reference Water Purification System, having a resistivity of 18.2 MΩ.cm at 25 °C and a TOC value < 5 ppb.

Table 3: List of all chemicals used.

Substance	**Supplier(s)**	**Purity**
Betaine hydrochloride (HbetCl)	Acros organics	99 %
Lithium bis(trifluoromethylsulfonyl)imide ($LiTf_2N$)	IOLITEC	99 %
YOX	Nichia Japan	99 %
HALO	Nichia Japan	99 %
LAP	Nichia Japan	99 %
BAM	Nichia Japan	99 %
Phosphor waste	Relight	
Nitric acid (HNO_3)	Chem-Lab	65 %
Hydrochloric acid (HCl)	VWR	37 %
Methanesulfonic acid (MSA)	Carl Roth	≥ 99.5 %
Ethanol	Fisher Chemical	Absolute
Oxalic acid (anhydrous)	J&K	99 %
Tributyl phosphate (TBP)	Chem-Lab	99 % +
Cyanex 923	Solvay	
Di-(2-ehtylhexyl)phosphoric acid (D2EHPA)	J&K or Across	95 %
N-dodecane	Merck	≥ 99.0 %
Xylene (mixture)	BDH	98 %
Silicon solution SERVA for siliconizing glass and metal (in isopropanol)	SERVA	
Deuterated DMSO with 0.03 v% TMS	Merck	99.9 %
96 – 98 % D_2SO_4 in D_2O	Merck	99.5 % D
1000 ppm Al ICP standard	Merck	
1000 ppm Ba ICP standard	Chem-Lab	
1000 ppm Ca ICP standard	Chem-Lab	
1000 ppm Ce ICP standard	Chem-Lab	
1000 ppm Cl^- ISE standard	Mettler Toledo	
1000 ppm Eu ICP standard	Chem-Lab	
1000 ppm Ga ICP standard	Merck	
1000 ppm In ICP standard	Chem-Lab	
1000 ppm La ICP standard	Chem-Lab	
1000 ppm Mg ICP standard	Merck	
1000 ppm Mn ICP standard	Chem-Lab	
1000 ppm P ICP standard	Chem-Lab	

1000 ppm PO_4^{3-} ICP standard	Chem-Lab	
1000 ppm S ICP standard	Merck	
1000 ppm Sb ICP standard	Chem-Lab	
1000 ppm Si ICP standard	Merck, Chem-Lab	
1000 ppm Sr ICP standard	Chem-Lab	
1000 ppm Tb ICP standard	Chem-Lab	
1000 ppm Y ICP standard	Merck, Chem-Lab	

2.2 Health, Safety and Environment

All performed experiments followed the *Code of Practice for safety in the lab*.[b] The hazards of all used chemicals were checked before handling. No new risk assessments were needed as the experiments have already been performed in the past with a risk assessment already available, but additions to previous risk assessments were made for all experiments, and these can be found on the HSE Core Facilities website.[c] All procedures and observations were documented in a lab book. During the experiments, a lab coat and safety goggles were worn at all times in any lab, and gloves were worn when handling chemicals. As much of the experiments as possible were performed in a fume hood. Waste was disposed of in the correct waste containers.

The most hazardous chemicals used were tributyl phosphate (TBP), Cyanex 923, di-(2-ethylhexyl)phosphoric acid (D2EHPA), lithium bis(trifluoromethylsulfonyl)imide ($LiTf_2N$) and methanesulfonic acid (MSA). TBP is a class E4 chemical (very dangerous) and is suspected for causing cancer next to causing irritation of the skin and being harmful when swallowed. Cyanex 923 (a mixture of trioctylfosfine oxide, hexyldioctylfosfine oxide and dihexyloctylfosfine oxide) is a class E3 chemical (dangerous) and can cause serious burns and eye damage. It is harmful for aquatic life, with long-lasting consequences. D2EHPA is a class E3 chemical (dangerous) is harmful when in contact with skin and can cause serious burns and eye damage. It is harmful for aquatic life, with long-lasting consequences. $LiTf_2N$ is a class E3 chemical (dangerous) and is poisonous when swallowed or in contact with skin, can cause serious burns and eye damage, and can cause damage to organs after prolonged or repeated ingestion. It is harmful for aquatic life, with long-lasting consequences. MSA is a class E3 chemical (dangerous) and can cause serious burns and eye damage.

A mandatory course was followed about the dangers of ionizing radiation and how to protect oneself from it before using the TXRF machine.

[b] Available at http://chem.kuleuven.be/en/hse/procedures/liab1.htm
[c] Available at https://www.groupware.kuleuven.be/sites/hsecorefacilities/Pages/RA/default.aspx

2.3 Experimental procedure

2.3.1 *Synthesis of [Hbet][Tf_2N]*

The ionic liquid (IL) needed for the leaching experiments of the YOX phosphor was synthesized following a method described in the literature.[55] Equimolar amounts of betaine hydrochloride (HbetCl) and lithium bis(trifluoromethylsulfonyl)imide ($LiTf_2N$) were added to water (approximately 50 mL per 60 g of HbetCl) in a round-bottom flask and stirred magnetically for at least one hour at room temperature. During this stirring, the HbetCl and the $LiTf_2N$ switch their ions to form the IL [Hbet][Tf_2N] in the organic phase, while the LiCl dissolves in the aqueous phase. The mixture was then transferred to a separatory funnel and some Milli-Q water with ice was added to cool the aqueous phase to decrease the mutual solubility.[52] The phases were mixed, left to settle for at least thirty minutes and then separated. The ice always melted before the separation, defeating its purpose. A bit of the aqueous phase was added to a small vial and some $AgNO_3$ was added, the formation of a precipitate indicated the presence of chloride as AgCl is insoluble in water. The IL was washed several times with ice-cold Milli-Q water to remove dissolved LiCl in the IL until the $AgNO_3$ test showed no more chloride was present in the washing water. The phases were left to settle at least for thirty minutes after each washing step. The IL was then dried on a rotavapor at a pressure below 1 mbar. Both a ^{1}H-NMR at 300 MHz and a ^{13}C-NMR spectrum at 400 MHz were taken, using deuterated DMSO as solvent, and TMS as reference. The obtained spectra can be found in Appendix 2.

The water content of the dried IL was measured using either a volumetric (METTLER TOLEDO Compact Volumetric KF Titrator V30s) or a coulometric Karl-Fischer titrator (METTLER TOLEDO COMPACT KF Coulometers C30s), depending which one was available. Based on the obtained water content, Milli-Q water was added to obtain an IL with 5 wt% of water, which was used in all the experiments unless otherwise stated.

2.3.2 *Leaching*

Leaching experiments were performed in closed glass vials of different sizes depending on the scale of the experiment (between 4 and 250 mL). A bar magnet was added to stir, and the vials were placed in a sand bath on a heating plate. The sample in 4 mL vials were stirred at 600 rpm, samples in bigger vials were stirred at the highest speed possible if 600 rpm was not feasible. The experiments were done in duplicate, except for the experiments performed on a larger scale. The temperature was controlled using a probe in a vial of glycerol placed in the sand bath.

For the IL leaching experiments the IL was added to an amount of phosphors corresponding to the used solid-to-liquid ratio and magnetically stirred while heated for the required time. After leaching, the PLS was filtrated via syringe filtration using 0.45 µm PET filters. Due to the high viscosity of the IL, centrifuge was discarded for the solid-liquid separation.

For the MSA leaching experiments MSA was added to an amount of phosphors corresponding to the used solid-to-liquid ratio and magnetically stirred while heated for the required time. After leaching, the samples were also not centrifuged as syringe filtration is faster. This has the

advantage of immediately stopping the leaching, while the phosphor could continue to be leached during the centrifugation, which is certainly undesirable for kinetics experiments.

2.3.3 *Solvent extraction*

For solvent extraction experiments, the extractant and the diluent were added to the pregnant leach solution in vials/tubes, and were shaken on a TMS-200 Turbo Thermo Shaker Incubator (supplied by Allsheng) at a speed of 2500 rpm and are centrifuged in an Eppendorf 5804 centrifuge for 10 min at a speed of 4000 rpm to facilitate phase separation. The phases were separated using glass pasteur pipettes.

2.4 Analytical techniques

2.4.1 *Microwave digestion*

To measure the compositions of the solid material, microwave digestion (MWD) was performed in a Speedwave Xpert from Berghof. Approximately 50 mg of solid material was placed in the MW digestion vessels (DAK-100), and 10 mL HCl was added. Each digestion was performed in quadruplicate. The samples were digested using the following program: (1) heat from room temperature to 145 °C in 10 min and hold for 10 min, (2) heat to 170 °C in 5 min and hold for 10 min, (3) heat to 200 °C in 5 min and hold for 10 min, (4) cool down to 50 °C and hold for 20 min.

The samples were then taken out and diluted in Milli-Q water to a known volume of around 40 – to 50 mL and then centrifuged to settle undissolved particles. The metal content of the samples was measured with ICP-OES after further dilution in 2 v% HNO_3 to obtain adequate metal concentrations for the analysis.

2.4.2 *Soxhlet extraction*

Soxhlet extraction was performed using a Büchi Extraction System B-811. To perform the Soxhlet extraction, 5 g of material was placed in a cellulose extraction thimble. The continuous extraction mode (Randall extraction) was selected and 100 mL Milli-Q water was used as solvent. For the determination of the Soxhlet extraction efficiency, HCl was added to the water and the obtained precipitate (to dissolve the precipitate), and the mixture was further diluted with Milli-Q water to a volume of 500 mL and analyzed via ICP-OES.

2.4.3 *TXRF*

The used TXRF (Total Reflection X-Ray Fluorescence (Analysis)) machine was a S2 PICOFOX from the brand Bruker, using a molybdenum anode target where electrons are shot at from a heated tungsten cathode to produce X-rays.

For liquid samples, the quartz carriers were treated with 30 µl of a silicon solution in isopropanol and dried in the oven at 60 °C until the isopropanol evaporated completely to siliconize the surface, making it hydrophobic. 100 µL of the samples and 50 µL of 1000 ppm Ga standard were added to 850 µL ethanol and shaken to obtain a tenfold dilution of the sample and a concentration of 50 ppm gallium as internal standard. A drop of this mixture was then added in the middle of a carrier for each sample, and the carriers were dried for at least 30 min in an oven at 60 °C before measuring them in the TXRF device.

A test was performed to verify if TXRF is suitable for measuring the metal content of the IL samples. Three calibration samples were made for europium, yttrium, strontium and calcium as those were the most abundant and important elements to measure in the IL. Four more samples with varying concentrations for europium, yttrium, calcium and strontium were prepared to compare them to the calibration samples.

For solid samples, the carriers were treated with some vacuum grease to obtain a thin sticky film, and some of the solids were added in the middle of the carrier using a cotton bud, as described in the manual of the machine. The carriers were not dried in the oven as the vacuum grease would not evaporate.

2.4.4 *ICP-OES*

The metal concentration of the liquid samples was measured using Inductive Coupled Plasma-Optical Emission Spectrometry (ICP-OES), an Optima 8300 of the brand PerkinElmer with a 1-slot Hybrid XLT Ceramic-Quartz torch, also from PerkinElmer. The Syngistix software was used to control the ICP-OES device and processes the results.

The samples were diluted sufficient times in 2 v% HNO_3 to obtain concentrations below 50 ppm. A blanc and at least six calibration samples were used every measurement (less for some early validation experiments), and a quality check sample was measured after the calibration sample, after every ten samples and at the end of a measurement. Every sample (blanc, calibration, quality check and actual samples) had 5 ppm of indium as internal standard. Every element was measured three times at two wavelengths (excepts for the standards of indium and argon) in an axial position (some also in a radial position), see Table 4. After each sample, the system was washed at least 60 seconds, usually 70 seconds, with a 2 v% HNO_3 solution. The calibration curve was forced through zero. Error bars in graphs are calculated from the duplicates.

Table 4: Measured wavelengths of the elements and their measuring position.

Element	First wavelength (nm)	Second wavelength (nm)	Radial/axial
Argon	420.069	-	Both
Indium	230.606	-	Both
Yttrium	324.227	371.029	Both
Europium	381.967	412.910	Both
Calcium	315.887	317.933	Both
Strontium	407.771	421.552	Both
Antimony	206.836	217.582	Axial
Manganese	257.610	259.372	Both
Barium	233.527	455.403	Axial
Magnesium	279.077	285.213	Axial
Aluminium	394.401	396.153	Axial
Lanthanum	379.478	408.672	Axial
Cerium	413.764	418.660	Axial
Terbium	350.917	384.873	Axial
Silicon	212.412	251.611	Axial
Phosphorus	213.617	214.617	Axial
Sulfur	180.669	181.975	Axial

2.4.5 *NMR*

^{1}H-NMR (Nuclear Magnetic Resonance) spectra were taken using a Bruker Advance 300 MHz device, and ^{13}C-NMR spectra were taken using either a Bruker Advance 300 MHz or a Bruker Advance 400 MHz device. Depending on the sample, deuterated DMSO or a solution of 96 – 98 % deuterated sulfuric acid in deuterated water was used as a solvent. The spectra were processed with the MestreNova software.

3 Results and discussion

3.1 TXRF suitability

As mentioned in section 2.4.3, a test was performed to check if TXRF was suitable to measure the content of the metals of interest from IL samples. A calibration line was performed using synthetic mixtures and samples of known concentration (prepared in an IL matrix) were measured. A plot of the actual concentration versus the measured concentration for each element can be seen in Figure 32 in Appendix 3, and it can be observed that although a linear correlation was obtained for the regression of the calibration samples, the metal concentration of the samples was not appropriately determined. This behavior could be attributed to a matrix effect of the IL. From this it was concluded TXRF could not be used to accurately measure the elements of interest, and that ICP-OES would be used instead.

Besides what has been already mentioned, there are other reasons to discard the TXRF as a suitable technique for the accurate determination of the metal content from complex mixtures. First, the peaks in a TXRF spectra are quite broad and easily interfere with each other (certainly if a lot of elements are to be measured), and elements can be wrongly identified. Second, the detection limits of TXRF are relatively high. For example, in Table 16 or Table 18, TXRF could not detect some elements that ICP-OES could measure, even though their concentrations were similar to those of other detected elements.

Despite all the aforementioned disadvantages, TXRF is a valuable technique for the qualitative detection of elements, and a rough estimate of their concentration.

3.2 Validation of some previous research and attempt at the original flowsheet

To validate the previous research,[55,86] and to determine the conditions for a first attempt to integrate the different leaching techniques, some experiments were performed. These include preparing the IL, confirming the leachability and the kinetics of synthetic YOX phosphor and the HALO phosphor in the IL, stripping experiments, and the kinetics and the effect of the solid-to-liquid ratio of leaching the LAP phosphor from real lamp phosphor waste with methanesulfonic acid (MSA). As the experiments performed on real waste were not satisfactory due to characterization issues, they are discussed in Appendix 4 and only a summary is given here.

3.2.1 *Synthesis of the IL [Hbet][Tf2N]*

The first synthesis of the IL [Hbet][Tf_2N] started with 60 g of betaine hydrochloride (HbetCl, 0.39 moles), and an equimolar amount of lithium bis(trifluoromethylsulfonyl)imide ($LiTf_2N$, 112.2 g) were added to 60 mL of Milli-Q water in a 500 mL round-bottom flask. The products were stirred for one hour and 25 min. After separating the IL from the water and washing the IL three times, the $AgNO_3$-test showed that no more chloride was present in the IL. The IL stayed liquid after several days due to the presence of water. After drying on the rotavapor,

the water content was measured using the volumetric Karl Fisher titrator, and the water content was 0.65 wt% (or, when calculated to molar fraction, 14 mol%). Now that the IL was quite dry, it slowly started solidifying. The yield of the IL was only 34 %, a lot lower than the 79 % reported in the literature.[55] TXRF was used to qualitatively verify the absence of chloride.

During the first extraction, the water phase was still milky when separated from the organic phase, thus containing some suspended IL; this is likely one of the reasons the yield was very low. Furthermore, not enough ice was present to keep both phases at 0 °C during the following washing steps as after shaking no ice was left in the aqueous phase. Since the solubility of the IL in water rises with temperature, some more IL was probably lost this way.

The experiment was repeated, but only 50 mL of Milli-Q water was added during the synthesis, and the products were stirred for 1 hour and 45 min. During the washing, more ice was added until some ice was still present after shaking. The amount of washing water was also kept lower. Four washing steps were needed until no more chloride could be detected using the $AgNO_3$-test. Under these conditions the yield was 72 %.

A bigger scale synthesis (double the amounts of the second) was performed, and a yield of 75.4 % was achieved. The yield was very similar to the previous synthesis, so the synthesis of the IL can be scaled up.

The IL prepared during the third synthesis was sufficient for the work performed in this master thesis. Still, a different way to improve the yield were identified: using the salting out effect. This consists of adding a salt to the aqueous phase during the washing to reduce the solubility of the IL in the water, which is around 14 wt% at room temperature. The best anion for sodium salts was found to be SO_4^{2-}, it reduces the solubility of the IL to 4 wt% in 1 M Na_2SO_4. The best cation in chloride salts was found to be Mg^{2+}, it reduces the solubility of the IL to approximately 7 wt% in 1 M $MgCl_2$.[4] It may be worthwhile for future research to combine the best cation and anion together and use $MgSO_4$ to test if the solubility of IL in the aqueous phase is reduced even further.

3.2.2 *Leaching experiments*

The most important results of the leaching experiments used to validate previous research or performed on unsieved waste are discussed here. The experiments are discussed fully, including figures, in Appendix 4.

Leaching individual artificial phosphors (section A.4.1 and section A.4.2 in Appendix 4) and a mixture of them (section A.4.3 in Appendix 4) with IL had the expected selectivity; YOX was leached, only a small percentage of HALO and no BAM or LAP were leached. The dissolution of YOX was slower however compared to the literature, and its loading capacity seemed to be lower as well.[55] The same experiments were performed on real phosphor waste (section A.4.4 in Appendix 4) and it was the selectivity towards HALO that was lost, contaminating the PLS with quite some calcium. BAM and LAP were, similar to the artificial phosphors, hardly leached. The calculated leaching efficiencies exceeded 100 %, and after careful evaluation of the results a mismatch between the provided characterization and the composition of the unsieved material was identified.

Leaching the LAP phosphor from real waste using MSA has slower kinetics than reported in the literature, and a lot of HALO phosphor is leached along the LAP, heavily contaminating the PLS with calcium (see section A.4.5 in Appendix 4). These experiments also suffered from unreliable leaching efficiencies (up to 150 %). The effect of the liquid-to-solid ratio was investigated (using already sieved and characterized waste) to see its effect on the leaching efficiencies of all the phosphors (see section A.4.6 in Appendix 4). The most optimal liquid-to-solid ratio according to literature is 15 mL/g as a lower ratio results in the formation of a gel.[86] Low L-to-S ratios favored the leaching of LAP over YOX, and no gel formation was observed below a L-to-S ratio of 15 mL/g, but the sample were leached not long enough at the used temperature. The samples with lower L-to-S ratios were harder to filter though, so the L-to-S ratio was kept at 15 mL/g.

It was noticed that every time the MSA PLS (which had a very dark color) was diluted in water or ethanol, a brown precipitate appeared, leaving the rest of the solution almost colorless. A small amount of this precipitation was isolated and characterized in section 3.11. It was first thought that this precipitation could have been decomposition from the MSA, as it was advised in the literature not to heat MSA above 200 °C to prevent any thermal decomposition.[86] In a small test, some pure MSA was heated at 200 °C for more than two hours. A ^{1}H-NMR spectrum was taken before and after, and these can be found in Appendix 5. Other than a small shift in the peak position of the acidic proton, no change in the spectra is observed.

3.2.3 Stripping of loaded IL

To validate the stripping of the IL used for leaching artificial phosphors, the two samples that were leached for the full 46 hours were then used to test the stripping efficiency with oxalic acid. A stoichiometric amount of oxalic acid (1.5 times the amount of moles of yttrium and europium combined) was added to 1 mL of each sample and this was heated at 70 °C for 20 min. The samples were then filtered using a syringe filter and prepared for ICP-OES measurement. One sample had 95.7 % of its yttrium and 96.2 % of its europium stripped, and the other 99.94 % of its yttrium and 99.67 % of its europium. The first sample may have received not enough oxalic acid or the stripping was not yet complete. This excellent stripping behavior corresponds with the literature.[55]

To check the reusability of the IL after leaching real waste, a stochiometric amount of oxalic acid (1.5 times the amount of moles of the total amount of yttrium and europium) was added to a combination of the two samples used for the data point of a solid-to-liquid ratio of 60 mg/mL and a leaching time of 64 hours (see section A.4.4 in Appendix 4). The sample was then heated at 70 °C for 20 min. The sample was then centrifuged, filtered and diluted for an ICP-OES measurement. The oxalic acid was not selective for the yttrium and europium in the IL as 71 % of the yttrium and 68 % of the europium was removed. The other elements were stripped partially too with varying efficiencies. The half-stripped IL was then used to leach some more real phosphor waste (solid-to-liquid ratio of 60 mg/mL, leaching time of 70 hours), but the leaching efficiency for all elements was a lot lower. As expected, the IL must thus be stripped completely for a chance to be re-usable.

Since oxalic acid is not selective for yttrium and europium, an attempt to strip all the metals from the loaded IL was performed to make the rather expensive IL at least reusable, even if

the oxalates would be contaminated with other elements The filtered samples from previous experiments were combined (around 60 mL) and analyzed with ICP-OES to determine the metal concentration of the mixture. From the metal concentrations calculated from the ICP-OES values, double the amount of oxalic acid needed to complex all the metals was added to the IL. The mixture was stirred and heated at 70 °C for 30 min, after which the precipitation was filtered using a sintered glass filter on a Büchner flask. Around 50 mL of the IL was recovered, and the metal concentration of the stripped IL was measured with ICP-OES. As the concentrations of some elements are so low in the IL, they fall outside the calibration range of the ICP-OES and sometimes appear negative. These can be assumed to be zero. The stripping efficiencies and the concentration of the elements left in the stripped IL can be found in Table 5. Only aluminium and antimony are hard to strip, but their concentrations are very low and comparable to those of the traces left of the stripped elements.

TXRF was used later on to measure the composition of the loaded IL and to verify the absence of elements in the stripped IL. The loaded IL also contained iron and traces of potassium, nickel, copper, zinc, bromine, gadolinium and lead. This iron might be the cause of the light brown coloration in the IL. Both the loaded and stripped IL were not measured again with ICP-OES to measure the concentration of iron as by that time a better opportunity to leach YOX came along. Gadolinium most likely originates from some $GdMgB_5O_{10}:Ce^{3+},Tb^{3+}$ phosphor present in the waste that dissolved a bit as well. The stripped IL only contained traces of iron and bromine. Bromine does not strip very well, but this is logical as oxalic acid forms complexes with cations and not presumably negatively charged bromine ions. The presence of iron in the stripped IL could be due to some contamination. As remarked during a meeting of the research group, the TXRF carriers are not always perfectly clean and particularly iron is more difficult to remove, so some iron could originate from the carrier and not the IL.

Table 5: Stripping efficiencies and concentrations of the elements before and after stripping the IL, grouped together per phosphor.

Element	Concentration before stripping (ppm)	Stripping efficiency (%)	Concentration after stripping (ppm)
Y	3680	100	2
Eu	257	100	< 1
Ca	1040	100	-1 (= 0)
Sr	53	100	< 1
Sb	3	19	3
Mn	10	98	< 1
Ba	34	100	< 1
Mg	16	97	< 1
Al	4	68	1
La	2	94	< 1
Ce	3	100	< 1
Tb	1	98	< 1
Si	4	89	< 1

3.3 Solution to encountered problems: characterization

To tackle the problem of the composition of phosphor waste not corresponding to the values given in the provided characterization, several characterization methods were attempted after sieving the waste to remove glass particles and pieces of junk.

3.3.1 *Sieving*

The phosphor waste was sieved using an Analysette 3 Spartan vibratory sieve shaker from the brand Fritsch in four different fractions: > 500 µm, 250 – 500 µm, 125 – 250 µm and < 125 µm. A picture of the different fractions is given in Figure 10. The < 125 µm fraction had a size of four of the plastic weighing boats while the other fractions all fitted in one boat.

Figure 10: Picture of the four fractions after sieving the phosphor waste, from left to right: < 125 µm, 125 – 50 µm, 250 – 500 µm and > 500 µm.

The > 500 µm fraction mostly consists of large glass particles, pieces of rock, sand, plastic and some straw. The 250 – 500 µm fraction consist of glass particles and what seems to be iron filings, the 125 – 250 µm fraction consists mainly of glass particles. The < 125 µm fraction most likely contains some glass as well next to the phosphor powder.

3.3.2 *Dissolution of phosphor waste in HNO_3 and in HCl*

The first attempt to characterize the sieved phosphor waste used 65 % nitric acid (HNO_3) or 37 % hydrochloric acid (HCl) in duplicate. 10 mL acid was added to 0.5 g sieved waste and was stirred at room temperature overnight. As not everything was dissolved, the mixture was stirred further for three more days, but still not everything was dissolved. Part of the solution was filtered with syringe filters and its composition measured using ICP-OES. The calculated values of both methods are found in Table 6 along with the values found in received characterization. For the YOX and HALO phosphors, the HNO_3 and HCl methods give similar results (strontium and antimony are dissolved better in HCl), and all values (except for strontium and antimony in HNO_3) are bigger than those from the received characterization. Part of this is the removal of glass particles through sieving, increasing the powder fraction, part of it is that the values of the received characterization were lower than the actual content before sieving. The phosphor waste could be somewhat inhomogeneous, or the earlier characterization could have been performed on a very small scale, which would explain part of the difference. The BAM and LAP phosphors apparently hardly dissolved in both HNO_3 as

HCl as their values are much lower. Silicon (glass) also hardly dissolved. This is not really an issue for the BAM phosphor as that is not a phosphor of interest, but it is an issue for the LAP phosphor.

3.3.3 *Microwave digestion of phosphor waste*

Another characterization attempt used microwave digestion (MWD). 10 mL HCl was added to approximately 50 mg of sieved waste and the mixture was heated following the program discussed in section 2.4.1 (performed in quadruplicate). The results can be found in Table 6. The values for the YOX and HALO phosphors are very similar to those found using HNO_3 and HCl. The LAP phosphor now has more realistic values, which are approximately one and a half times bigger than those previously used. It is thought that the BAM phosphor did not dissolve very well in all used techniques as the concentrations of its elements are lower than the delivered characterization. Thus, MWD is a usable technique to accurately characterize the YOX, HALO and LAP phosphors in lamp phosphor waste. Using these values to recalculate all experiments that used unsieved waste would still give inaccurate results as the relative phosphor content was lower compared to the sieved waste. As dissolving the BAM phosphor is problematic, its leaching efficiencies are not shown in the figures, but the concentration of its elements in the PLS's still is to show the size of their contamination. From now on, sieved waste was used for all experiments.

Table 6: Content of the phosphor waste, sieved for the HNO_3 and HCl methods and MWD, unsieved for the delivered characterization.

Element	HNO_3 (wt%)	HCl (wt%)	MWD (wt%)
Y	9.51 ± 0.04	10.37 ± 0.14	10.1 ± 0.7
Eu	0.666 ± 0.006	0.65 ± 0.02	0.67 ± 0.05
Ca	7.781 ± 0.017	7.28 ± 0.08	7.9 ± 0.7
Sr	0.047 ± 0.001	0.378 ± 0.002	0.37 ± 0.04
Sb	0.052 ± 0.005	0.107 ± 0.006	0.110 ± 0.017
Mn	0.184 ± 0.001	0.172 ± 0.006	0.172 ± 0.014
Ba	0.028	0.097 ± 0.002	1.47 ± 0.15
Mg	0.075 ± 0.001	0.106 ± 0.003	0.19 ± 0.02
Al	0.043 ± 0.001	0.339 ± 0.011	1.7 ± 0.3
La	0.017 ± 0.001	0.080 ± 0.003	1.47 ± 0.08
Ce	0.024 ± 0.001	0.081 ± 0.003	0.97 ± 0.03
Tb	0.014	0.044 ± 0.001	0.48± 0.04
Si	0.006 ± 0.001	0.013 ± 0.001	-

3.4 Solution to encountered problems: selective leaching of HALO

The selective removal of the HALO phosphor would minimize the contamination of calcium in the following leaching steps. Different methods were tested: Soxhlet extraction, leaching with HCl, and leaching with MSA, both pure and diluted. MSA was chosen to be investigated as at

the end of the solvent extraction of lanthanum, cerium and terbium from pure MSA, barren 40x diluted (2.5 vol%) MSA emerges. It would be favorable if this diluted MSA could be used to remove HALO.

3.4.1 *Soxhlet extraction with water*

First, a Soxhlet extraction was attempted using pure water to dissolve the HALO phosphor. During a Soxhlet extraction, the leaching agent is removed from the solid sample continuously or in batches, and it ends up in a beaker on a hot plate. The leaching agent is distilled, leaving the dissolved elements behind, and it is condensed after which it ends up at the solid sample again. This way, the sample is constantly brought into contact with fresh leaching agent, facilitating the leaching reaction.[89]

Around 5 g of sieved phosphor waste and more than 100 mL of water was used. The experiment was performed four times for four different lengths of time in a continuous mode (usually called Randall). After the leaching, the water was recovered in the beakers and HCl was added to dissolve precipitated material. The metal concentrations of the solution were determined with ICP-OES. The result is in Figure 11. Only a small amount of calcium leached, while all the other elements did not seem to leach, even after eight hours. Soxhlet extraction is thus not a suitable technique to remove HALO from the waste prior to leaching YOX and LAP.

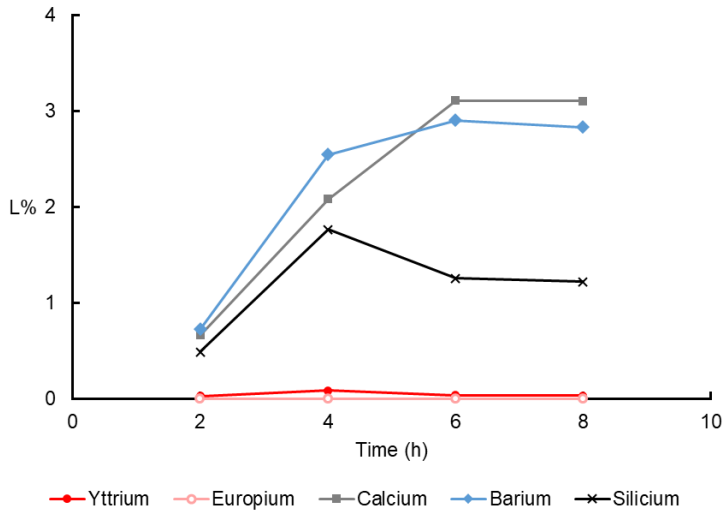

Figure 11: Leaching efficiencies of the main elements of the four phosphors after different leaching times in a Soxhlet extraction.

3.4.2 *Leaching HALO with HCl*

The next attempt to selectively dissolve HALO used different concentrations of HCl and different leaching times at room temperature. According to the literature, the HALO phosphor can be leached in five minutes at room temperature using 2 M HCl. Almost 95 % of calcium dissolves, but 4.2 % of the yttrium and 6.6 % of the europium are leached too.[77] Using 1 M

HNO_3 achieves similar results.[47] Around 0.3 g of sieved material and 3 mL aqueous HCl was used. The results are in Figure 12.

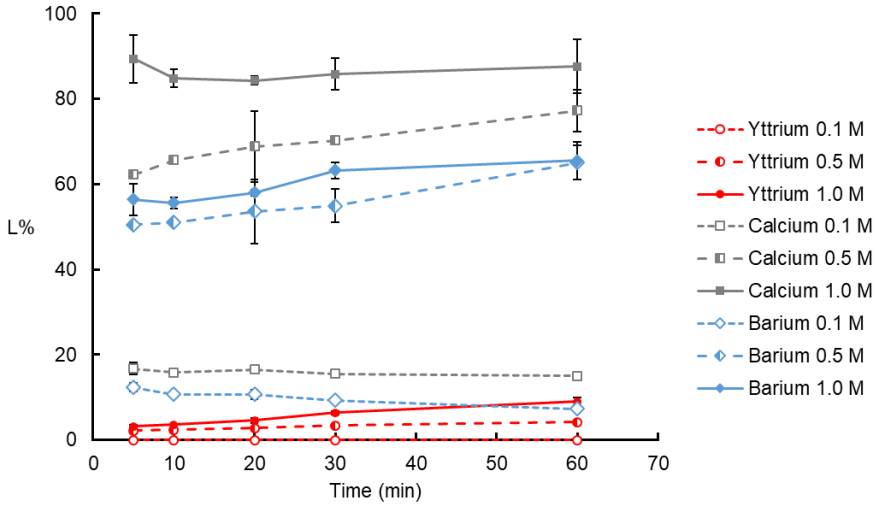

Figure 12: Leaching efficiencies of the main elements of HALO, YOX and BAM using various concentrations of HCl and leaching times.

HALO dissolves very fast when using 1 M HCl and barium from the BAM phosphor dissolves quite well too, but a small part of the YOX is dissolved as well. Leaching for a longer time has no influence on the leaching of HALO, but the YOX phosphor increased with time. Using lower acid concentrations suppresses the leaching of YOX, completely preventing it when using 0.1 M HCl, but HALO and barium are suppressed too. Although the technique works with values similar to those found in the literature,[47,77] it is not selective enough to solve the problem of calcium in the process without leaching part of the valuable YOX phosphor.

3.4.3 *Leaching of HALO with MSA*

The next attempt to selectively leach HALO used different dilutions of MSA. As can be seen in Figure 40 in Appendix 4, pure MSA dissolves most of the HALO phosphor. In an attempt to increase the selectivity of leaching HALO over the other phosphors, lower temperatures and different concentrations of MSA were tested. Samples were prepared with a liquid-to-solid ratio of 15 mL MSA solution per g of phosphor waste. They were heated at 80 °C for 2 hours. The samples with pure MSA were black afterwards, and the samples with more diluted MSA had less and less color. The leaching efficiencies are given in Figure 13. In almost all cases, the YOX phosphor is leached along with the HALO phosphor, but pure MSA seems to leach HALO selectively over YOX. The leaching efficiency of yttrium and europium are around 10 %. Most of the antimony and manganese of the HALO phosphor are leached as well, but strontium is leached around 60 %. For an unknown reason, HALO is leached less when using 50 – 80 vol% MSA. The leaching efficiencies and content of the elements in pure MSA are listed in Table 7 to get a sense of the purity of the PLS. This experiment was originally performed on unsieved waste using more dilute MSA concentrations, and the leaching efficiencies of all elements steeply drop below a concentration of 5 vol% MSA.

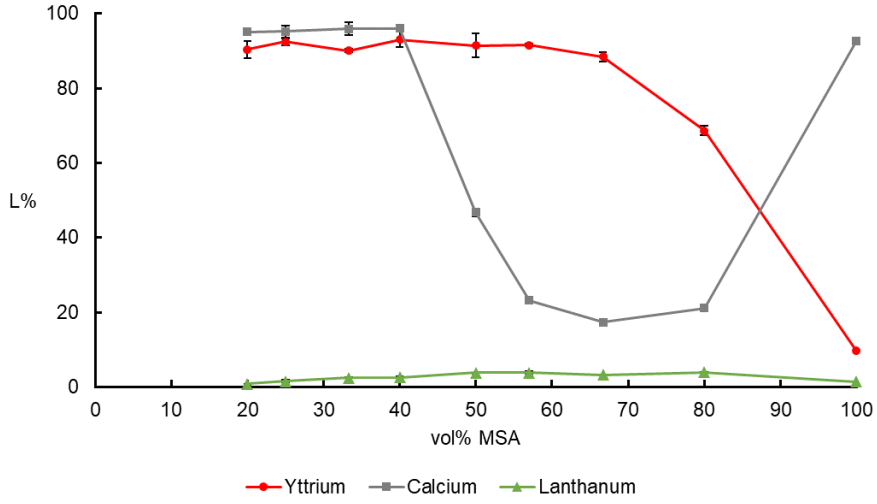

Figure 13: Leaching efficiencies of the main elements of the four phosphors. L-to-S ratio: 15 mL/g, temperature: 80 °C, leaching time: 2 hours.

Table 7: Leaching efficiencies and concentrations of all elements in pure MSA after leaching at 80 °C.

Element	Leaching efficiency (%)	Concentration (mg/mL)
Y	9.4	0.64
Eu	10.0	0.04
Ca	92.7	4.91
Sr	53.0	0.13
Sb	87.6	0.06
Mn	90.5	0.10
Ba	-	0.22
Mg	-	0.03
Al	-	0.14
La	1.3	0.01
Ce	1.1	< 0.01
Tb	1.7	< 0.01
Si	-	0.03

Although leaching with pure MSA at 80 °C is not more selective than the method using HCl, there is a trend in increased selectivity of HALO over YOX when compared to leaching with pure MSA at 160 or 200 °C (see section A.4.5 in Appendix 4). For that reason, leaching in the even colder room temperature (23 – 25 °C) was attempted, with the same conditions as the previous experiment. The results can be found in Figure 14. The samples leached with pure MSA were orange-brown after filtration, the other samples were colorless. Similar to the previous experiment, there is a dip in the leaching efficiency of HALO. Compared to leaching at 80 °C, LAP now dissolves less than 1 %, and the leaching of YOX is greatly suppressed. HALO on the other hand is leached the same amount, so reducing the temperature had the desired effect of increasing the leaching selectivity of MSA for HALO over YOX. For pure MSA, YOX is leached around 1 %. This is more selective than found in both the literature[77] and the previous experiment at 80 °C. This experiment was originally also performed on unsieved waste using more dilute MSA solutions, and the leaching efficiencies of the elements drop below a concentration of 10 vol% MSA. The leaching efficiencies and

concentrations of all elements in the pure MSA are given in Table 8. Due to this excellent result, there is a renewed hope of a working flowsheet. Lowering the leaching temperature for an even better selectively is not possible as MSA has a melting point of 20 °C according to the manufacturer (Carl Roth).

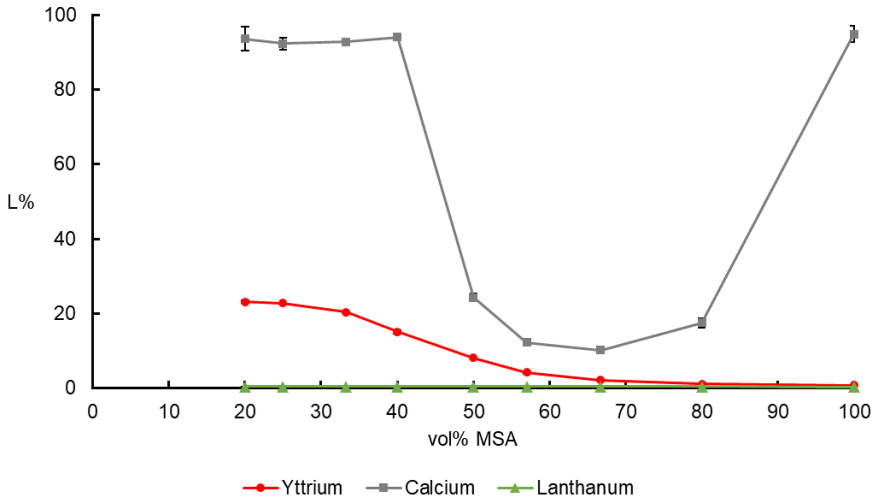

Figure 14: Leaching efficiencies of the main elements of the four phosphors. L-to-S ratio: 15 mL/g, temperature: RT, leaching time: 2 hours.

Table 8: Leaching efficiencies and concentrations of all elements in pure MSA after leaching at RT.

Element	Leaching efficiency (%)	Concentration (mg/mL)
Y	0.8	0.05
Eu	1.4	< 0.01
Ca	96.3	5.12
Sr	53.0	0.13
Sb	62.1	0.05
Mn	90.7	0.10
Ba	-	0.17
Mg	-	0.03
Al	-	0.06
La	0.4	< 0.01
Ce	0.3	< 0.01
Tb	0.5	< 0.01
Si	-	0.01

3.4.4 *Optimization of leaching HALO with MSA at room temperature*

To optimize the leaching of HALO with pure MSA at room temperature, the kinetics and the effect of the liquid-to-solid ratio were investigated. The kinetics of the leaching reaction are shown in Figure 15.

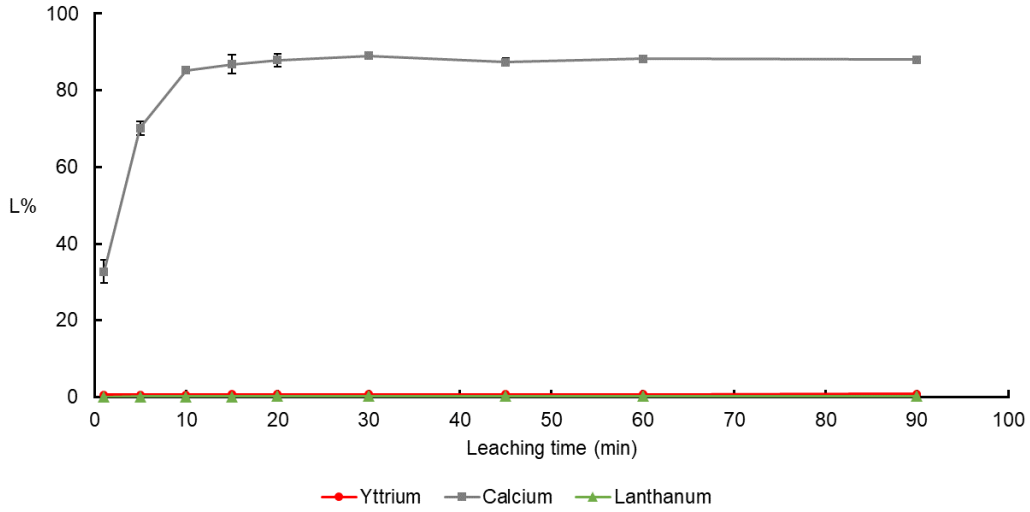

Figure 15: Kinetics of leaching HALO with pure MSA at room temperature. Liquid-to-solid ratio: 15 mL/g, temperature: RT (23 – 24 °C).

It can be seen that the leaching reaction reaches equilibrium after approximately half an hour. Calcium is leached 89 % at that moment, while YOX and LAP stay below 1 %.

To determine the most optimal liquid-to-solid ratio, liquid-to-solid ratios smaller than 15 mL/g were chosen as a higher liquid-to-solid ratio might facilitate the leaching of YOX, which is undesirable. The samples were leached for two hours at room temperature (23 – 25 °C). The results can be found in Figure 16, and a composition and leaching efficiencies of all elements in the MSA are given in Table 9.

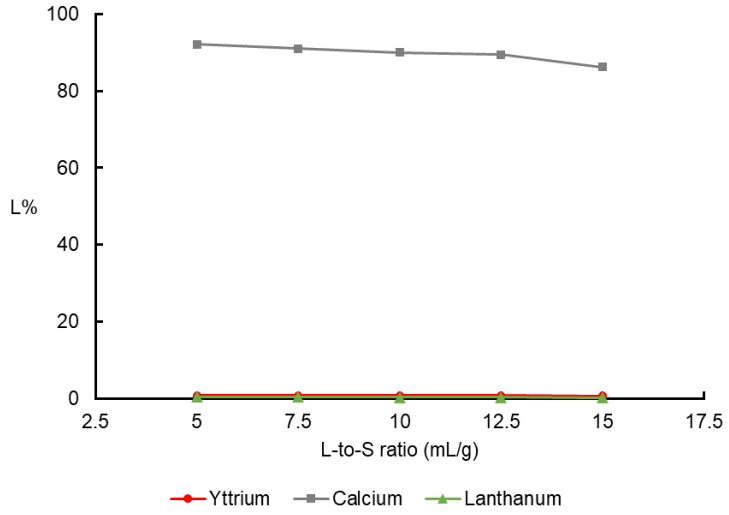

Figure 16: Effect of the liquid-to-solid ratio on the leaching behavior of the main elements of the four phosphors using pure MSA at room temperature. Leaching time: 2 hours.

A lower liquid-to-solid ratio increases the selectivity of leaching HALO over YOX even more, improving the leaching efficiency from 86 to 92 % while YOX is leached less than 1 % with hardly any difference between the solid-to-liquid ratios. The optimal leaching conditions to selectively remove HALO using pure MSA from phosphor waste are now found: a leaching time of half an hour (for small samples), a liquid-to-solid ratio of 5 mL/g and a temperature of around 23 °C.

Table 9: Leaching efficiencies and concentrations of all elements in pure MSA after leaching at RT with a liquid-to-solid ratio of 5 mL/g.

Element	Leaching efficiency (%)	Concentration (mg/mL)
Y	0.7	0.15
Eu	1.1	0.01
Ca	92.5	14.6
Sr	54.6	0.41
Sb	33.1	0.07
Mn	79.7	0.27
Ba	-	0.53
Mg	-	0.09
Al	-	0.22
La	0.4	0.01
Ce	0.3	< 0.01
Tb	0.5	< 0.01
Si	-	0.03

3.5 First attempt at a new integrated flowsheet

Now that the problem of removing HALO is solved, a second attempt was made to make an integrated flowsheet. The flowsheet is shown in Figure 17. Only the leaching parts have been performed as the rest of the flowsheet depends on the purity of the PLS's.

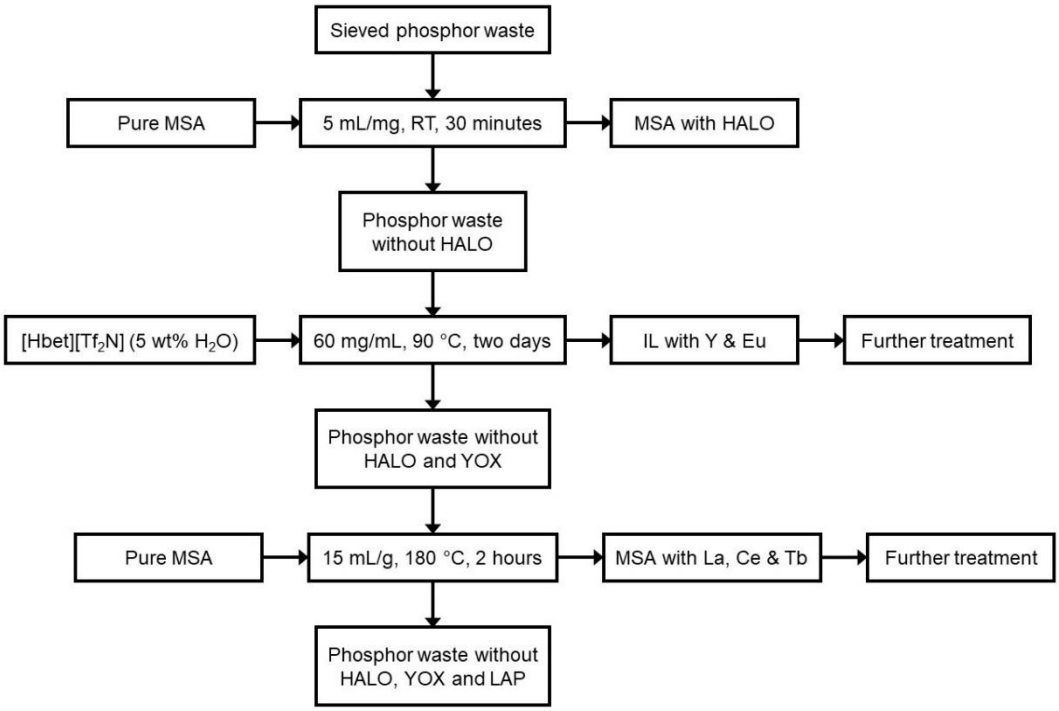

Figure 17: First integrated flowsheet.

4 g sieved waste and 20 mL pure MSA were put in a glass vial and the sample was stirred at room temperature for 30 min. The mixture was then filtered with a sintered glass filter on a

Büchner flask. Some powder stayed afloat on the MSA during the leaching, and what seemed like iron particles gathered on the ends of the magnetic stirring bar after washing the vial and stirring bar with some water to remove all the MSA and undissolved phosphors. The latter is a good thing as this (presumed) iron is removed from the phosphor waste, taking away its ability to contaminate something further in the flowsheet. If this step is to be scaled up, usually a stirrer will be used and not a magnetic stirring bar, so a magnet should then be added to collect the magnetic particles. The filtered phosphors were washed with water and then dried in an oven overnight at 90 °C. Around 2.7 g of waste was recovered. Microwave digestion was performed on the dried phosphors, and the metal concentrations in the MWD solutions along with the PLS were determined with ICP-OES. The leaching results are shown in Table 10 and the changes in waste composition are shown in Table 13. Most of the calcium is removed and practically all of the REEs stay behind in the phosphor waste.

Table 10: Leaching efficiencies and concentrations in the MSA PLS.

Element	Leaching efficiency (%)	Concentration (mg/mL)
Y	0.6	0.12
Eu	1.1	0.01
Ca	75.9	12.01
Sr	43.2	0.32
Sb	25.4	0.06
Mn	67.6	0.23
Ba	-	0.38
Mg	-	0.06
Al	-	0.16
La	0.3	0.01
Ce	0.3	< 0.01
Tb	0.3	< 0.01
Si	-	0.01

1.2 g of the phosphor waste from the previous step and 20 mL IL were added to a vial, and they were stirred at 600 rpm and heated at 90 °C for 66 hours and 20 min. The mixture was then filtered using a sintered glass filter on a Büchner flask. Around 14 mL of the 20 mL IL could be recovered. The filtrate was washed with water and then dried overnight in an oven at 90 °C. Around 0.87 g of phosphors waste was recovered. Microwave digestion was performed on the dried phosphors and ICP-OES was performed on the MWD solutions and a sample of the IL. The results are shown in Table 11 for the leaching and in Table 13 for the change in composition of the waste. Although some remaining HALO phosphor was leached, the total amount is very low compared to yttrium and europium, which take up 88.8 and 5.9 wt% of all the dissolved elements. BAM and LAP are hardly leached. The leachability of YOX from the waste where HALO was removed also proves that the YOX phosphor is not dissolved along with HALO in the previous step and precipitated again as a mixture of phosphates. If this were the case, the IL would not have been able to leach yttrium and europium anymore, and the flowsheet would have been a failure. This step does have two disadvantages however; (1) it is very slow, and (2) the IL is very expensive, costing € 1539 per 5 kg of $LiTf_2N$.

Table 11: Leaching efficiencies and concentrations in the IL PLS.

Element	Leaching efficiency (%)	Concentration (mg/mL)
Y	93.8	7.10
Eu	90.9	0.47
Ca	24.2	0.07
Sr	84.9	0.10
Sb	19.2	< 0.01
Mn	43.9	< 0.01
Ba	-	0.02
Mg	-	0.04
Al	-	0.12
La	0.07	< 0.01
Ce	3.5	0.03
Tb	4.6	0.02
Si	-	< 0.01

For the third step, 0.6 g of the waste from the previous step and 9 mL pure MSA were heated at 180 °C for two hours. A small sample was taken from the PLS and filtered using a syringe filter to measure its content with ICP-OES. The mixture was filtered in a sintered glass funnel on a Büchner flask. The filtered phosphors were washed with water and were dried in an oven at 90 °C overnight. 0.46 g was recovered. The leaching efficiencies and concentrations of the elements in the PLS are given in Table 12, and the change of composition of the waste is given in Table 13.

Table 12: Leaching efficiencies and concentrations in the MSA PLS.

Element	Leaching efficiency (%)	Concentration (mg/mL)
Y	123	0.15
Eu	48.1	0.01
Ca	27.0	0.06
Sr	57.0	0.01
Sb	93.4	0.02
Mn	69.4	< 0.01
Ba	-	0.06
Mg	-	0.03
Al	-	0.20
La	84.8	1.24
Ce	78.3	0.77
Tb	82.5	0.37
Si	-	< 0.01

Table 13: Composition of the waste at the start and after each leaching step measured using MWD.

Element	Initial composition (wt%)	Composition after leaching HALO (wt%)	Composition after leaching YOX (wt%)	Composition after leaching LAP (wt%)
Y	10.1	12.6	0.2	0.047
Eu	0.67	0.87	0.04	0.005
Ca	7.9	0.51	0.36	0.12
Sr	0.37	0.206	0.022	0.002
Sb	0.110	0.046	0.034	0.001
Mn	0.172	0.009	0.005	0.001
La	1.47	2.07	2.18	< 0.001
Ce	0.97	1.34	1.46	0.001
Tb	0.48	0.636	0.666	0.002

Even though the leaching efficiencies of the LAP elements are below 85 %, they are completely removed from the waste, probably during the washing step. Since the PLS is to be diluted ten times with water anyway, the washing water can be used for this dilution. It is also possible that the LAP particles are severely reduced in size due to the leaching and get stuck deeper in the glass filter, in this case they are lost instead. Quite some yttrium is present in the waste along with aluminium, 5 and 6.7 wt% of all elements in the PLS, but only yttrium is problematic as it ends up in the terbium fraction of the solvent extraction part. The amount of yttrium and europium in the waste compared to terbium is much lower compared to that from the HydroWEEE process. The HydroWEEE residue contained 2.2 wt% yttrium, 0.3 wt% europium and 0.5 wt% terbium, resulting in five times more combined yttrium and europium as there is terbium, resulting in a terbium fraction only containing 13.1 wt% Tb_4O_7. The residue used for this experiment after leaching HALO and YOX only contains 0.2 wt% yttrium, 0.04 wt% europium and 0.67 wt% terbium, giving a ratio of three times for terbium than yttrium and europium combined, a ratio fifteen times higher than in the HydroWEEE residue. A rough calculation shows that the terbium fraction after solvent extraction would consist of around two thirds terbium oxide. As the technique has already been performed on real waste and no aluminum is reported to end up with the recovered REEs,[86] the aluminum is probably not extracted in the solvent extraction part.

3.6 Leaching YOX with MSA after removal of HALO

Although the leaching parts of the second integrated flowsheet work, and the subsequent steps should work too, leaching YOX with the IL takes too long (more than two days) and the source for the anion of the IL (lithium bis(trifluoromethylsulfonyl)imide) is very expensive while the high viscosity of the IL causes quite some loss. The experiments discussed in section 3.4.3 show that diluted MSA can leach around 90 % of the YOX phosphor while the LAP phosphor hardly dissolves. This happens both faster and a lot cheaper (2.5 liter costs € 166.10), so some experiments were performed to check the viability of this new method.

Before performing the necessary experiments, quite some phosphor waste was needed from which HALO was already removed. The leaching reaction of HALO was thus performed on a

bigger scale, using 50 g sieved waste and 250 mL pure MSA. The mixture was stirred at room temperature for over an hour to ensure a good leaching performance. After leaching, again what seems to be iron powder was found on the ends of the stirring bar. There were some issues filtrating the filters from the PLS as the pore size of the sintered glass filter was wrongly selected, causing the MSA to hardly go through the filter. Adding some water to reduce the viscosity so it would flow through the filter faster also failed. After most of the now diluted MSA got through the filter overnight, it was decided to use a different, smaller filter and washing the residue from the large filter in smaller batches. Microwave digestion was performed on the dried phosphor powder (around 34.8 g was recovered) to determine its composition, and the leaching efficiencies were measured using a sample of the MSA before diluting it. The leaching efficiencies and the relative change in content of elements in the phosphor waste are summarized in Table 14.

Table 14: Leaching efficiencies and relative change in content of the phosphor after leaching with pure MSA at room temperature at a larger scale.

Element	Leaching efficiency (%)	Relative change in phosphor content based on MWD (%)
Y	0.9	-19
Eu	1.4	-17
Ca	92.8	-97
Sr	52.5	-66
Sb	33.3	-91
Mn	89.1	-98
La	1.0	+44
Ce	0.8	+40
Tb	1.2	+34

It can be seen that part of the YOX was leached when adding water to the MSA when it did not go through the filter, as diluted MSA at room temperature is capable of leaching it (see section 3.4.3). This is not really a big problem as the mass percent of yttrium and europium are still in the same range, from 10.1 to 8.2 wt% for yttrium and from 0.67 to 0.56 wt% for europium. This phosphor powder was used for the next experiments. It is probably better to wash the residue with acetone or another solvent instead that dissolves the MSA. Of course, this solvent should not facilitate the leaching of the YOX phosphor, but this has not been investigated.

3.6.1 *Leaching YOX with different concentrations of MSA at 80 °C*

First, the optimal concentration of MSA in water was determined. As the end product of the solvent extraction part to separate terbium from lanthanum and cerium is 40x diluted MSA (or 2.5 vol% MSA) in water, this specific concentration was among the concentrations used. The previous experiments using diluted MSA did not use this specific concentration, and as the leachability of most elements dropped steeply close to this point, it was unknown if this concentration would work or not. Samples were prepared with a liquid-to-solid ratio of 15 mL

MSA solution per g of phosphor waste from which HALO was removed and they were heated at 80 °C for 2 hours. The leaching efficiencies are shown in Figure 18. The data points using 2.5 vol% MSA are the second from the left. The highest leaching efficiency of the YOX phosphor coincidently uses 2.5 vol% MSA. Note that the leaching efficiencies rise above 100 %, but the cause of this is some evaporation of the water from diluted MSA as some condensation was found in the upper half of all the sample vials. This increased the concentration of the elements in PLS, pushing the calculated leaching efficiencies to a higher value. It could even be that the maximum at 2.5 vol% MSA just happened to have more water removed via evaporation compared to the others samples. Even then, it still shows that 2.5 vol% MSA is capable of leaching a large part of the YOX phosphor. The average leaching efficiencies and concentrations of all elements in the 2.5 vol% MSA PLS and the corresponding errors are given in Table 15, as the values of the duplicates are a bit different from each other.

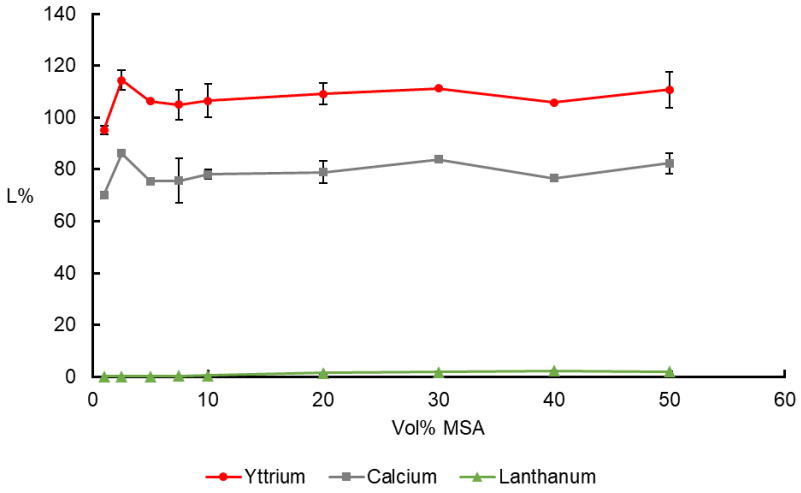

Figure 18: Leaching efficiencies of the main elements of the four phosphors in function of the MSA concentration. Temperature: 80 °C, L-to-S ratio: 15 mL/g, time: 2 hours. The second set data point from the left used 2.5 vol% MSA.

Table 15: Average leaching efficiencies and concentrations of all measured elements of the phosphors in 2.5 vol% MSA.

Element	Leaching efficiency (%)	Concentration (mg/mL)
Y	114 ± 4	5.7 ± 0.6
Eu	108 ± 4	0.37 ± 0.04
Ca	86.2 ± 1.2	0.11 ± 0.01
Sr	107 ± 3	0.07 ± 0.02
Sb	101.6 ± 1.8	< 0.01
Mn	20 ± 5	< 0.01
Ba	-	0.31 ± 0.07
Mg	-	0.02 ± 0.01
Al	-	0.08 ± 0.05
La	0.07 ± 0.01	< 0.01
Ce	3.1 ± 1.0	0.02 ± 0.02
Tb	4.2 ± 1.4	0.01 ± 0.01
Si	-	0.04 ± 0.02

Although lanthanum itself is hardly leached, cerium and terbium are leached a few percent. HALO is only present as traces in the waste, so its high leaching efficiency is not as problematic as it appears. Yttrium and europium take up 84.8 and 5.4 wt% of the dissolved elements. After that, barium (4.6 wt%), calcium (1.6 wt%), aluminium (1.2 wt%) and strontium (1.1 wt%) take up most of the rest fraction. This may not be a problem, as solvent extraction was attempted later on to extract yttrium and europium from the PLS (see section 3.9).

3.6.2 *Optimization of leaching YOX with 2.5 vol% MSA*

Now that it is known that 2.5 vol% MSA can leach the YOX phosphor, the remaining two parameters of the reaction were determined: the optimal leaching time and the optimal liquid-to-solid ratio. To determine the optimal leaching time, samples containing 15 mL 2.5 vol% MSA per g of phosphor waste from which HALO was removed were and heated at 80 °C for different amounts of time. The results are in Figure 19. One hour seems to be enough to leach YOX completely. Cerium and terbium on the other hand are leached more than a percent less compared to leaching for two hours, so this increases the selectivity of YOX over LAP slightly.

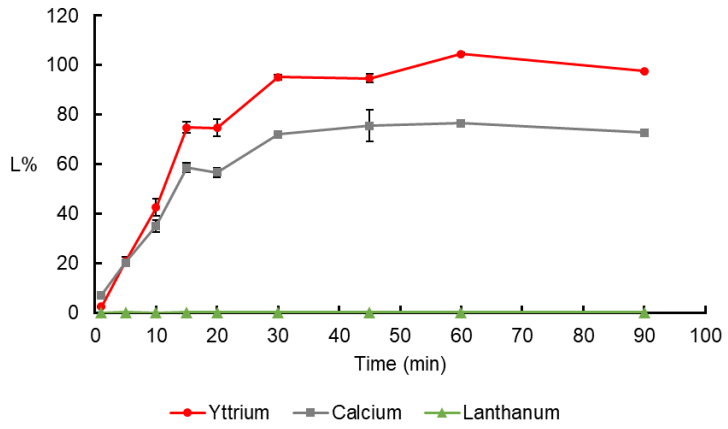

Figure 19: Kinetics of the leaching reaction of the main elements of the four phosphors. Temperature: 80 °C, L-to-S ratio: 15 mL/g.

Samples with different liquid-to-solid ratios were heated at 80 °C for two hours. The results are shown in Figure 20. The highest leaching efficiency for yttrium (and also europium) was achieved at a liquid-to-solid ratio of 10 mL/g, but the error on the value is quite high while that of a liquid-to-solid ratio of 12.5 mL/g is much smaller. It seems that a liquid-to-solid ratio of 10 mL/g is too close to the drop-off at lower liquid-to-solid ratios to be reliable, so 12.5 mL/g is chosen instead. It does have a slightly higher leaching efficiency than the 15 mL/g used in the previous two experiments. The leaching of cerium and terbium is also slightly suppressed compared to a liquid-to-solid ratio of 15 mL/g.

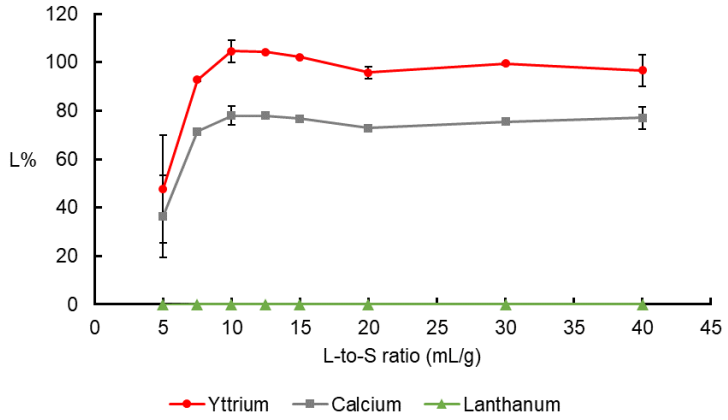

Figure 20: Effect of the L-to-S ratio on the leaching efficiency of the main elements of the four phosphors. Temperature: 80 °C, time: 2 hours.

3.7 Current integrated flowsheet

The current flowsheet using 2.5 vol% MSA to leach YOX instead of the IL is given in Figure 21. Performing all the leaching steps after each other is discussed later on in section 3.11.

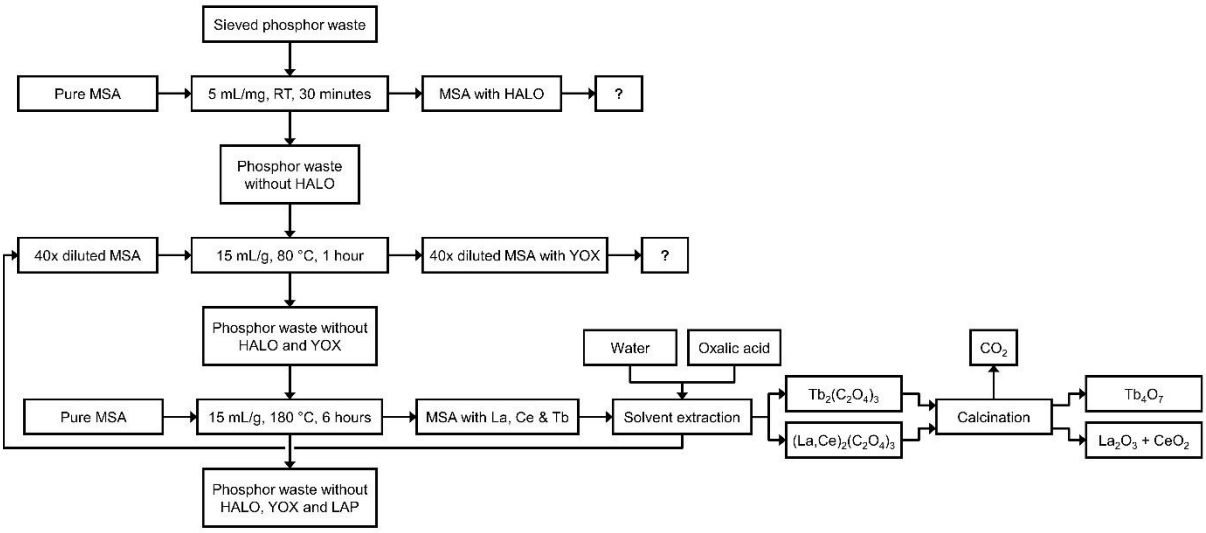

Figure 21: Second integrated flowsheet, with some loose ends.

Although all the leaching parameters of the three steps (removing HALO, leaching YOX and leaching LAP) are now known, there are still some loose ends in the flowsheet. The 2.5 vol% MSA emerging after the solvent extraction of lanthanum, cerium and terbium can be recycled to leach the YOX phosphor from the next batch, but three others remain: (1) the pure MSA containing the unwanted HALO, (2) extracting and purifying the yttrium and europium from the 2.5 vol% MSA PLS, and (3) the barren 2.5 vol% MSA left after removing the yttrium and europium. These three issues are worked out in their own sections.

3.8 Closing the loop: purification of HALO-rich MSA PLS

The first issue tackled is the HALO-rich MSA. Two techniques were attempted: solvent extraction and vacuum distillation.

3.8.1 *Preparation of HALO rich MSA PLS*

Since solvometallurgy (and also hydrometallurgy) are featured in this master thesis, it would be fitting if HALO could be extracted from the pure MSA using solvent extraction. HALO consists of mostly calcium phosphate, so possible extractants for removing these two compounds were searched. First, some pure MSA containing HALO was needed to perform possible solvent extraction experiments on. 20 g of sieved waste and 100 mL pure MSA were stirred for one hour at room temperature. The PLS was filtered using syringe filters. These also clogged rather fast so it was decided to leave the mixture to settle overnight, and the next morning most of the solids had settled on the bottom, making the filtering using syringe filters much easier. Although the kinetics of the leaching reaction in Figure 15 suggest that equilibrium is achieved after 30 min, some further leaching might have occurred, but for reason to be explained later this was not important. A TXRF measurement afterwards showed concentrations similar to those after leaching for only 30 min.

As HALO also consists of phosphor (in the form of phosphate) and chlorine (in the form of chloride) and MSA consists of sulfur, a small test was performed to see if ICP-OES could reliably detect these elements, as it should be able to according to a periodic table distributed by the manufacturing company of the ICP-OES device. The reason to measure sulfur is to see if some MSA gets extracted as well, which would be undesirable. Sulfur was measured quite accurately at a concentration it was expected at. Phosphor was measured, but at a very low intensity, making its measurements not entirely accurate Chlorine cannot be measured in a nitric acid solution because it is oxidized to volatile molecular chlorine (Cl_2) and then adsorbs on the plastic tubing. The possible solutions are: measuring in pure water (which could precipitate the calcium phosphate) or diluted sulfuric acid (removing the ability to measure sulfur). [d] It was decided not to measure it as it would have taken too much time to prepare and measure all the measurement samples twice for only one element present as a trace in the HALO phosphor.

3.8.2 *Solvent extraction*

The extraction of calcium using di-(2-ethylhexyl)phosphoric acid (D2EHPA)[90] and extracting phosphoric acid (H_3PO_4) using tributyl phosphate (TBP)[91–94] as described in the literature was tested. As the presence of $CaCl_2$ improves the extraction of H_3PO_4 from water,[94] it was decided to extract phosphoric acid first as the presence of calcium in the MSA might have the same effect. According to PubChem,[e] MSA is immiscible in hexane, but dodecane was chosen as a solvent as it is less dangerous and has a much higher flash point. Pure dibutyl sulfoxide is also

[d] As described in an ICP operations guide written by Paul R. Gaines, PhD, from Inorganic Ventures™
[e] https://pubchem.ncbi.nlm.nih.gov/

capable of extracting H_3PO_4,[95] but this might be too polar to be immiscible with MSA, so this was not attempted. To strip H_3PO_4 from the organic phase, deionized water can be used.[91] As calcium triphosphate ($Ca_3(PO_4)_2$) is not very soluble in water (0.01 – 0.10 g/L),[96] the aqueous H_3PO_4 stream from extracting phosphoric acid could be used to facilitate the stripping of calcium as it would precipitate, pulling the equilibrium towards stripping. The water could be recycled back to the stripping of phosphoric acid. The clean MSA can be sent back to the leaching step to remove HALO. The proposed flowsheet is presented in Figure 22. It was advised to check Cyanex 923 (a mixture of alkyl phosphine oxides) if it was also capable to extract H_3PO_4.

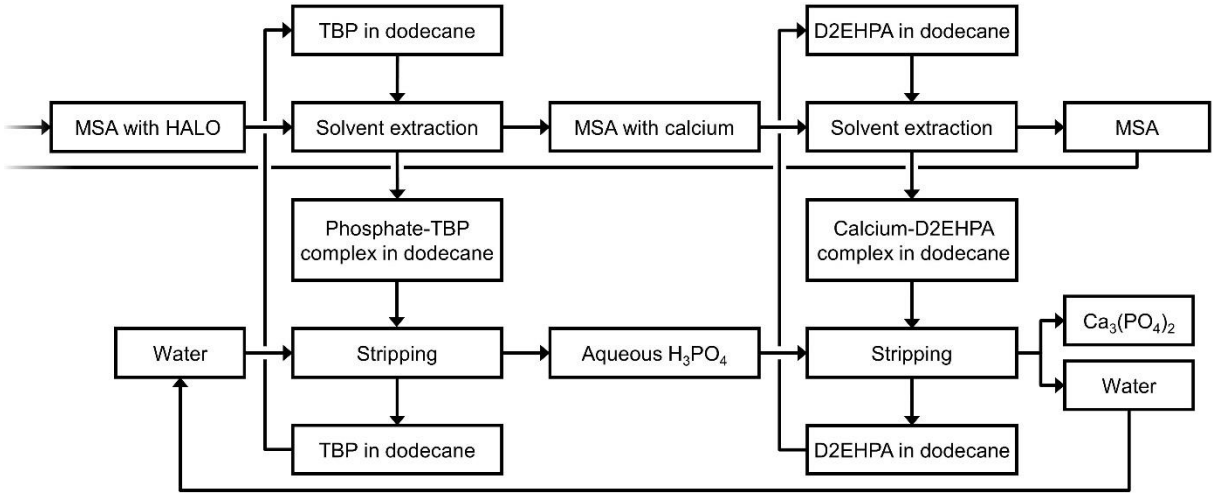

Figure 22: Proposed flowsheet to recover calcium and phosphate from the MSA. The recycled MSA is sent back to the leaching of HALO from the phosphor waste.

Several concentrations of either TBP, Cyanex 923 or D2EHPA in dodecane (20, 35, 50, 65 and 80 vol%) were made for the extraction of calcium and H_3PO_4. For extracting phosphoric acid, samples in duplicate were made using the HALO in MSA PLS and every concentration of both TBP and Cyanex 923 in O/A phase ratios of 1 and 2. After shaking and centrifuging the samples, the phase ratio differed greatly from what they were before; the heavier MSA phase had a larger volume, and the samples with an increasing concentration of extractant had an increasing volume of the MSA phase. A short test showed that Cyanex 923, TBP and D2EHPA all dissolve into pure MSA, whether they are added pure or dissolved in dodecane. Cyanex 923 even heats up when dissolving in the MSA. So instead of extracting phosphate or calcium from MSA to dodecane, the extractant itself switches from the dodecane phase to the MSA phase.

In an attempt to save the method, some other diluents were tried, and an aromatic diluent was suggested. Toluene, *p*-cymene and a mixture of dodecane and toluene were all immiscible with MSA, but all three extractants in these diluents migrated to the MSA phase every time. Adding some decanol as a modifier did not help and it migrated to the MSA too. In the case of Cyanex 923, the extractant is capable of making the MSA and toluene mutually miscible. It is clear that solvent extraction is not an option to remove calcium phosphate from the MSA PLS. Diluting the MSA with water might work as no extractants are reported to migrate,[86] but after a successful extraction the diluted MSA has to be purified using distillation. The next method is very similar to distillation, so compared to that, performing solvent extraction on diluted MSA seems like an unnecessary step, making it more complex.

3.8.3 *Vacuum distillation*

Vacuum distillation was actually performed before the failed solvent extraction experiments, and a PLS was prepared by combining the filtered samples of the leaching experiments using pure MSA. The solvent extraction experiments were still performed as it could have been more elegant, but the miscibility of the extractant in MSA sabotaged that. The MSA was distilled off at a pressure of 1.1 mbar and a temperature of 140 °C, and the residue left in the flask looked very similar to pitch. ICP-OES was used to measure the concentration of the elements in the MSA before and after the vacuum distillation. All measured elements were removed for more than 99 %. Only the silicon content increased, but this is most likely due to some vacuum grease used to seal the setup that ended up in the distilled MSA. The amount of phosphate (in the form of H_3PO_4 as no cations are present) was measured to be 44 ± 3 mg H_3PO_4 per liter MSA. TXRF could not detect any elements left in the distilled MSA. A ^{1}H-NMR was also taken of the distilled MSA, of which the spectrum can be found in Figure 41 in Appendix 5. No degradation seems to occur as the spectrum is almost identical to that of clean MSA. The dark matter was dried on the Schlenk line and around 0.2 g was dissolved in either pure HCl or pure HNO_3 and stirred at room temperature for a day. The HCl-sample was black at first, but a while after the stirring was stopped a black precipitate was formed, leaving a yellow colored solution. The HNO_3-sample was clear and orange, and its color was slightly lighter after filtering some with a syringe filter. The metal concentrations of the filtered samples were measured using ICP-OES and TXRF, and the mass fractions of the components are given in Table 16.

Table 16: Composition of the HALO waste obtained after distilling off the MSA, using different techniques.

Element	Mass fraction HNO_3 (wt%)	Mass fraction HCl (wt%)	Mass fraction solid TXRF (wt%)
Y	0.11	0.11	0.11
Eu	0.01	0.01	0.13
Ca	7.81	7.23	1.32
Sr	0.11	0.23	0.21
Sb	0.12	0.06	-
Mn	0.18	0.18	-
Ba	0.06	0.20	0.15
Mg	0.06	0.05	-
Al	0.13	0.13	-
La	0.01	0.01	< 0.01
Ce	< 0.01	< 0.01	-
Tb	< 0.01	< 0.01	-
Si	0.02	0.02	-
PO_4	3.92	4.00	-
MSA	77.6	72.12	-
Fe	-	-	0.27
Zn	-	-	0.02
W	-	-	0.01
Pb	-	-	0.02

The dark matter itself was also measured with TXRF, using the known concentration of yttrium from the ICP-OES value as an internal standard to quantify the other elements. TXRF also showed traces (< 0.01 wt%) of potassium, nickel, copper, bromine and mercury (1 ppm) in the solid sample. The tungsten measured is probably originating from the tungsten electrodes of the fluorescent tubes (see section 1.4.1).

Because of the full removal of dissolved elements, the very low concentration of phosphoric acid left and no apparent degradation, the MSA seems fully reusable, but this was not tested anymore due to time constraints. Vacuum distillation thus seems a successful technique to close the loop of leaching HALO, only the loss of some MSA during the distillation and the price of such a low vacuum needed are disadvantages.

3.9 Closing the loop: purification of YOX rich diluted MSA PLS

The next loose end in the flowsheet is getting the yttrium and europium out of the 2.5 vol% MSA in which YOX was dissolved. As the solvent extraction to extract terbium from the diluted LAP PLS also extracted yttrium and europium that were leached from traces of YOX left in the HydroWEEE residue,[86] the same extraction procedure was attempted. This consists of bringing the diluted MSA PLS into contact with 70 vol% D2EHPA in xylene three times, combining the tree D2EHPA fractions and precipitating the REEs by contacting it with a concentrated oxalic solution. The full flowsheet of this is discussed in detail in section 1.6.6.

3.9.1 *Solvent extraction*

To perform the solvent extraction experiments, a rather large volume PLS was needed, so the filtered samples of the leaching experiments using 2.5 vol% MSA were combined. 6 mL of this PLS was mixed with 6 mL 70 vol% D2EHPA in xylene (thus with an A/O ratio of 1) on a shaker for 10 min, centrifuged to facilitate the phase separation and its two phases separated as described in section 2.3.3. The following two steps each used 0.5 mL less to leave some PLS for ICP-OES and TXRF analysis. The (cumulative) extraction efficiencies of each step compared to the original PLS is calculated from the change in composition of the PLS using the ICP-OES values, and they are given in Table 17. Some values were negative, most likely because the concentration of these elements was below the detection limit of ICP-OES. These can be assumed to be close to zero. It can be seen that, as predicted, yttrium and europium are extracted completely in three steps, and most of the traces of cerium and terbium too. The only unwanted and significant extraction is that of calcium. After every extraction step, the amount of phosphorus measured rose with around 0.07 mg PO_4 per mL, probably indicating small losses of D2EHPA from the organic phase to the PLS.

Table 17: Cumulative extraction efficiencies of all measured elements and their original concentration in the PLS.

Element	PLS concentration (mg/mL)	Extraction efficiency step 1 (%)	Extraction efficiency step 2 (%)	Extraction efficiency step 3 (%)
Y	5.30	98.3	100.0	100.0
Eu	0.34	94.1	99.9	100.0
Ca	0.10	94.4	96.2	96.6
Sr	0.07	-	-	-
Sb	0.01	14.6	29.6	21.6
Mn	< 0.01	5.6	4.4	6.0
Ba	0.31	-	-	-
Mg	0.02	-	-	-
Al	0.06	2.5	4.9	19.6
La	< 0.01	-	-	27.1
Ce	0.02	47.0	77.8	91.1
Tb	0.01	94.1	98.6	99.5
Si	0.04	-	-	-

For the stripping part, the three D2EHPA in xylene fractions were combined, except for a small amount to measure its contents using TXRF. A concentrated aqueous oxalic acid solution was prepared by adding an excess of oxalic acid to Milli-Q water, shaking the mixture for some minutes and filtering it. For the stripping, 10 mL of combined D2EHPA in xylene and 0.5 mL of the concentrated oxalic acid solution (O/A ratio of 20) was shaken for forty minutes, centrifuged and separated, using the same conditions as used in the literature.[86] A white precipitate appeared in the aqueous phase. It was possible to separate this precipitate by sucking it up along with some water with a pasteur pipette and then evaporating the water off in an oven overnight at 90 °C. The precipitate was not filtered off and washed to remove oxalic acid as the amount was quite low and there was the risk of losing it during these steps, so it most likely contained some oxalic acid too. The aqueous oxalic acid solution only contained small traces of most elements, and the most abundant is aluminium at 0.12 mg/mL. 2 mg of the oxalates were dissolved in HNO_3 and analyzed using ICP-OES and TXRF, and TXRF was performed directly on the solid as well, using the yttrium concentration obtained from the ICP-OES measurement as an internal standard. The weight fractions of the oxalate salts are given in Table 18. Apparently, yttrium is not stripped very well from the D2EHPA phase as its mass fraction is around the same value for europium while it is more than ten times more abundant in the PLS. Calcium on the other hand is stripped, forming a contamination of the product. The TXRF measurements on the D2EHPA phase before and after stripping confirm this trend of yttrium not being stripped very well, and the stripping efficiencies and starting concentrations for all measured elements are given in Table 19.

Table 18: Composition of the oxalates measured using ICP-OES and TXRF.

Element	Mass fraction oxalate in HNO3 (ICP-OES) (wt%)	Mass fraction oxalate in HNO3 (TXRF) (wt%)	Mass fraction (solid TXRF) (wt%)
Y	38.17	37.3	38.17
Eu	33.88	29.0	43.23
Ca	0.85	3.4	
Sr	0.01	-	
Sb	-0.15 (= < 0.01)	-	
Mn	< 0.01	-	
Ba	0.01	-	
Mg	0.02	-	
Al	1.14	-	
La	0.01	-	
Ce	1.40	1.71	1.63
Tb	0.64	-	
Si	0.05	-	-
PO_4	0	-	-
MSA	0.02	-	-
Gd	-	-	2.72
Zn	-	-	< 0.01
Pb	-	-	0.28

Table 19: Starting concentration of the organic phase before stripping and the stripping efficiencies.

Element	Loaded D2EHPA concentrations (mg/mL)	Stripped D2EHPA concentrations (mg/mL)	Stripping efficiency (%)
Y	2.00	1.78	11.1
Eu	0.11	-	100
Ca	0.01	-	100
Ce	< 0.01	-	100
Fe	< 0.01	< 0.01	1.64
Zn	< 0.01	-	100

It can be seen that the calcium is stripped completely, so a way must be found to remove it. Either the waste obtained after removing most of the HALO can be leached again to remove the last traces of HALO, or a step can be added somewhere in the flowsheet to selectively remove calcium. An aqueous sulfuric acid solution could be used either before, during or after the solvent extraction step to remove calcium selectively as calcium sulfate has a lower solubility in water (2.01 g $CaSO_4$ per liter water at 18 °C)[96] than yttrium sulfate (74.6 g $Y_2(SO_4)_3$ per liter water at 20 °C)[97] or europium sulfate (25.6 g $Eu_2(SO_4)_3 \cdot 8H_2O$ per liter water at 20 °C).[96]

To strip yttrium completely, either a lower O/A-ratio can be used (a ratio of 20 is not feasible in industrial mixer-settlers anyway), a longer contact time or a different method can be used. In

industry, aqueous nitric acid is used to strip the REEs after solvent extraction to separate them using acidic extractants like D2EHPA. From this the REEs can be precipitated as oxalates using oxalic acid, as hydroxides using aqueous ammonia or sodium hydroxide or as carbonates using ammonium or sodium bicarbonate. The precipitated REEs are then calcined to produce their oxides.[48]

3.10 Closing the loop: recovery of pure MSA from 2.5 vol% MSA

The last loose end in the flowsheet is the recovery of pure MSA from 2.5 vol% MSA in water so it can be re-used to leach the LAP phosphor. A simulation using the OLI Studio software shows that water and MSA form an azeotropic mixture at 90 vol% MSA at atmospheric pressure, so direct distillation to remove MSA from the water is not possible. The simulation shows that the composition of the azeotropic mixture is dependent on the pressure, and lower pressures lead to azeotropic mixtures containing less water. Figure 23 shows the bubble point and dew point curves for the MSA-H_2O mixture for different pressures, and the azeotropes are located where both curves meet. This opens up the option for a pressure swing distillation. In this method, the diluted MSA is heated at a low pressure to distill off pure water and obtain the azeotropic mixture characteristic for that pressure. By then increasing the pressure, the mixture is now positioned on the other side of the azeotropic mixture characteristic for the new higher pressure, so heating this mixture now results in the distillation of pure MSA from the mixture. This mixture can then be added to the next batch of 2.5 vol% MSA to reduce losses. Both pressures should be low enough so that no temperatures above 200 °C are needed as MSA decomposes when distilled at atmospheric pressure,[98] and no thermal stability can be guaranteed above 200 °C.[86] The only source found was a safety document from the company Arkema, stating that MSA decomposes above 215 °C.[f] The difference in position of the azeotrope between the two pressures must be large enough for the pressure swing distillation to be feasible however. At a pressure of 0.001 atm, the azeotrope has a composition of 98 vol% MSA (93 mol%) and a temperature of 119 °C, and at a pressure of 0.050 atm, and the azeotrope has a composition of 94 vol% MSA (81 mol%) and a temperature of 206 °C. These two pressures meet the criteria of both temperature and difference in composition, if the simulation is accurate of course. There are also other techniques available to separate azeotropic mixtures, like performing a reaction selectively on one of the two components to make it possible to distill only one of the two compounds (reactive distillation) or adding a salt that changes the volatilities of the compounds enough so they can be separated.[99] Using pressure swing distillation has the advantage that trace elements present in the 2.5 vol% MSA cannot contaminate the MSA when evaporating it in the second step, making the MSA more reusable.

[f] Found at https://www.arkema.com/export/shared/.content/media/downloads/socialresponsability/safety-summuries/Thiochimicals-AMS-Metanesulphonic-acid-GPS-2014-07-31-V0.pdf

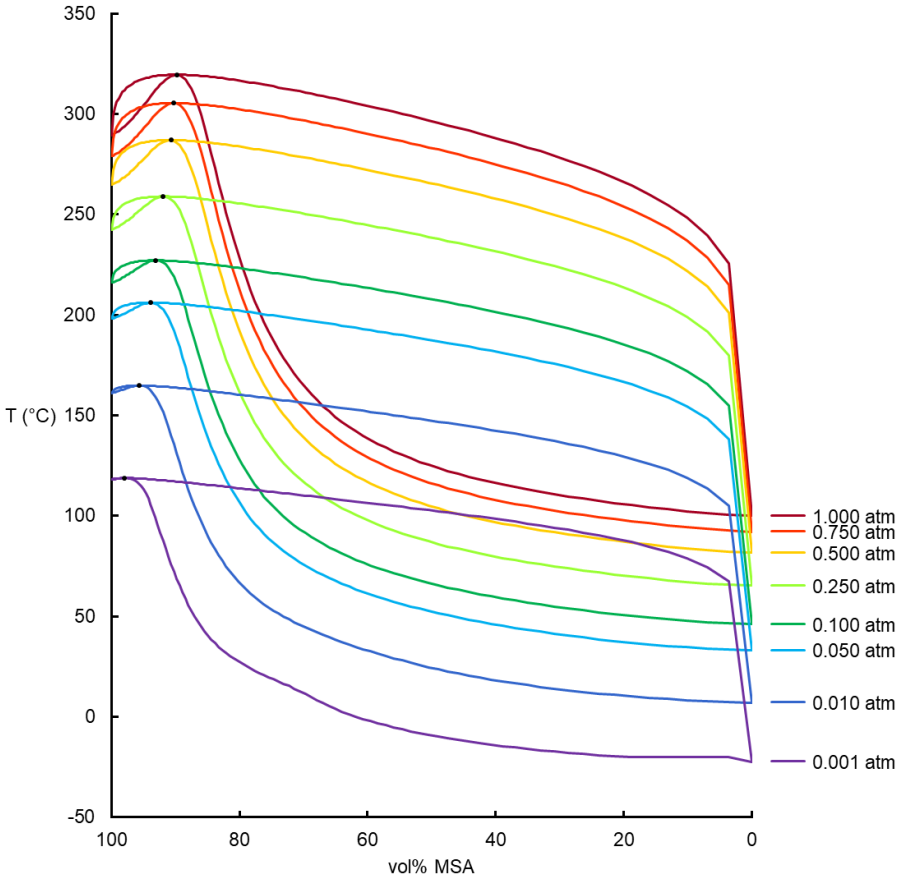

Figure 23: Bubble point (bottom) curve and dew point (top) curve of the MSA-H_2O mixture at different pressures. The azeotrope is located where both curves meet.

3.11 Second attempt at a new integrated flowsheet

With all the loose ends now closed, the proposed flowsheet given in Figure 24 is now complete.

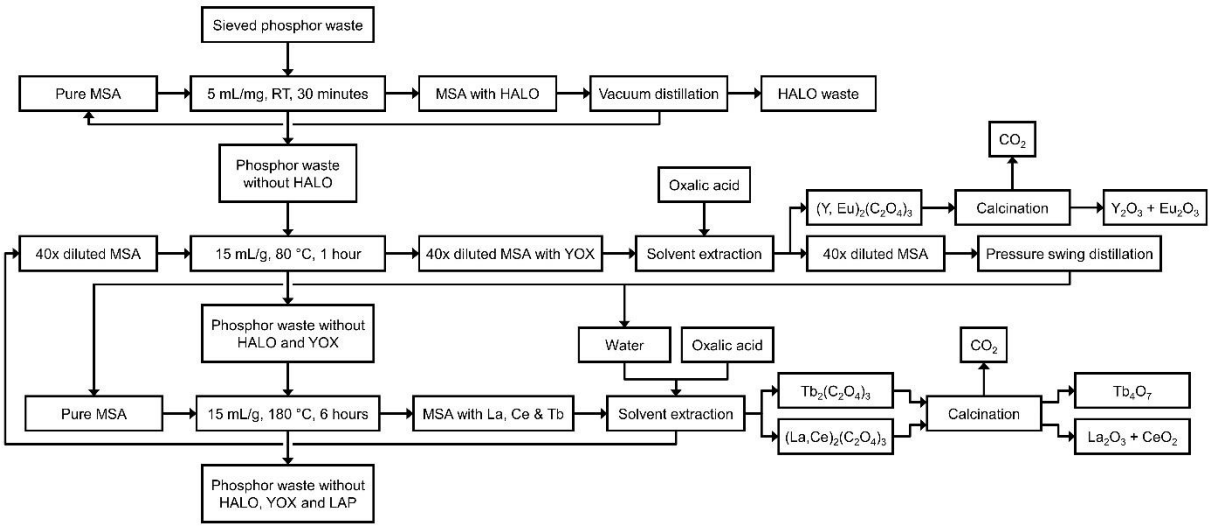

Figure 24: Final version of the proposed flowsheet with all loops closed.

The first leaching step was already performed as the starting material was the waste from which HALO was removed, discussed in section 0. Around 3.2 g waste and 40 mL 2.5 vol% MSA were stirred at 80 °C for one hour. The sample was filtered using a sintered glass funnel on a Büchner flask and washed with water. Using water to wash the residue is not a problem compared to the leaching of HALO as all phosphors are leached less with lower MSA concentrations. A small sample of the PLS had its composition measured using ICP-OES. Around 2.7 g residue was recovered and MWD was used to characterize it. The leaching efficiencies, concentrations in the PLS and relative change in composition in the residue are given in Table 20. The values for antimony should not be trusted as its concentration is too low to be measured accurately. Apart from some traces of the HALO and BAM phosphors, the PLS is rather pure. TXRF also measured traces (< 0.01 mg/mL) of copper, zinc and lead.

Table 20: Leaching efficiencies, concentrations of the elements in the 2.5 vol% MSA PLS and relative change in residue composition.

Element	Leaching efficiency (%)	Concentration (mg/mL)	Relative change in phosphor content based on MWD (%)
Y	94.7	6.20	-93
Eu	89.1	0.40	-90
Ca	68.8	0.11	-30
Sr	67.0	0.07	-66
Sb	(171.5)	0.01	(+414)
Mn	14.4	< 0.01	-27
Ba	-	0.37	-
Mg	-	0.01	-
Al	-	0.05	-
La	< 0.1	< 0.01	-7
Ce	0.6	0.01	-8
Tb	0.8	< 0.01	0
Si	-	0.04	-
PO_4	-	0.05	-

For leaching LAP, around 1 g of the previous residue and 15 mL MSA were stirred and heated at 180 °C for six hours. The mixture was filtered in a sintered glass filter on a Büchner flask and washed with water. The leaching efficiencies and concentrations of the elements are given in Table 21. The LAP elements leached slightly above 100 %, but this can be due to a small error in the MWD measurements. The HALO and YOX elements are only present as traces in the residue, so their high and inaccurate leaching efficiencies only cause small impurities. Only yttrium is present in quite a high concentration. The remaining residue was not characterized anymore. The compositions of the phosphor waste at the start and after each step is given in Table 22.

Table 21: Leaching efficiencies and concentration of the elements in the pure MSA PLS.

Element	Leaching efficiency (%)	Concentration (mg/mL)
Y	112	0.43
Eu	80.5	0.03
Ca	44.6	0.04
Sr	98.7	0.03
Sb	53.1	0.02
Mn	90.4	< 0.01
Ba	-	0.01
Mg	-	0.04
Al	-	0.23
La	105 (=100)	1.39
Ce	106 (=100)	0.88
Tb	106 (=100)	0.46
Si	-	0.18
PO_4	111	2.09

Table 22: Change in composition of the phosphor waste at the start and after each step.

Element	Initial composition (wt%)	Composition after leaching HALO (wt%)	Composition after leaching YOX (wt%)
Y	10.1	8.2	0.6
Eu	0.67	0.56	0.06
Ca	7.9	0.20	0.14
Sr	0.37	0.127	0.043
Sb	0.110	0.010	0.052
Mn	0.172	0.004	0.003
La	1.47	2.12	1.98
Ce	0.97	1.35	1.24
Tb	0.48	0.647	0.647

The same brown precipitation appeared in the flask when washing the residue, leaving the rest of the solution almost completely colorless, and a very small amount of it could be isolated. It was measured as a solid using TXRF as the same precipitation formed in the ICP-OES samples of previous measurements, making ICP-OES not usable. The composition is given in Table 23. The major part of it consists of aluminium and iron, both of which are not important for this master thesis, so this precipitation is actually a good thing as it removes these unwanted elements. Iron is probably responsible for the brown color of the precipitation, and partially for the black color of the MSA after leaching. A small amount was also dissolved in a solution of deuterated sulfuric acid in deuterated water to take a ^{1}H-NMR and a ^{13}C-NMR spectrum to see if any organic components were present too as TXRF cannot measure light elements like carbon or hydrogen. No hydrogen or carbon could be detected, so the precipitate was purely of inorganic nature, meaning that the MSA did not decompose.

Table 23: Composition of the precipitate.

Element	Concentration (%)
Y	0.21
Eu	0.01
Ca	0.34
Sr	0.02
Mn	0.08
Ba	3.03
Al	73.6
La	1.01
P	2.51
S	3.05
K	0.94
Cr	2.78
Fe	10.3
Ni	1.03
Cu	0.07
Br	0.32
W	0.29
Hg	0.39
Pb	0.07

4 Conclusion

The original flowsheet using the IL [Hbet]Tf_2N] to leach the red YOX phosphor and then leaching with methanesulfonic acid (MSA) to leach the green LAP phosphor selectively was not satisfactory as the white HALO phosphor contaminated the pregnant leach solutions. Many options were attempted, and in the end a selective removal of the HALO phosphor was achieved using pure MSA at room temperature. This removal dissolves less valuable YOX than what is already proposed in the literature,[77] making it a more interesting option.

With this newly discovered removal step, the leaching of YOX with the IL and the leaching of LAP with MSA is improved by severely lowering the concentrations of contaminants in the pregnant leach solutions. The leaching of the YOX phosphor with the IL takes a very long time, and making the IL is very costly, so a different leaching agent was searched for. From some experiments with the purpose of searching a way to remove HALO selectively, it seemed possible to leach the red YOX phosphor a lot faster using MSA diluted in water. As the solvent extraction part to separate the valuable terbium from lanthanum and cerium produced an aqueous MSA solution with a concentration of 2.5 vol%, it was attempted to leach the YOX phosphor with this, recycling it and reducing the waste generated. This attempt was successful, and this leaching process with 2.5 vol% MSA is much cheaper and faster than leaching with the IL, so the latter was replaced by the former.

Not only the leaching steps of a flowsheet are important, ways must be found to separate the wanted products from the unwanted ones. There were three such steps needed to close all the loops in the flowsheet. The first was to recycle the pure MSA from the removal step for HALO. Solvent extraction was attempted, but several investigated extractants did not stay in the organic phase and dissolved in the MSA phase. Vacuum distillation was much more successful, and is also more effective to drastically reduce the amount of trace elements present as only the MSA is removed. Even if the solvent extraction was successful, it was only designed to remove calcium and phosphate from the MSA and the other trace elements present in HALO might not have been removed.

The second loop that needed closing was recovering the yttrium and europium from the 2.5 vol% MSA they were dissolved in. Solvent extraction was attempted using the same conditions as they were used in the previous research to separate terbium from lanthanum and cerium as small amounts of yttrium and europium heavily contaminated the terbium fraction but not the fraction of lanthanum and cerium.[86] The extraction part using 70 vol% D2EHPA in xylene was successful, but stripping using aqueous oxalic acid was not so selective for yttrium as it was for europium. Traces of calcium present in the waste are extracted and stripped as well, so a way must be found to remove it.

The third and final loop that was still open was turning the 2.5 vol% MSA left after extracting yttrium and europium back to water and MSA. A simulation using the OLI software showed that although water and MSA form an azeotrope making normal distillation impossible, the composition of the azeotrope was dependent on the pressure. This allows the use of a pressure swing distillation where the pressure is changed between two distillation steps to shift the position of the azeotrope from one side of a certain composition of the mixture to the other, so pure fractions can be obtained.

Outlook

Some future research is still needed to optimize the flowsheet. First, the waste still contains traces of HALO as the removal is not fully complete. A second leaching step with pure MSA could remove these traces.

Second, a better stripping step for yttrium and europium is needed. Using techniques already used in industry, like nitric acid, would be interesting.[48]

Third, if the removal of traces of HALO from the waste using a second leaching step is not successful, a way to remove it is needed as it is leached along the YOX phosphor. There is the possibility to selectively precipitate the calcium as a sulfate as it is less soluble than the yttrium and europium sulfates. It can be investigated of this extra step can be done before, after or during the solvent extraction.

Lastly, the reusability of the chemicals used in the flowsheet should be checked, and see if it is possible to scale-up.

Appendices

Appendix 1: Spectra of the lamp phosphors

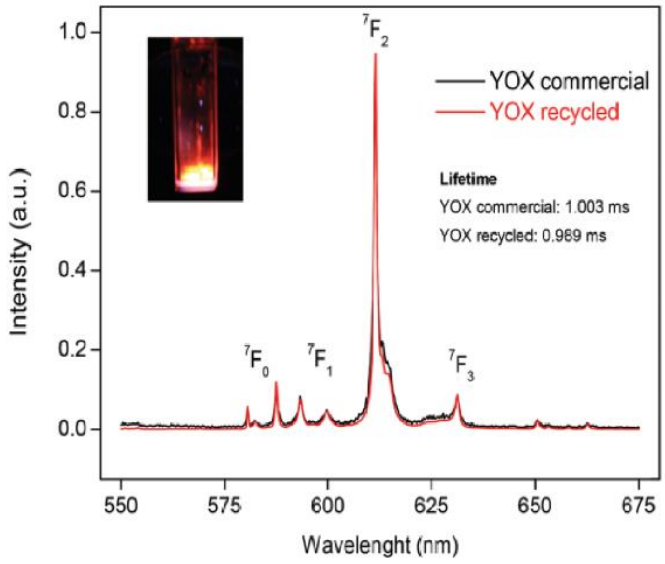

Figure 25: Emission spectrum of the red YOX phosphor. Notice how the peaks are narrow. The inserted picture shows some YOX phosphor held under UV light. The black curve is the spectrum of commercial phosphor, the red curve is phosphor recycled using an ionic liquid, see page 19.[55]

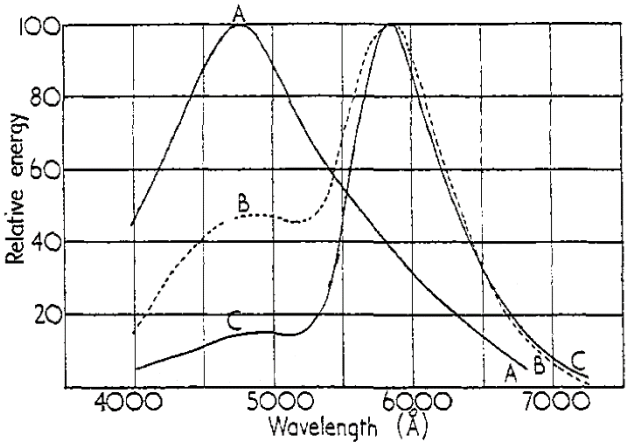

Figure 26: Emission spectrum of the white HALO phosphor with different levels of manganese. A: no manganese, only antimony, light blue color. B: both manganese and antimony, color similar to daylight. C: manganese and more antimony, warm white color. All spectra are adjusted, for a comparison between energies, spectrum C should be multiplied with a factor of 1.3.[64] *(adapted)*

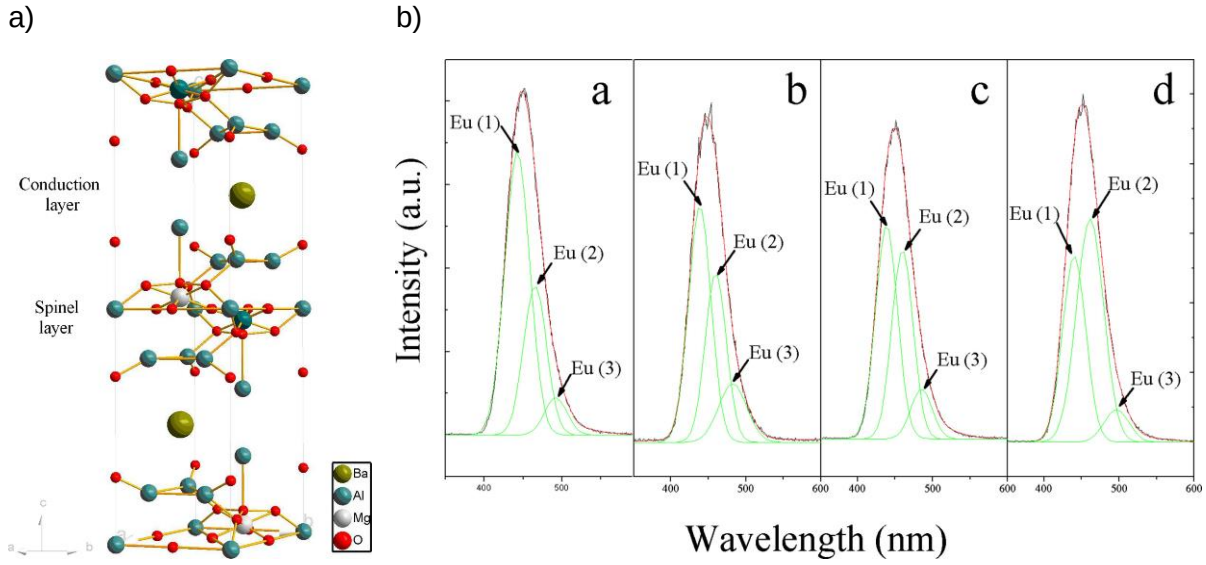

Figure 27: a) Crystal structure of the blue $BaMgAl_{10}O_{17}:Eu^{2+}$ phosphor. The spinel layer consists of AlO_4 tetrahedrons and AlO_6 octahedrons. Magnesium replaces one aluminium atom per lattice cell.[65] b) Emission spectra of the $BaMgAl_{10}O_{17}:Eu^{2+}$ phosphor prepared under different atmospheres using an excitation wavelength of 254 nm (a wavelength emitted by mercury). Eu (1) refers to europium replacing barium atoms, Eu (2) and Eu (3) refer to europium in interstitial positions. Each has a different emission spectrum (green curves).[65]

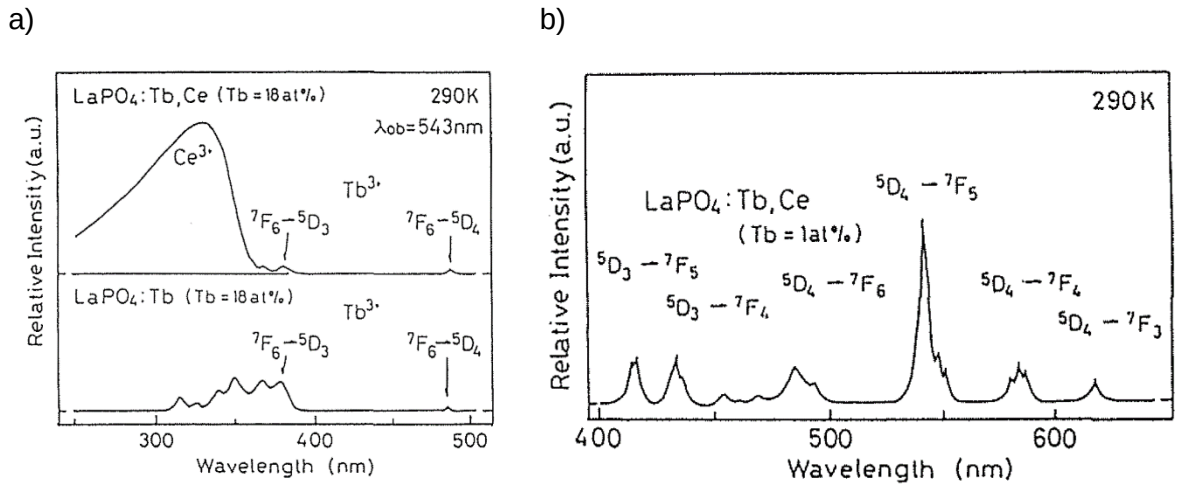

Figure 28: a) Absorption spectrum of the LAP phosphor measured at the green emission of 543 nm, with (top) and without (bottom) Ce^{3+}, showing the need of it to absorb the UV light emitted by mercury. Notice that the absorption band of Ce^{3+} is broad as discussed earlier. b) Emission spectrum of the LAP phosphor after excitation at 365 nm. The highest peak is around 544 nm, which causes the green color of the phosphor. Notice that the peaks of Tb^{3+} are narrow as discussed earlier, and are accompanied by the specific electronic transition responsible for them.[58] (adapted)

Appendix 2: NMR-spectra of the IL [Hbet][Tf_2N]

A ^{1}H-NMR spectrum was recorded (300 MHz, deuterated DMSO, TMS) which showed that the IL was pure and the positions (in ppm) and intensities of the peaks correspond to the literature values:[55] δ (ppm): 3.23 (9 H, s, 3 × CH_3), 4.28 (2 H, s, CH_2) and 11.50 (1 H, s, COOH). The concentration of the IL was quite high in the NMR-sample, causing the very broad peak of the acidic proton of the betaine cation to be visible, something that usually is not. The spectrum can be found in Figure 29, and an enlarged spectrum can be found in Figure 30. The concentration of the IL in the sample was quite high, as can be seen by comparing the size of peak 1 and peak 2 of the IL with the size of the peak caused by the internal standard Me_4Si present in the solvent at δ = 0.00 ppm.

Peak 1 and peak 2 also have some very small satellite peaks lying symmetrically around them, these are caused by the coupling of the hydrogen atoms with the ^{13}C- atoms which have a natural occurrence of around 1 %. Peak 3 is also visible now, and it is so broad because the acidic hydrogen of the [Hbet]-cation is donated in a hydrogen bond with either some water or the negatively charged imide-part of the [Tf_2N] anion.

The small peak at 2.09 ppm is a trace of acetone, which was probably present in the NMR-tube from cleaning it. The small peak at 2.52 ppm is a trace of non-deuterated DMSO present in the deuterated DMSO. The small peak at 3.37 ppm corresponds to water in DMSO solvent and is a small amount of water present in the IL.[100]

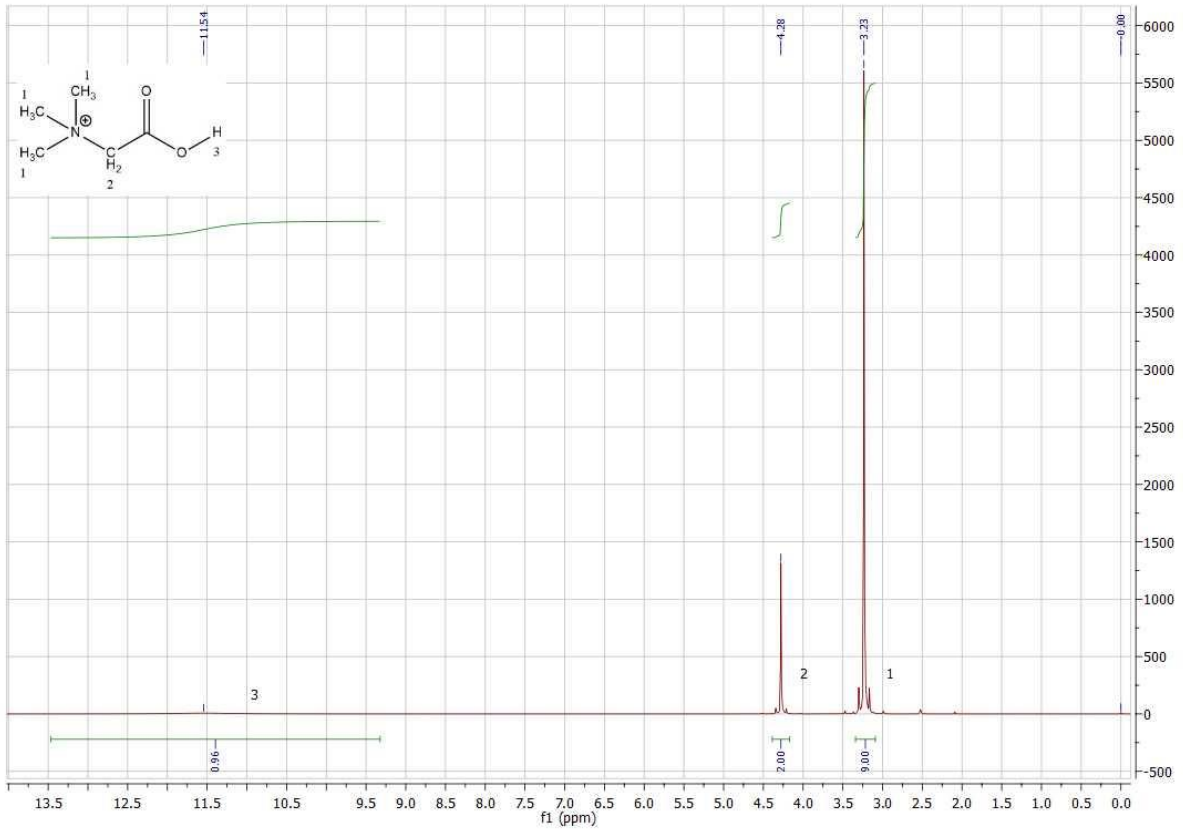

Figure 29: ^{1}H-NMR spectrum of [Hbet][Tf_2N].

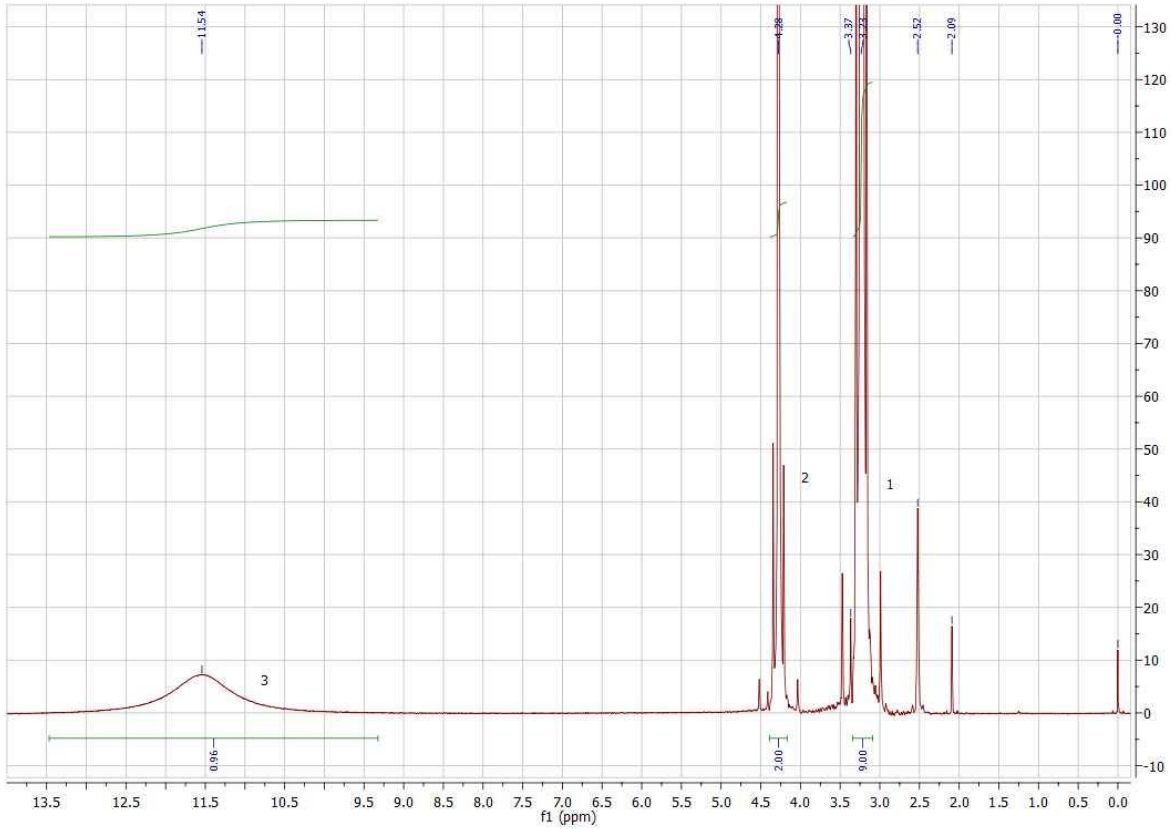

Figure 30: Enlargement of the ^{1}H-NMR spectrum of [Hbet][Tf_2N], making the peak of the acidic proton more visible.

A ^{13}C-NMR was recorded as well (100 MHz, deuterated DMSO, Me_4Si) and the positions of the peaks (in ppm) and coupling constants *J* (in Hz) correspond to the values mentioned in the literature:[55] δ (ppm): 53.09 (s, 3 x CH_3), 63.03 (s, CH_2), 119.68 (q, 2 x CF_3, *J* = 320) and 166.26 (s, COOH). The solvent of deuterated DMSO shows up as a septet and the spectrum was calibrated to let this peak appear at 39.52 ppm.[100] The spectrum can be found in Figure 31.

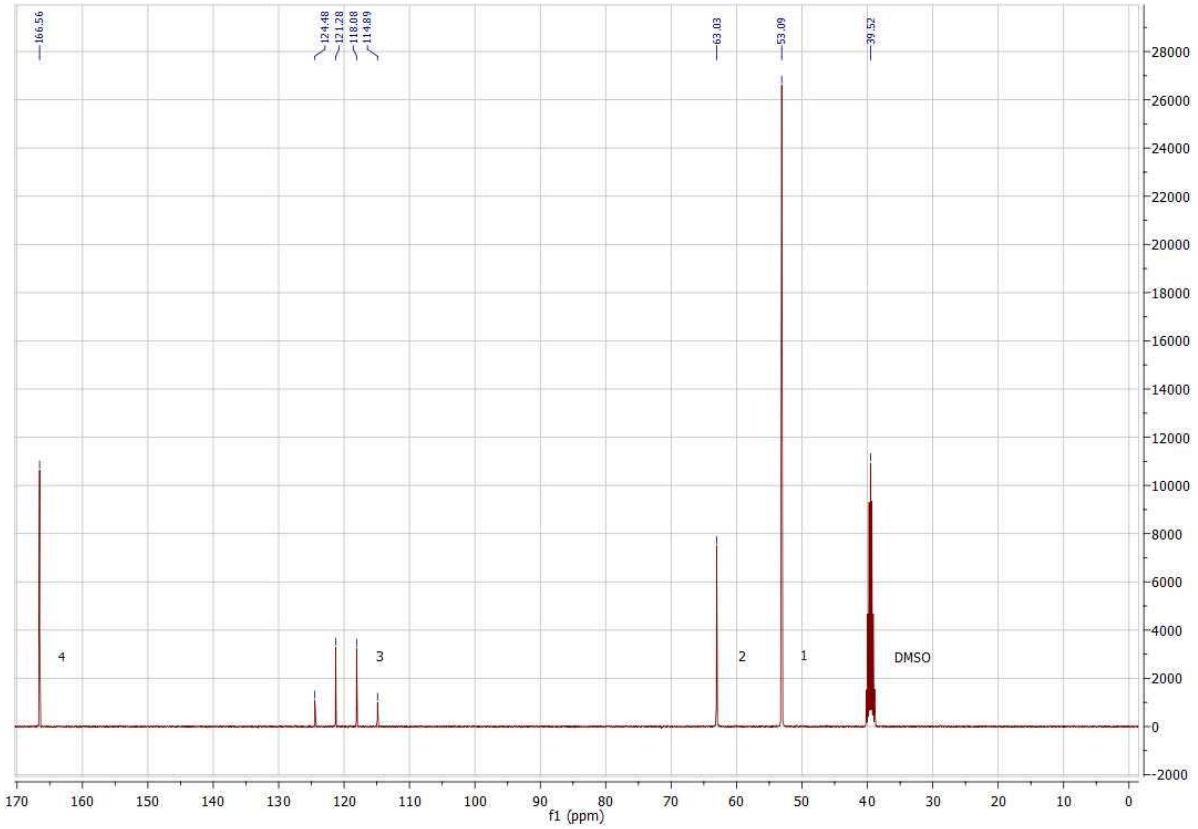

Figure 31: ^{13}C-NMR spectrum of [Hbet][Tf_2N].

Appendix 3: TXRF unreliability

Seven samples were prepared containing different concentrations of europium, yttrium, strontium and calcium along with a fixed amount of IL. Gallium was added as an internal standard, and ethanol was used to end up at the same volume for every sample. The results are shown in Figure 32. The blue colored circles were samples used to make a calibration curve (blue dashed line), the orange colored squares were samples to see if they followed the calibration curve. It seems that high concentrations of europium cannot be measured accurately, and that calcium cannot be measured accurately at both high and low concentrations. The values of yttrium and strontium seem to be more reliable, but the slope of the calibration curve is not equal to one, indicating that the values calculated by the machine do not correspond with the real values.

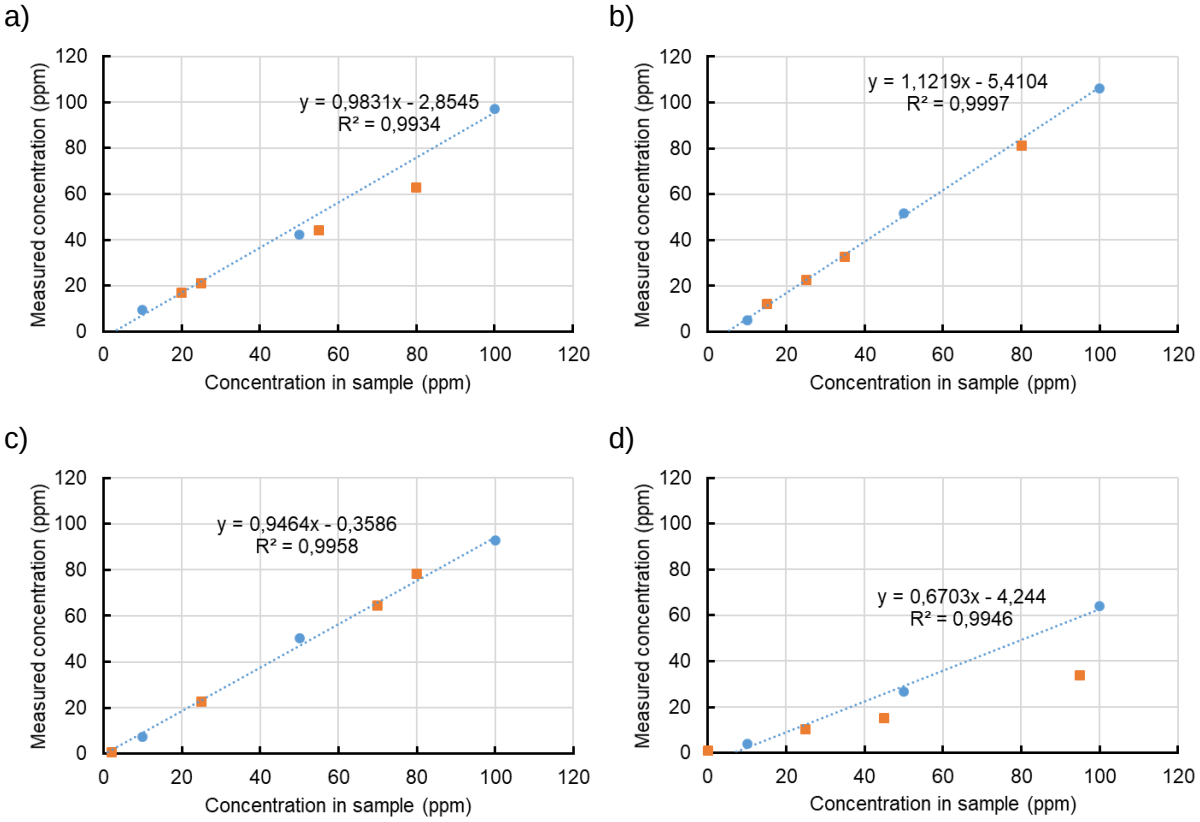

Figure 32: Measured concentrations of a) europium, b) yttrium, c) strontium and d) calcium in function of the real concentrations. The blue squares are the calibration samples and their calibration curve is drawn in a dashed blue line, accompanied by its formula and R^2-value. The orange squares were the samples used to check the reliability of the calibration curve.

Appendix 4: Validation experiments and leaching of unsieved phosphor waste

All the experiments mentioned here instead of in the section 'Results and discussion' were performed either to get familiar with the used techniques or performed on unsieved waste. The results of experiments using unsieved waste were unreliable due to the delivered characterization not corresponding to the actual content. The leaching efficiencies of unwanted phosphors was also higher when trying to leach YOX or LAP selectively.

A.4.1 Confirmation of the leachability of artificial YOX and HALO in IL

The objective of this experiment was to confirm the leaching efficiencies of the YOX and HALO phosphors in the IL containing 5 wt% H_2O. The loading capacity of YOX in the IL according to the literature is 40 mg YOX per g IL after leaching for 40 hours at 90 °C.[55] Calculations show that this is equal to 42 % of the IL forming a complex with the yttrium and europium.

The results obtained for the leaching of the YOX samples can be found in Figure 33, and are compared to the equivalent literature values. For an unknown reason, the errors on the values are very large. The loading capacity seems to be lower than in the literature.[55]

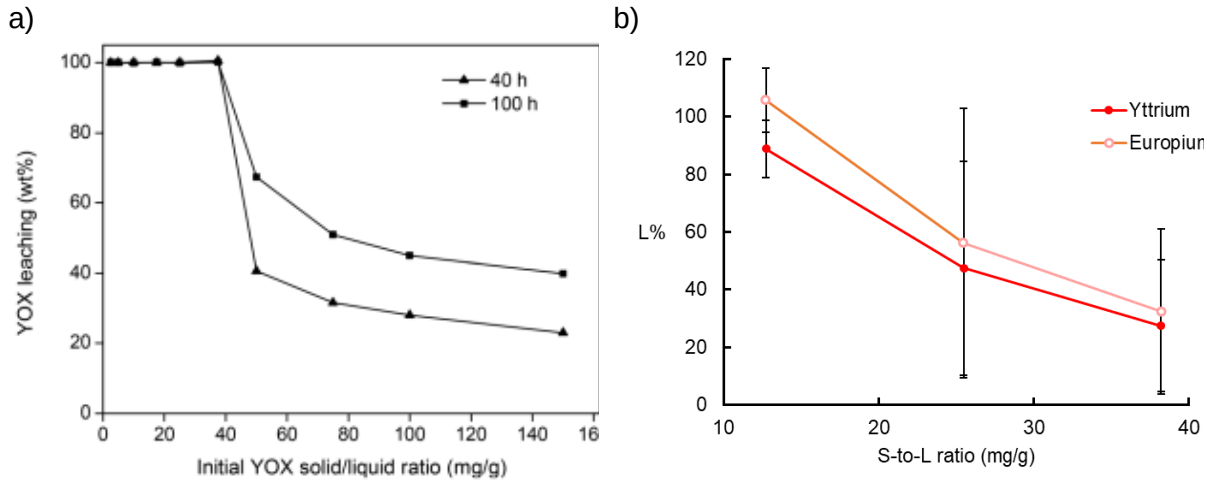

Figure 33: a) Dissolution of YOX in the IL (5 wt% H_2O) in function of the solid-to-liquid ratio, carried out at 90 °C for both 40 hours and 100 hours, as discussed in the literature.[55] b) Leaching efficiencies of yttrium (filled red circles) and europium (open pink circles) after 40 hours in function of the solid-to-liquid ratio.

The leaching efficiency (L%) of calcium from the HALO phosphor was very small as expected. The content of antimony and strontium in the samples were much smaller than in the calibration samples used for ICP-OES, so these could not be measured accurately. The result can be seen in Figure 34.

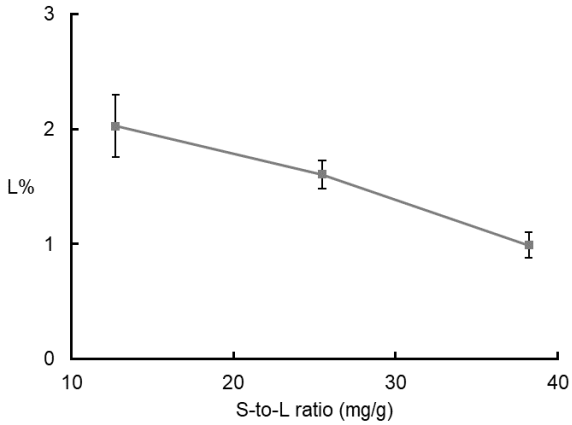

Figure 34: Leaching efficiency of calcium from the HALO phosphor depending on the solid-to-liquid ratio.

A.4.2 Confirming kinetics of leaching artificial YOX with IL and stripping

In this experiment, the YOX leaching kinetics were compared to the literature, using a S-to-L ratio of 20 mg phosphor per mL IL (equal to 12.7 mg phosphor per g IL) and heating at 90 °C. A comparison can be found in Figure 35. YOX seems to leach slower compared to the literature. It is not mentioned in the literature if the IL is pre-heated before adding it to the phosphors.[55] If the IL was pre-heated, it would explain the less steep start of the curve as the IL was cold when it was added to the YOX at time zero, so the phosphor was leached slower until the samples reached 90 °C.

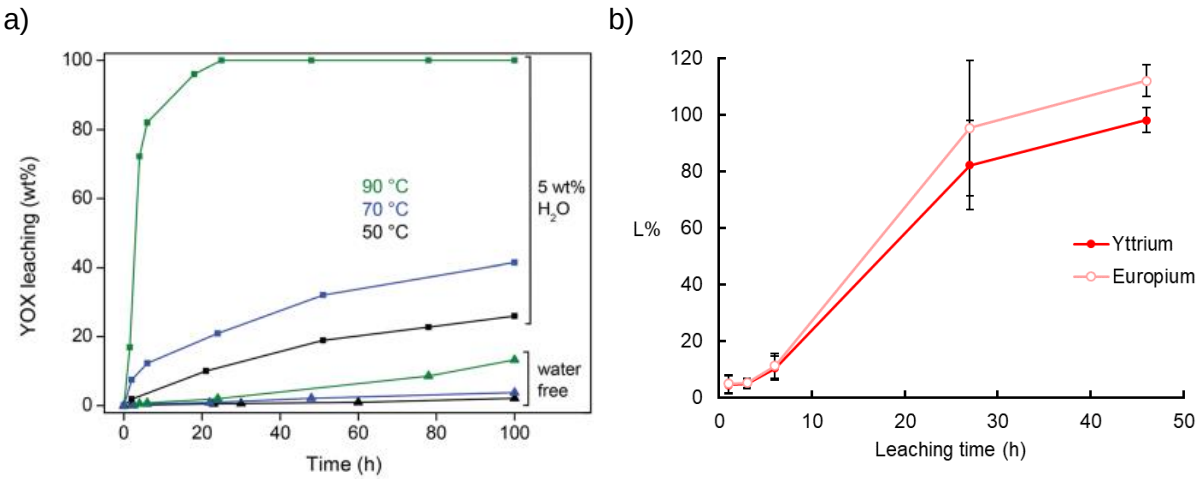

Figure 35: a) Kinetics of leaching YOX depending on the temperature and the water content of the IL as in the literature. S-to-L ratio: 20 mg YOX per g IL.[55] b) Measured kinetics of leaching YOX in IL (5 wt%). S-to-L ratio: 12.7 mg YOX per g IL.

A.4.3 Leaching of a synthetic phosphor mixture in IL

The previous experiments were all performed on individual artificial phosphors, the next step was to verify if it works on a synthetic mixture of phosphors as well. This synthetic mixture was prepared by adding the artificial phosphors together in ratios that are similar to those found in phosphor waste;[55] 2.50 g of HALO, 1.00 g of YOX, 0.25 g of LAP and 0.25 g of BAM were

added to a vial and this was shaken for 2 hours at room temperature to mix them. The samples had S-to-L ratios of 20, 40 or 60 mg/mL, and they were heated at 90 °C for either 22 or 64 hours. The results are in Figure 36. Barium is not included as it only consisted of traces. Only the main element of each phosphor is shown, the other cations of the phosphor have similar values. It can be seen that approximately one day is not enough to leach the YOX phosphor as seen in the literature,[55] but 64 hours certainly is. The LAP phosphor is not leached at all, and HALO leaches a small amount. The S-to-L ratio does not have a very large influence on the leaching behavior compared to the experiment discussed section A.4.1, but the presence of other phosphors in the mixture lowers the amount of YOX per IL, which prevents reaching the maximum loading capacity. These results looked very promising.

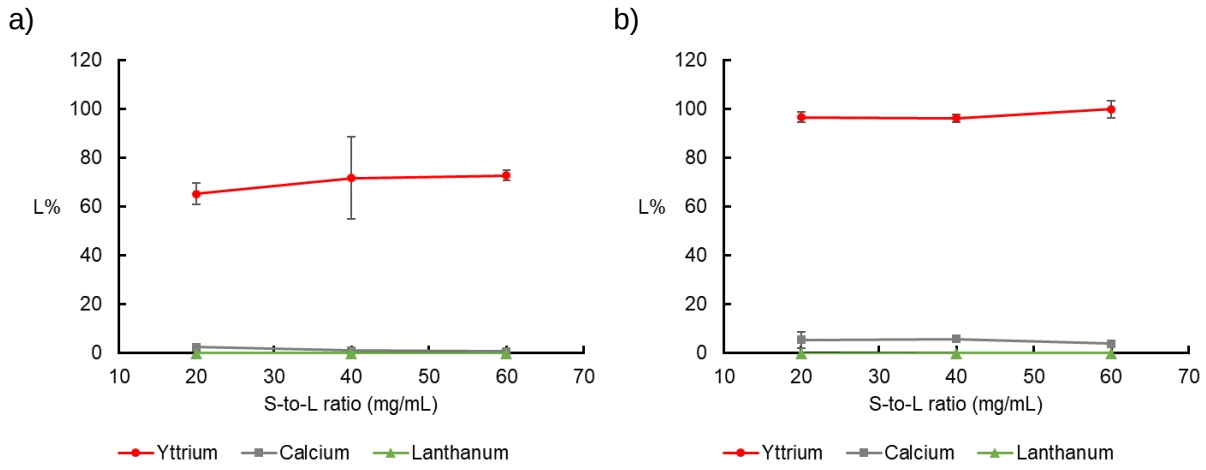

Figure 36: Leaching efficiencies of yttrium, calcium and lanthanum from the artificial phosphor blend in function of the S-to-L ratio after a) 22 hours and b) 64 hours.

A.4.4 Leaching of real phosphor waste in IL

The previous experiment was repeated using the same conditions with real phosphor waste instead of a synthetic mixture of phosphors. The obtained leaching efficiencies are depicted in Figure 37, and the composition of the PLS is shown in Table 24. While the IL in the experiments on synthetic phosphors stayed clear, the IL now has a light brown color. The YOX from the real phosphor waste leaches easier than the artificial counterpart as after 22 hours, the values are closer to those from leaching 64 hours. Note that the leaching efficiency exceeds 100 %. Either there is an error in the ICP-OES values, which is unlikely as good results were obtained from previous measurements on samples with a known composition, or that the characterization provided together with the phosphor waste deviated from the actual composition. The europium on the other hand is lower, in the range of 60 – 70 % after 22 hours and 70 – 80 % after 64 hours. The LAP phosphor still is not leached (less than 0.1 % for lanthanum, maximum 1.5 % for cerium), but the BAM phosphor is leached, and the HALO phosphor is leached more than in the artificial phosphor blend. The strontium in the HALO phosphor is leached significantly, reaching 64 % at one point, but the total concentration is still low as strontium is only a minor element in the HALO phosphor. Silicon is measured as well since the phosphor waste also contains glass particles, but the leaching efficiency stayed under 0.1 % at all times. The composition of one of the two samples used for the data point of a S-to-L ratio of 20 mg/mL and a leaching time of 64 hours is given in Table 24. Similar to the

experiments performed on the synthetic mixture, the S-to-L ratio does not have a large influence on the leaching.

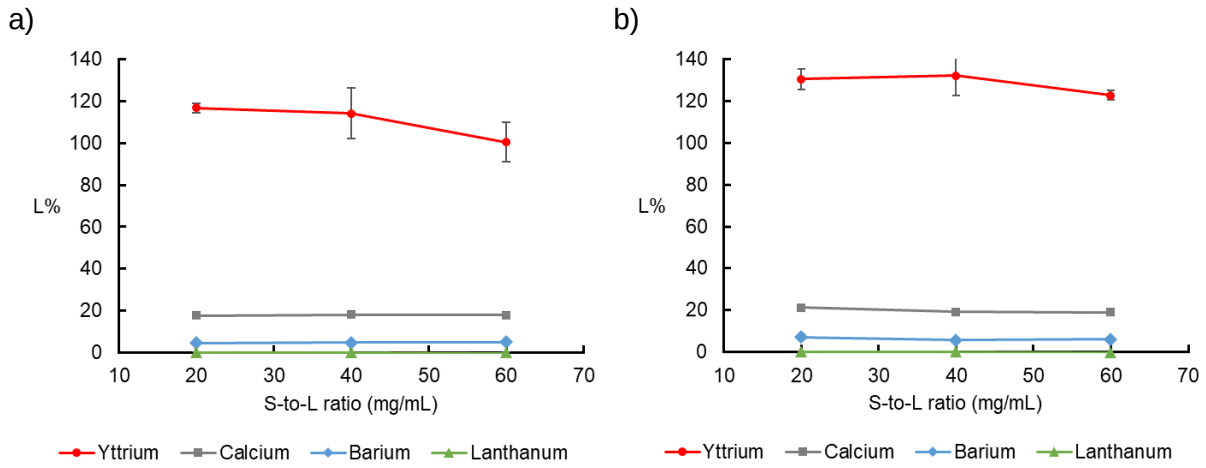

Figure 37: Leaching efficiencies of yttrium, calcium, barium and lanthanum from the real phosphor waste in function of the solid-to-liquid ratio after a) 22 hours and b) 64 hours.

Table 24: Composition of the IL after leaching 22 and 64 hours with a S-to-L ratio of 20 mg/mL.

Element	Concentration leaching time of 22 hours (mg/mL)	Concentration leaching time of 64 hours (mg/mL)
Y	1.47	1.67
Eu	0.09	0.10
Ca	0.27	0.35
Sr	0.029	0.049
Sb	< 0.001	< 0.001
Mn	0.002	0.003
Ba	0.016	0.026
Mg	0.008	0.011
Al	0.019	0.029
La	< 0.001	< 0.001
Ce	0.001	0.002
Si	0.001	0.002

A.4.5 Kinetics of leaching real waste in MSA at 200 °C and 160 °C

Now that the leaching of YOX with IL has been shown to more or less work with a higher leaching efficiency for HALO, the next step was to validate the leaching of LAP with pure methanesulfonic acid (MSA). First the kinetics of the leaching reaction were studied on real phosphor waste. Samples with a liquid-to-solid ratio of 15 mL MSA per g of phosphor waste were heated at 200 °C between 5 min and 2 hours. All samples were black after leaching. The composition of the PLS was analyzed and the results are in the left-hand side of Figure 38a. Compared to the kinetics discussed in the literature for the residue of the HydroWEEE process, see Figure 39, the green LAP phosphor leaches a lot slower, reaching a leaching efficiency of 100 % after 2 hours while only half an hour suffices for the HydroWEEE residue according to

the literature.[86] The other three phosphors are also leached, and much faster than the LAP phosphor. For the YOX phosphor, europium leaches more than yttrium, but both practically are not leached further after the first couple of minutes. For the BAM phosphor, barium dissolves the easiest, magnesium and aluminium stay below 10 %. For HALO, all trace elements are leached easier than calcium, easily going above 100 %, again indicating that the characterization delivered with the waste deviated from the actual composition. For LAP, cerium and terbium are below lanthanum and follow its trend. After the ICP measurements, a small amount of brown precipitation was observed in the samples, at the moment thought to probably be decomposition products from the MSA. In other experiments, this was observed too when adding water to the MSA, and a small amount of the precipitation could be isolated (see section 3.11).

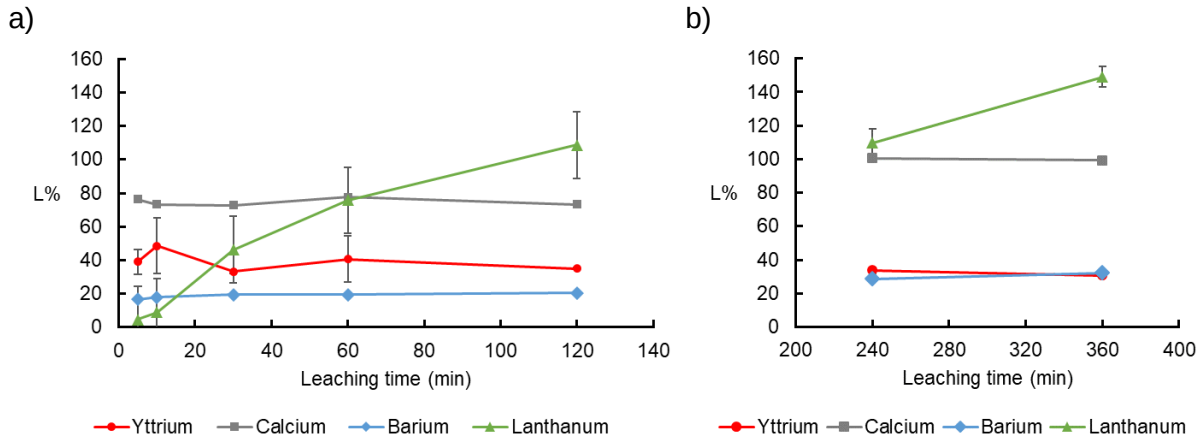

Figure 38: Leaching kinetics of the main elements of the four phosphors at a) 200 °C and b) 160 °C. Used L-to-S ratio: 15 mL/g

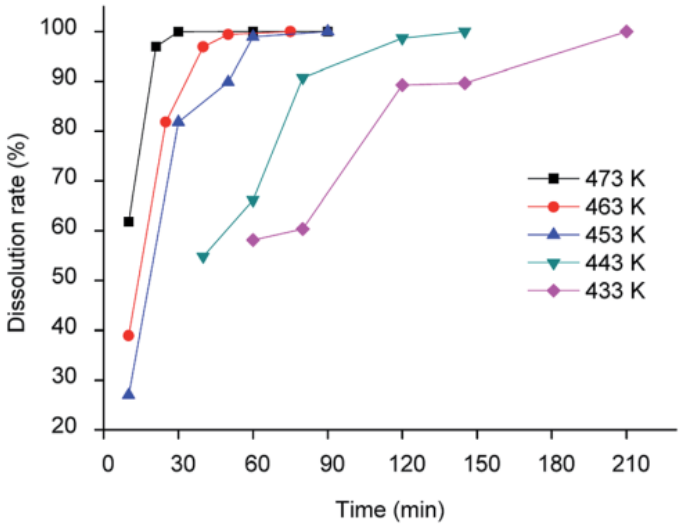

Figure 39: Kinetics of the leaching of the green LAP phosphor depending on the temperature according to the literature. 473 K equals 200 °C, 433 K equals 160 °C. Used L-to-S ratio: 15 mL/g.[86]

Since the MSA might already be decomposing (higher temperatures are not advised due to decomposition),[86] some samples were leached at 160 °C for a longer time. According to Figure 39, 3.5 hours should be enough to completely leach the LAP phosphor, so 4 and 6 hours were used to ensure full leaching of all the metals present. All samples were again black after leaching and filtering. The results are in Figure 38b. The YOX and BAM phosphors leach approximately the same amount and HALO leaches more. The trace elements follow the

same trends as when leached at 200 °C. The LAP phosphor however is not completely leached after four hours when it has the same value as when leaching at 200 °C for two hours, and after six hours, lanthanum is leached more than 140 %. A composition of one of the two samples used for the leaching time of two hours is given in Table 25. Both ICP-OES values and TXRF values are given. TXRF measured quite some iron, and traces of nickel, copper, zinc, germanium, bromine and gadolinium in the sample. Similar to the test shown in Appendix 3, calcium cannot be measured reliably using TXRF.

Table 25: Composition of the MSA after leaching two hours at 200 °C.

Element	Concentration TXRF (mg/mL)	Concentration ICP-OES (mg/mL)
Y	1.612	1.463
Eu	0.234	0.200
Ca	1.142	3.266
Sr	0.066	0.239
Sb	-	0.048
Mn	-	0.089
Ba	0.116	0.222
Mg	-	0.048
Al	-	0.081
La	0.298	0.651
Ce	0.225	0.410
Tb	0.099	0.143
Si	-	0.001
Fe	0.275	-

To see what happens to the MSA when heating it to 200 °C, a sample of pure MSA was heated at 200 °C for two hours and a quarter. The sample only had a small discoloration afterwards, contrary to the black samples of leaching the phosphor waste. A ^{1}H-NMR was taken before and after heating the MSA, see Figure 41 in Appendix 5. Other than a small shift in the peak of the acidic proton, no change between the spectra is observed. It seems that pure MSA is stable at 200 °C for at least two hours. It was thought that one of the metals leached from the phosphor waste somehow facilitated decomposition of the MSA.

A.4.6 Effect of the liquid-to-solid ratio in leaching LAP with MSA

Although the literature mentions the liquid-to-solid ratio to be optimal at 15 mL/g for leaching LAP with MSA, no graph was shown. It was also reported that a gel formed at lower liquid-to-solid ratios.[86] Samples with varying liquid-to-solid ratios were heated at 160 °C for two hours. For this experiment, sieved phosphor waste was used (see section 3.3.1). It was overlooked that the LAP phosphor leaches a lot slower at 160 °C than the literature suggests, so the leaching was not complete. The results can be found in Figure 40. For the BAM phosphor, the liquid-to-solid ratio has no effect on the leaching. Magnesium leached between 40 and 50 %, aluminium leached less than 10 %. All elements of the HALO phosphor leached above 90 % independent of the L-to-S ratio except when using a L-to-S ratio of 5 mL/g. At this same value,

the LAP phosphor dissolves easier than at higher L-to-S ratios. Cerium is leached a few percent more selectively and terbium is leached a couple of percent less. The dissolution of YOX is inhibited at lower L-to-S ratios, but it still leaches considerably, and europium has leaching efficiencies more than double those of yttrium.

No gel formation was observed, but the samples with the lowest L-to-S ratios were difficult to filter using syringe filters due to the larger amount of solids present, blocking the filter more. This effect would also be present at a larger scale when filtering with a glass filter. These samples also produced a precipitation when diluting them in 2 v% HNO_3 for the ICP-OES measurements. Because of these reasons, the used L-to-S ratio was kept at 15 mL/g.

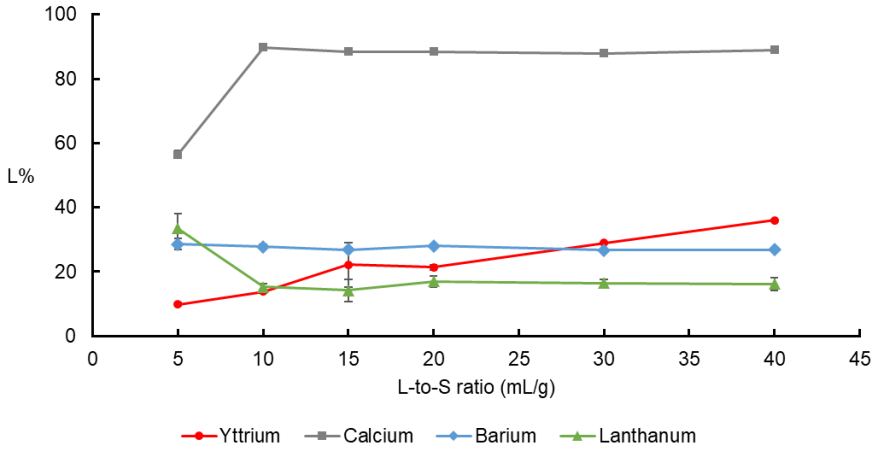

Figure 40: Effect of the liquid-to-slid ratio on leaching LAP from sieved phosphor waste. Heated at 160 °C for 2 hours.

Appendix 5: ^{1}H-NMR-spectra of MSA

All ^{1}H-NMR spectra were taken at 300 MHz. The MSA was dissolved in deuterated DMSO containing some TMS. As the concentration of the MSA was quite high in the DMSO to make it easier to spot impurities, coupling with ^{13}C is visible as small satellite peaks around the large peaks.

The spectra of clean MSA, MSA heated at 200 °C (see section 3.2.2) for two hours and a quarter, and distilled MSA (see section 3.8.3) are given in Figure 41. The only difference between the heated MSA and the clean MSA is a small shift in the position of the acidic proton. No other peaks are visible and the hydrogen ratio of the two peaks fit, so no degradation seems to occur. The spectrum of the distilled MSA is almost identical to that of clean MSA, so it does not seem to degrade during the distillation.

Clean MSA: δ (ppm): 2.54 – 2.58 (3 H, s, CH_3) and 14.10 (1 H, s, SO_3H).

Heated MSA: δ (ppm): 2.54 – 2.57 (3 H, s, CH_3) and 13.84 (1 H, s, SO_3H).

Distilled MSA δ (ppm): 2.54 – 2.59 (3 H, s, CH_3) and 14.12 – 14.14 (1 H, s, SO_3H).

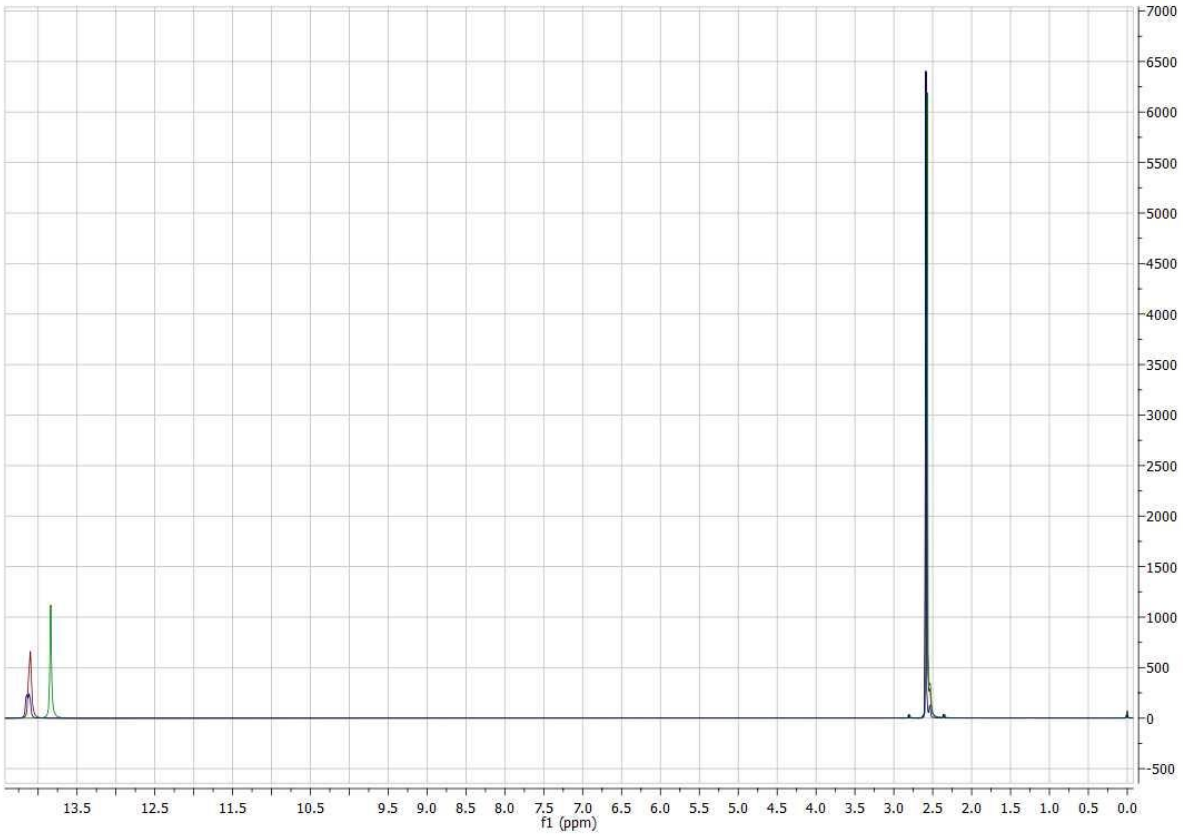

Figure 41: ^{1}H-NMR spectra of clean MSA (red), MSA heated at 200 °C (green) and distilled MSA (blue).

References

1 J.-C. G. Bünzli and I. Mcgill, in *Ullmann's Encyclopedia of Industrial Chemistry*, Wiley-VCH Verlag GmbH & Co. KGaA, Weinheim, Germany, 7th edn., 2018, pp. 1–53.

2 K. Binnemans, P. T. Jones, T. Müller and L. Yurramendi, *J. Sustain. Metall.*, 2018, **8**, 126–146.

3 K. M. Goodenough, F. Wall and D. Merriman, *Nat. Resour. Res.*, 2018, **27**, 201–216.

4 D. Dupont and K. Binnemans, *Green Chem.*, 2015, **17**, 2150–2163.

5 S. Soleille, M. A. Kong, M. Planchon, N. Saidi, D. Chloé, E. Petavratzi, G. Gunn, T. Brown, R. Shaw, G. Lefebvre, M. Le Gleuher, E. Rietveld, J. de Jong, T. Nijland and T. Bastein, *Study on the review of the list of Critical Raw Materials*, 2017.

6 U.S. Geological Survey, *Rare Earths*, 2017.

7 U.S. Geological Survey, *Rare Earths*, 2018.

8 U.S. Geological Survey, *Rare Earths*, 2019.

9 J. Kooroshy, G. Tiess, A. Tukker and A. Walton, *Strengthening the European rare earths sypply chain: Challenges and policy options. Final report of the European Rare Earths Competency Network (ERECON).*, Brussels, 2015.

10 R. Kim, H. Cho, K. Han, K. Kim and M. Mun, *Minerals*, 2016, **6**, 63.

11 A. Ferdowsi and H. Yoozbashizadeh, *Trans. Nonferrous Met. Soc. China*, 2017, **27**, 420–428.

12 K. Stone, A. M. T. S. Bandara, G. Senanayake and S. Jayasekera, *Hydrometallurgy*, 2016, **163**, 137–147.

13 A. Battsengel, A. Batnasan, A. Narankhuu, K. Haga, Y. Watanabe and A. Shibayama, *Hydrometallurgy*, 2018, **179**, 100–109.

14 M. Alemrajabi, Å. C. Rasmuson, K. Korkmaz and K. Forsberg, *Hydrometallurgy*, 2017, **169**, 253–262.

15 S. Wu, L. Wang, L. Zhao, P. Zhang, H. El-Shall, B. Moudgil, X. Huang and L. Zhang, *Chem. Eng. J.*, 2018, **335**, 774–800.

16 D. Xu, Z. Shah, Y. Cui, L. Jin, X. Peng, H. Zhang and G. Sun, *Hydrometallurgy*, 2018, **180**, 132–138.

17 M. Chen and T. E. Graedel, *J. Clean. Prod.*, 2015, **91**, 337–346.

18 Y. Shen, Y. Jiang, X. Qiu and S. Zhao, *JOM*, 2017, **69**, 1976–1981.

19 L. K. Sinclair, D. L. Baek, J. Thompson, J. W. Tester and R. V. Fox, *J. Supercrit. Fluids*, 2017, **124**, 20–29.

20 S. Dai, I. T. Graham and C. R. Ward, *Int. J. Coal Geol.*, 2016, **159**, 82–95.

21 W. Zhang, M. Rezaee, A. Bhagavatula, Y. Li, J. Groppo and R. Honaker, *Int. J. Coal Prep. Util.*, 2015, **35**, 295–330.

22 P. L. Rozelle, A. B. Khadilkar, N. Pulati, N. Soundarrajan, M. S. Klima, M. M. Mosser, C. E. Miller and S. V. Pisupati, *Metall. Mater. Trans. E*, 2016, **3**, 6–17.

23 R. S. Blissett, N. Smalley and N. A. Rowson, *Fuel*, 2014, **119**, 236–239.

24 J. F. King, R. K. Taggart, R. C. Smith, J. C. Hower and H. Hsu-Kim, *Int. J. Coal Geol.*, 2018, **195**, 75–83.

25 W. Franus, M. M. Wiatros-Motyka and M. Wdowin, *Environ. Sci. Pollut. Res.*, 2015, **22**, 9464–9474.

26 R. Q. Honaker, W. Zhang, X. Yang and M. Rezaee, *Miner. Eng.*, 2018, **122**, 233–240.

27 R. Lin, B. H. Howard, E. A. Roth, T. L. Bank, E. J. Granite and Y. Soong, *Fuel*, 2017, **200**, 506–520.

28 P. K. Parhi, K. H. Park, C. W. Nam and J. T. Park, *J. Rare Earths*, 2015, **33**, 207–213.

29 V. L. Brisson, W.-Q. Zhuang and L. Alvarez-Cohen, *Biotechnol. Bioeng.*, 2016, **113**, 339–348.

30 M. I. Aly, B. A. Masry, M. S. Gasser, N. A. Khalifa and J. A. Daoud, *Int. J. Miner. Process.*, 2016, **153**, 71–79.

31 F. Sadri, F. Rashchi and A. Amini, *Int. J. Miner. Process.*, 2017, **159**, 7–15.

32 R. Panda, A. Kumari, M. K. Jha, J. Hait, V. Kumar, J. Rajesh Kumar and J. Y. Lee, *J. Ind. Eng. Chem.*, 2014, **20**, 2035–2042.

33 E. H. Borai, M. S. A. El-Ghany, I. M. Ahmed, M. M.Hamed, A. M. S. El-Din and H. F. Aly, *Int. J. Miner. Process.*, 2016, **149**, 34–41.

34 A. Kumari, R. Panda, M. K. Jha, J. R. Kumar and J. Y. Lee, *Miner. Eng.*, 2015, **79**, 102–115.

35 A. Kumari, R. Panda, M. K. Jha, J. Y. Lee, J. R. Kumar and V. Kumar, *J. Ind. Eng. Chem.*, 2015, **21**, 696–703.

36 P. Davris, S. Stopic, E. Balomenos, D. Panias, I. Paspaliaris and B. Friedrich, *Miner. Eng.*, 2017, **108**, 115–122.

37 S. M. El Hady, A. R. Bakry, A. A. S. Al Shami and M. M. Fawzy, *Hydrometallurgy*, 2016, **163**, 115–119.

38 C. Ayora, F. Macías, E. Torres, A. Lozano, S. Carrero, J.-M. Nieto, R. Pérez-López, A. Fernández-Martínez and H. Castillo-Michel, *Environ. Sci. Technol.*, 2016, **50**, 8255–8262.

39 K. Binnemans, P. T. Jones, B. Blanpain, T. Van Gerven, Y. Yang, A. Walton and M. Buchert, *J. Clean. Prod.*, 2013, **51**, 1–22.

40 Y. Wang, C. Huang, F. Li, Y. Dong and X. Sun, *Hydrometallurgy*, 2017, **169**, 158–164.

41 K. M. Goodenough, J. Schilling, E. Jonsson, P. Kalvig, N. Charles, J. Tuduri, E. A. Deady, M. Sadeghi, H. Schiellerup, A. Müller, G. Bertrand, N. Arvanitidis, D. G. Eliopoulos, R. A. Shaw, K. Thrane and N. Keulen, *Ore Geol. Rev.*, 2016, **72**, 838–856.

42 S. Jaireth, D. M. Hoatson and Y. Miezitis, *Ore Geol. Rev.*, 2014, **62**, 72–128.

43 K. Reinhardt and H. Winkler, in *Ullmann's Encyclopedia of Industrial Chemistry*, Wiley-VCH Verlag GmbH & Co. KGaA, Weinheim, Germany, 2000, pp. 1–16.

44 K. Binnemans and P. T. Jones, *J. Sustain. Metall.*, 2017, **3**, 570–600.

45 J. Régnier, in *Essential Reading in Light Metals - Volume 1: Alumina and bauxite*, eds. D. Donaldson and B. E. Raahauge, 1988, pp. 3–20.

46 M. L. Free, *Hydrometallurgy*, John Wiley & Sons, Inc., Hoboken, New Jersey, 2013.

47 C. Tunsu, PhD thesis, Chalmers University of Technology, 2016.

48 J. Lucas, P. Lucas, T. Le Mercier, A. Rollat and W. Davenport, *Rare Earths: Science, Technology, Production and Use*, Elsevier, 2014.

49 S. Özdemir and İ. Girgin, *Miner. Eng.*, 1991, **4**, 179–184.

50 S. Wongnawa, P. Boonsin and T. Sombatchaikul, *Hydrometallurgy*, 1997, **45**, 161–167.

51 G. W. Meindersma, M. Maase and A. B. De Haan, in *Ullmann's Encyclopedia of Industrial Chemistry*, Wiley-VCH Verlag GmbH & Co. KGaA, Weinheim, Germany, 2007, vol. 19, pp. 547–575.

52 P. Nockemann, B. Thijs, S. Pittois, J. Thoen, C. Glorieux, K. Van Hecke, L. Van Meervelt, B. Kirchner and K. Binnemans, *J. Phys. Chem. B*, 2006, **110**, 20978–20992.

53 N. Schaeffer, X. Feng, S. Grimes and C. Cheeseman, *J. Chem. Technol. Biotechnol.*, 2017, **92**, 2731–2738.

54 S. Wellens, T. Vander Hoogerstraete, C. Möller, B. Thijs, J. Luyten and K. Binnemans, *Hydrometallurgy*, 2014, **144**–**145**, 27–33.

55 D. Dupont and K. Binnemans, *Green Chem.*, 2015, **17**, 856–868.

56 P. Davris, E. Balomenos, D. Panias and I. Paspaliaris, *Hydrometallurgy*, 2016, **164**, 125–135.

57 G. Mawire and L. van Dyk, *Extr. 2018*, 2018, 2723–2734.

58 K. A. Franz, W. G. Kehr, A. Siggel, J. Wieczoreck and W. Adam, in *Ullmann's Encyclopedia of Industrial Chemistry*, Wiley-VCH Verlag GmbH & Co. KGaA, Weinheim, Germany, 2000, pp. 1–41.

59 S. Fukumoto and Y. Hayashi, *J. Light Vis. Environ.*, 1996, **20**, 36–41.

60 S. Cotton, *Lanthanide and Actinide Chemistry*, John Wiley & Sons, Ltd, Chichester, UK, First., 2006.

61 W. J. van den Hoek, A. G. Jack† and G. M. J. F. Luijks, in *Ullmann's Encyclopedia of Industrial Chemistry*, Wiley-VCH Verlag GmbH & Co. KGaA, Weinheim, Germany, 2001, pp. 1–42.

62 K. Binnemans and P. T. Jones, *J. Rare Earths*, 2014, **32**, 195–200.

63 G. R. Fonda, *Br. J. Appl. Phys.*, 1955, **6**, S69–S72.

64 M. Doherty and W. Harrison, *Br. J. Appl. Phys.*, 1955, **6**, S11–S16.

65 B. Liu, Y. Wang, J. Zhou, F. Zhang and Z. Wang, *J. Appl. Phys.*, 2009, **106**, 053102.

66 S. Van Loy, K. Binnemans and T. Van Gerven, *Engineering*, 2018, **4**, 398–405.

67 C. Tunsu, C. Ekberg and T. Retegan, *Hydrometallurgy*, 2014, **144**–**145**, 91–98.

68 G. T. Silveira and S.-Y. Chang, *Waste Manag. Res.*, 2011, **29**, 656–668.

69 J. Hobohm, O. Krüger, S. Basu, K. Kuchta, S. van Wasen and C. Adam, *Chemosphere*, 2017, **169**, 618–626.

70 V. Innocenzi, I. De Michelis and F. Vegliò, *J. Taiwan Inst. Chem. Eng.*, 2017, **80**, 769–778.

71 T. Hirajima, A. Bissombolo, K. Sasaki, K. Nakayama, H. Hirai and M. Tsunekawa, *Int. J. Miner. Process.*, 2005, **77**, 187–198.

72 T. Takahashi, A. Takano, T. Saitoh, N. Nagano, S. Hirai and K. Shimakage, *Shigen-to-Sozai*, 2001, **117**, 579–585.

73 T. Hirajima, K. Sasaki, A. Bissombolo, H. Hirai, M. Hamada and M. Tsunekawa, *Sep. Purif. Technol.*, 2005, **44**, 197–204.

74 G. Mei, P. Rao, M. Mitsuaki and F. Toyohisa, *J. Wuhan Univ. Technol. Sci. Ed.*, 2009, **24**, 418–423.

75 G. Mei, P. Rao, M. Matsuda and T. Fujita, *J. Wuhan Univ. Technol. Sci. Ed.*, 2009, **24**, 603–607.

76 G. Mei and K. Xie, in *2008 2nd International Conference on Bioinformatics and Biomedical Engineering*, IEEE, Shanghai, 2008, pp. 4674–4679.

77 S. Van Loy, K. Binnemans and T. Van Gerven, *J. Clean. Prod.*, 2017, **156**, 226–234.

78 M. A. Rabah, *Waste Manag.*, 2008, **28**, 318–325.

79 M. Yu, S. Pang, G. Mei and X. Chen, *Minerals*, 2016, **6**, 109.

80 F. Beolchini, L. Rocchetti, P. Altimari, I. Michelis, L. Toro, F. Pagnanelli, E. Moscardini, B. Kopacek, B. Ferrari, V. Innocenzi and F. Veglio, *Environ. Eng. Manag. J.*, 2013, **12**, 69–72.

81 I. De Michelis, F. Ferella, E. F. Varelli and F. Vegliò, *Waste Manag.*, 2011, **31**, 2559–2568.

82 N. M. Ippolito, V. Innocenzi, I. De Michelis, F. Medici and F. Vegliò, *J. Clean. Prod.*, 2017, **153**, 287–298.

83 V. Innocenzi, N. M. Ippolito, I. De Michelis, F. Medici and F. Vegliò, *J. Environ. Manage.*, 2016, **184**, 552–559.

84 C. Liao, Z. Li, Y. Zeng, J. Chen, L. Zhong and L. Wang, *J. Rare Earths*, 2017, **35**, 1008–1013.

85 S.-G. Zhang, M. Yang, H. Liu, D.-A. Pan and J.-J. Tian, *Rare Met.*, 2013, **32**, 609–615.

86 L. Gijsemans, F. Forte, B. Onghena and K. Binnemans, *RSC Adv.*, 2018, **8**, 26349–26355.

87 R. Shimizu, K. Sawada, Y. Enokida and I. Yamamoto, *J. Supercrit. Fluids*, 2005, **33**, 235–241.

88 C. Tunsu, C. Ekberg, M. Foreman and T. Retegan, *Solvent Extr. Ion Exch.*, 2014, **32**, 650–668.

89 M. D. Luque de Castro and F. Priego-Capote, *J. Chromatogr. A*, 2010, **1217**, 2383–2389.

90 X. Ren, W. Lu and Q. Wei, *AASRI Procedia*, 2012, **3**, 341–350.

91 H. Shlewit and S. A. Khorfan, *Solvent Extr. Res. Dev. Japan&*, 2002, **9**, 59–68.

92 C. Ye and J. Li, *J. Chem. Technol. Biotechnol.*, 2013, **88**, 1715–1720.

93 D. Zou, Y. Jin, J. Li, Y. Cao and X. Li, *Sep. Purif. Technol.*, 2017, **172**, 242–250.

94 Y. Jin, D. Zou, S. Wu, Y. Cao and J. Li, *Ind. Eng. Chem. Res.*, 2015, **54**, 108–116.

95 M. Chen, J. Li, Y. Jin, J. Luo, X. Zhu and D. Yu, *J. Chem. Technol. Biotechnol.*, 2018, **93**, 467–475.

96 W. F. Linke and A. Seidell, *Solubilities, inorganic and metal-organic compounds - Volume 1*, American Chemical Society, Washington, D.C., 4th ed., 1958.

97 W. F. Linke and A. Seidell, *Solubilities, inorganic and metal-organic compounds - Volume 2*, American Chemical Society, Washington, D.C., 4th ed., 1958.

98 K. Kosswig, in *Ullmann's Encyclopedia of Industrial Chemistry*, Wiley-VCH Verlag GmbH & Co. KGaA, Weinheim, Germany, 2000, pp. 1–4.

99 J. G. Speight, in *The Refinery of the Future*, ed. J. G. B. T.-T. R. of the F. Speight, William Andrew Publishing, Boston, 2011, pp. 117–145.

100 H. E. Gottlieb, V. Kotlyar and A. Nudelman, *J. Org. Chem.*, 1997, **62**, 7512–7515.

AFDELING MOLECULAIR DESIGN EN SYNTHESE
Celestijnenlaan 200 F Chem&Tech
3001 LEUVEN, BELGIË
tel. + 32 16 32 74 46
koen.binnemans@kuleuven.be
https://chem.kuleuven.be/solvomet